STUDIES ON THE RING-OPENING/CROSS METATHESIS OF 8-OXABICYCLO[3.2.1]OCTENE DERIVATIVES AND ITS APPLICATION TOWARDS THE SYNTHESIS OF LATRUNCULIN B

By

MARÍA E. ESTRELLA-JIMÉNEZ

A DISSERTATION PRESENTED TO THE GRADUATE SCHOOL
OF THE UNIVERSITY OF FLORIDA IN PARTIAL FULFILLMENT
OF THE REQUIREMENTS FOR THE DEGREE OF
DOCTOR OF PHILOSOPHY

UNIVERSITY OF FLORIDA

2005

Copyright 2005

by

María E. Estrella-Jiménez

Dedicated to my family, the most important thing in my life, and to all of those who have taught me in some way

ACKNOWLEDGMENTS

I need to thank my big and wonderful family; they are my life's engine. Especially, I thank my parents, Sheila Jiménez and Félix A. Estrella, my brother Félix A. Estrella Jr., and my sister Johanna Estrella for their unconditional love and support. In addition, a special thank you goes to Wilfredo Ortiz, who has always been there to give me his love, help, support and positive input. Without him, everything would have been overwhelming. I would like to thank my friends for keeping my social life in healthy status.

Professionally, I would like to thank my undergraduate advisor, Dr. John A. Soderquist. I am very grateful for the trust he gave me as a student and for giving me the opportunity to start organic chemistry in his research group. I also thank him for his help in numerous opportunities and fellowships.

I thank my advisor, Dr. Dennis L. Wright, for giving me the opportunity of being part of his research group and for respecting my decision of staying at the University of Florida, after he moved to Dartmouth College for a new faculty position. I also thank him for his advices and exciting chemistry discussions.

I offer special thanks to Professor Merle A. Battiste. He was a key person in my final year at University of Florida. I could not be more grateful of his support, positive input, confidence and friendship. I really appreciated the concern and interest he took in me. He always had the time to listen, regardless of the matter.

I would like to thank the other members of my committee, Professor William R. Dolbier, Professor Ken Sloan and Professor David H. Powell, for taking their time to be part of my professional development. Dr. Ion Ghiviriga needs to be given special thanks for all his help with the NMR and for his friendship. He was a great collaborator and friend. No matter how busy he was, he would always take some time to help me. In addition, the mass spectroscopy team needs to be thanked for their suggestions and work in getting the molecular weight of my compounds. I am very grateful for my former and present colleagues for offering me their knowledge and friendship, especially Lynn Usher, Chris Whitehead and Ravi Orogunty. Lynn Usher trained me during my first year as a graduate student and offered me tremendous help through the years with her advice, friendship and, I need to add, the English lessons. I will always remember Chris Whitehead; he mentored me on many occasions with lab techniques. I appreciate Ravi Orogunty for sharing his wisdom with me many times. In addition, I would like to thank Chris Baker for his friendship during this past year.

Furthermore, I would like to express my thanks to my colleagues and friends, Theodore Martinot and Jed Hasting. I thank Theodore Martinot for all the help and advice he offered me this past year. Jed Hasting is truly appreciated for his wonderful friendship, help and patience in listening to me during stressful times. Dave Pirman, the undergraduate that worked with me during my last year, also deserves special mentioning for all the help he provided in the lab. Last, but not least, for all the non-research-related work, I am very grateful for secretaries Lori Clark and Gwen McCann from the Department of Chemistry. They are efficient, friendly and wonderful secretaries.

Finally, I would like to thank the University of Florida for giving me the opportunity of coming here to pursue my graduate studies and for the fellowship provided.

TABLE OF CONTENTS

page

ACKNOWLEDGMENTS iv

ABSTRACT ix

CHAPTER

1 INTRODUCTION 1

Ring-Opening of 8-Oxabicyclo[3.2.1]Octene Derivatives and its Application in Synthesis 3
Cleavage of the Unsaturated Double Bond, C6-C7, of the Oxabicyclo[3.2.1] System 4
Cleavage of the Carbonyl and the α-Carbon, C3-C4, of the Oxabicyclo[3.2.1] System 8
Cleavage of the Carbon-Oxygen Bridgehead Bond, C1-C2, of the Oxabicyclo[3.2.1] System 9
Olefin Metathesis 13
Types of Olefin Metathesis Reactions 16
Ring-opening metathesis polymerization 16
Acyclic diene metathesis 17
Cross metathesis 18
Ring-closing metathesis 19
Ring-opening cross metathesis 23
Tandem Metathesis 26
Catalytic Asymmetric Olefin Metathesis 29
The Latrunculins 36
Total Syntheses of Latrunculin B 37
Smith's total synthesis 37
Fürstner's total synthesis 39
Total Syntheses of Latrunculin A 40
Smith's total synthesis 40
White's total synthesis 41
Kashman's Approach to the Latrunculin Synthon 44
Kashman's Synthesis of Latrunculin M and C 45

2 RESULTS/DISCUSSION 47

Intermolecular Ring-Opening Cross Metathesis (ROCM) 47
Kinetic Studies 49
Bridgehead Substituted 8-Oxabicyclo[3.2.1]Octene Derivatives 59
Intramolecular Ring-Opening Cross Metathesis (ROCM) 65
Approaches Towards Latrunculin B from Ring-Opening Metathesis of 8-Oxabicyclo[3.2.1]Octene Derivatives 71

3 CONCLUSIONS AND FUTURE WORK 80

4 EXPERIMENTAL PROCEDURES 82

APPENDIX

A SELECTED SPECTRA 118

B LIST OF TABLES FOR KINETIC STUDIES 151

C LIST OF GRAPHS FOR KINETIC STUDIES 157

LIST OF REFERENCES 188

BIOGRAPHICAL SKETCH 194

Abstract of Dissertation Presented to the Graduate School
of the University of Florida in Partial Fulfillment of the
Requirements for the Degree of Doctor of Philosophy

STUDIES ON THE RING-OPENING/CROSS METATHESIS OF 8-OXABICYCLO[3.2.1]OCTENE DERIVATIVES AND ITS APPLICATION TOWARDS THE SYNTHESIS OF LATRUNCULIN B

By

María E. Estrella-Jiménez

May 2005

Chair: Dennis L. Wright
Cochair: Merle A. Battiste
Major Department: Chemistry

The pyran moiety is a common structural feature found in many natural products, and often seen as an integral part of carbohydrates and macrolides of marine origin. This work discloses the use of ring-opening cross metathesis (ROCM) of 8-oxabicyclo[3.2.1]octene derivatives for the preparation of substituted pyrans, using Grubbs' ruthenium-based metathesis catalyst. The oxabicyclic systems were synthesized using Föhlish conditions, which involve the [4+3] cycloaddition between furan and an oxallyl cation. An unusual influence in the reactivity and selectivity of the ROCM reactions was discovered upon substituent variation at the C3 position of the oxabicyclo. These results led to further investigations that involved the synthesis of a series of 8-oxabicyclo[3.2.1]octene derivatives with different substituents at C3. Kinetic experiments were conducted with the substrates, using NMR to monitor the reactions. These experiments provided relative rates of ring-opening metathesis polymerization for

the series of oxabicyclic derivatives when compared with 4,10-dioxa-tricyclo[5.2.1.0 ^{2,6}]dec-8-ene-3,5-dione (adduct of furan and maleic anhydride). The relative rate trend observed among the substrates showed that their reactivity is affected by the combination of electronic and steric effects. The knowledge obtained can be used to accelerate sluggish ROCM reactions in the synthesis of pyrans from these types of substrates. Substitution at the bridgehead position of the oxabicycle decreases the reactivity of the system and brings into focus the problem of regioisomers. However, the careful consideration of the substituent at the C3 position gave good yields of the pyrans, and excellent regioselectivity was obtained having an *endo*-alcohol as a substituent at that position. In addition, the intramolecular ROCM of oxabicyclic system having a tethered alkene at the C2 position was studied and led to linear-fused pyrans.

Furthermore, preliminary work was done towards the synthesis of latrunculin B using the ROCM approach.

CHAPTER 1
INTRODUCTION

Polycyclic systems can be seen as a method to achieve stereoselectivity in organic synthesis. The ring strain contained in some polycyclic compounds fixes them in a conformation that accesses contiguous stereocenters as well as helps in the control of stereocenters from successive reactions. Oxabicyclic compounds are polycyclic systems that possess an oxygen atom as part of the cyclic framework. The developments of ring cleavage reactions of oxabicyclic compounds have made them attractive starting materials in organic synthesis. Ring-opening of oxabicyclic derivatives can lead to a wide variety of compounds by selective cleavage of specific bonds. These compounds are frequently highly substituted ethers, particularly tetrahydrofurans and tetrahydropyrans.[1] A large number of natural products and sugars have been synthesized from oxabicyclic compounds.[1]

A particular substrate is 8-oxabicyclo[3.2.1]oct-6-en-3-one **1**, which allows the construction of different oxygen-containing compounds by specific bond disconnections. Cleavage between the bridged-carbon, C1, and the oxygen (path *a*) generates a cycloheptenol, whereas cleavage between the carbonyl, C3, and the adjacent α carbon, C2, (path *b*) gives a 2,4 dihydrofuran moiety, and cleavage of the unsaturated double bond, C6-C7, (path *c*) produces a pyrone derivative (Scheme1-1).

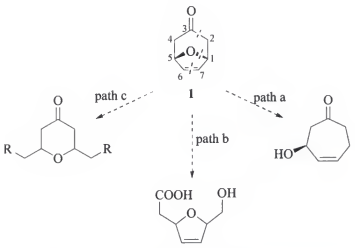

Scheme 1-1. Different oxygen-containing compounds by specific bond disconnections of 8-oxabicyclo[3.2.1]oct-6-en-3-one

The availability of this oxabicyclo, which can be synthesized by a [4+3] cycloaddition with protocols amenable to large scale preparations,[2] and the availability of alternative ring-opening reactions make this compound an interesting starting unit in organic synthesis.[1]

Our research focused on the cleavage of the double bond (path *c*) of **1** and its derivatives using ruthenium-based olefin metathesis to generate a pyran moiety. To prove the efficiency of the method, it was also applied in an approach to latrunculin B. The precursors were readily obtained by a [4+3] cycloaddition, employing Föhlish's conditions, which involves the [4+3] cycloaddition of furan and trichloroacetone in the presence of sodium trifluorethoxide, and subsequent reduction using zinc/copper couple in methanol saturated with ammonium chloride.[3] The presence of the pyran moiety in many natural products (Figure 1-1) sparked our interest in developing this methodology.

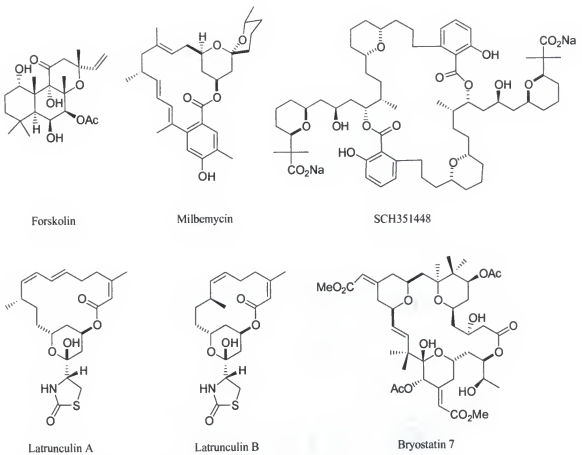

Figure 1-1. Natural products displaying the pyran moiety

This dissertation will present the studies on the ring opening cross metathesis of 8-oxabicyclo[3.2.1]octene derivatives and its application in an approach to latrunculin B. Relevant to this dissertation is to mention different types of ring-opening of 8-oxabicyclo[3.2.1]octene derivatives and their application to the synthesis of a variety of natural products, as well as a background on the olefin metathesis reaction. In addition, a brief history of the latrunculins is included.

Ring-Opening of 8-Oxabicyclo[3.2.1]Octene Derivatives and its Application in Synthesis

This section is devoted to demonstrating the versatility of 8-oxabicyclo[3.2.1]octene derivatives in the synthesis of natural products via different ring openings. 8-oxabicyclo[3.2.1]octene derivatives present some advantages that make

them excellent precursors in organic synthesis. Among these, specific bond disconnections in the system allow for the construction of different oxygen-containing moieties that are commonly seen in natural products. Moreover, the system is readily accessible in large scale from a [4+3] cycloaddition.[4] The defined conformation and rigidity of the system allows access to multiple stereocenters in one step from the cycloaddition reaction. Furthermore, methods have been developed towards asymmetric [4+3] cycloadditions.[4,5] In addition, chiral derivatives can be accessed from desymmetrization of *meso* 8-oxabicyclo[3.2.1]octene compounds.[6]

Cleavage of the Unsaturated Double Bond, C6-C7, of the Oxabicyclo[3.2.1] System

Tetrahydropyrans are common features in many natural products and sugars. They can be accessed by cleavage of the unsaturated bond of the oxabicyclo[3.2.1] system.

Yadav and coworkers elaborated a strategy of asymmetric hydroboration for the desymmetrization and subsequent opening of 8-oxabicyclo[3.2.1]octene **2** in the asymmetric synthesis of the C(19)-C(25) polypropionate unit of Rifamycin.[7] Cleavage of the double bond, C6-C7, of bicyclic ketone **2** was performed in several steps. The sequence involves reduction and protection of **2**, asymmetric hydroboration of ether **3** with (+)-Ipc_2BH (Bis (isopinocampheyl) borane), PCC oxidation of the resulting alcohol **4**, and Baeyer-Villiger oxidation of ketone **5**. After a diastereoselective α-methylation, the system was opened by an exhaustive reduction that lead to the resolved acyclic compound **8,** which is relevant to **9,** the C(19)-C(25) segment of Rifamycin (Scheme 1-2). The sequence elaborated by Yadav et al. was exploited by Hoffmann et al., who proved the efficacy of the methodology in the enantioselective synthesis of various δ-valerolactones and polyacetate segments of natural products (Scheme 1-3).[8]

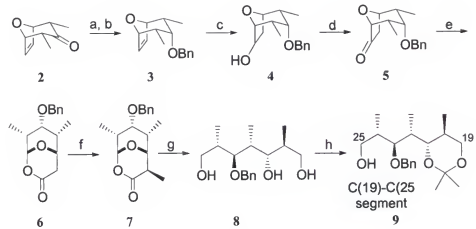

Scheme 1-2. Yadav's asymmetric synthesis of the C(19)-C(25) unit of Rifamycin. a) DIBAL-H, CH_2Cl_2, -10°C b) NaH, BnBr, THF, 65°C c) (+)-Ipc_2BH, -20°C, 24h, 96% (>99% ee) d) PCC, CH_2Cl_2, rt, 95% e) H_2O_2, SeO_2, *t*BuOH, reflux, 40% f) LDA, MeI, THF, -78°C g) $LiAlH_4$, THF, 0°C, h) 2,2-dimethoxypropane, P-TsOH, acetone, r.t.

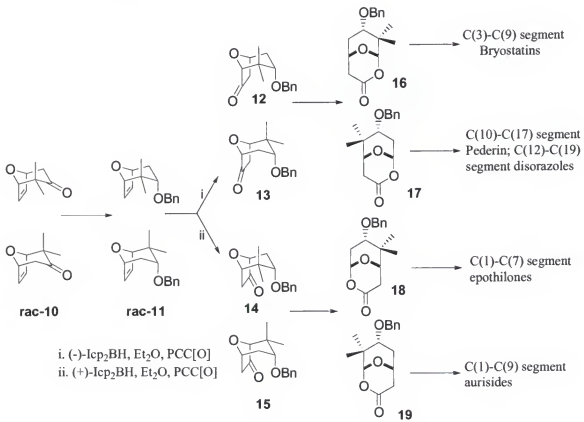

Scheme 1-3. Structural and stereochemical diversity from racemic oxabicyclo **10**

Hoffmann and coworkers demonstrated the utility of 8-oxabicyclo[3.2.1]octene derivatives as versatile scaffolds in the approach to numerous natural products containing the tetrahydropyran unit. These include Bryostatins,[9] Phorboxazoles,[10] Discodermolide,[11] Lasonolide A,[12] Spongistatin 1,[13] and mevinic acids[14] among others. They approached the tetrahydropyran unit by oxidative cleavage of the unsaturated double bond, C6-C7, of the system. In the approach to the Bryostatins, two strategies that involved the cleavage of the unsaturated double bond were employed. The C(1)-C(16) segment of the molecule was synthesized starting from 8-oxabicyclo[3.2.1]oct-6-en-3-one **1** and racemic 2,2-dimethyl-8-oxabicyclo[3.2.1]oct-6-en-3-one **10**.[9b]

To synthesize the C(1)-C(9) unit, Hoffmann et al. started with racemic 2,2-dimethyl-8-oxabicyclo[3.2.1]oct-6-en-3-one **10**. The synthesis of that segment involves the preparation of lactone **16** using the strategy developed by Yadav et al. (Scheme 1-3).[7] This protocol prepared the system for cleavage under standard basic conditions that resulted in the asymmetric tetrahydropyran **20**. Further manipulations including ring-opening with borontrifluoride and Claisen condensation afforded **23**, the C(1)-C(9) segment of the Bryostatins (Scheme 1-4).

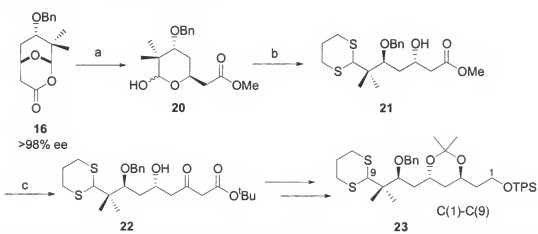

Scheme 1-4. Synthesis the C(1)-C(9) segment of the Bryostatins. a) K_2CO_3, MeOH, rt, 99% b) 2 equiv $HS(CH_2)_3SH$, 3 equiv $BF_3{\cdot}Et_2O$, $MeNO_2$, -20 to -15°C, 95% c) 5 equiv CH_3CO_2But, LDA, -78 to 0°C, 94%

For the synthesis of the C(10)-C(16) fragment, ring-opening of the *meso* oxabicyclic ketone **1** was performed by ozonolytic olefin cleavage. Tetrahydropyran **25**, the key intermediate in Hoffmann's synthesis of the C(10)-C(16) unit, was obtained in 5 steps in 35% overall yield from **1** (Scheme 1-5). The enantioselectivity of **25** was achieved by enzymatic desymmetrization of ketal **24**.

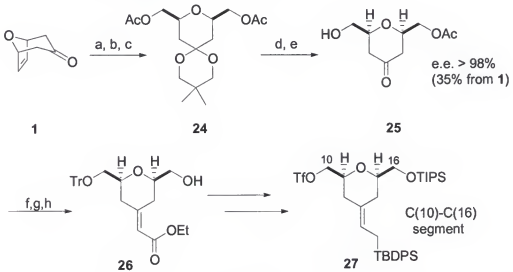

Scheme 1-5. Synthesis of the C(10)-C(16) unit of the Bryostatin. a) 2,2,5,5-tetramethyl-1,3-dioxane, cat. p-TsOH, 35-45 mm Hg, 50% b) i. O_3, $MeOH/CH_2Cl_2$, -78°C ii. $NaBH_4$, -20°C, 98% c) Ac_2O, cat 4-DMAP, py, r.t. 91% d) lipase PS, toluene/phosphate buffer (1:4) pH 7, r.t. 88% e) Acetone, cat. $Pd(CH_3CN)_2Cl_2$ r.t. 89% f) Trityl chloride, Et_3N, cat. 4-DMAP, CH_2Cl_2, r.t. g) K_2CO_3 5% H_2O in MeOH (79% two steps) h) ethyl diisopropoxyphosphonoacetate, NaH, toluene, -50 to -35 °C then -25°C (72%)

After various transformations including protection, deprotection and Horner-Wadsworth-Emmons olefination, tetrahydropyrone **25** was converted to **27**, the C(10)-C(16) fragment of the Bryostatins, (Scheme 1-5). Finally, coupling of the C(1)-C(9) segment **23** and the C(10)-C(16) unit **27** achieved the northern hemisphere of the Bryostatins **28** (Scheme 1-6).

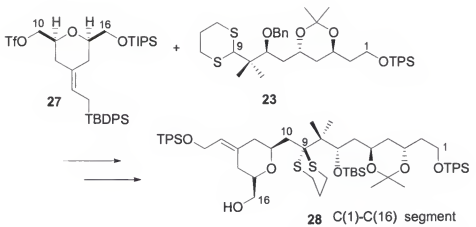

Scheme 1-6. Synthesis of the C(1)-C(16) segment of the Bryostatins

Cleavage of the Carbonyl and the α-Carbon, C3-C4, of the Oxabicyclo[3.2.1] System

Tetrahydrofurans can also be derived from oxabicyclo[3.2.1] systems. Tetrahydrofuran **33**, a key intermediate in the synthesis of the C-nucleoside showdomycin,[15] was synthesized by Simpkins and coworkers by cleavage of the C2-C3 bond of the bicyclic ketone **1** (Scheme 1-7).[16]

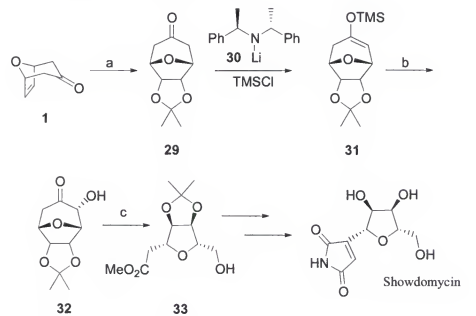

Scheme 1-7. Cleavage of C2-C3 of an oxabicyclo[3.2.1] from a chiral silyl enol ether. a) OsO_4, *t*BuOH, Et_2O, H_2O_2, acetone b) PhIO, $BF_3{\cdot}OEt_2$, H_2O, 67% c) $Pb(OAc)_4$, MeOH; then $NaCNBH_3$, 93%

The protocol involves the preparation of a chiral enol silane **31** with homochiral lithium amide **30**. Enol silane **31** was oxidized with PhIO (iodosobenzene) producing α-hydroxyketone **32** with the hydroxyl group in an equatorial position. Oxidative cleavage of recrystallized α-hydroxyketone **32** was effected by treatment with lead tetraacetate in methanol, followed by reduction with $NaCNBH_3$, in the same pot, yielding the C-nucleoside **33** with high enantiomeric excess (>98% ee).

Cleavage of the Carbon-Oxygen Bridgehead Bond, C1-C2, of the Oxabicyclo[3.2.1] System

Cleavage of the carbon-oxygen ether bond allows the access to functionalized seven-membered rings, avoiding entropically disfavored cyclization approaches to it. In addition, further cleavage of the seven-membered ring provides an efficient route to polysubstituted acyclic chains.

Also involving enolate formation, Grieco and Hunt performed opening at the bridgehead of an oxabicyclo[3.2.1] system.[17] Thus, enol ether **34**, generated from treatment of bicyclic ketone **2** with LDA, THF, HMPA and TBSCl, was mixed with 2.0 equiv. of 1-methoxy-1-(tert-buthyldimethylsiloxy)-ethylene **35** in a 4.0 M solution of lithium perchlorate in diethyl ether (LPDE) at room temperature affording cycloheptadienes **36** and **37** in a ratio of 4:1 in quantitative yields (Scheme 1-8).

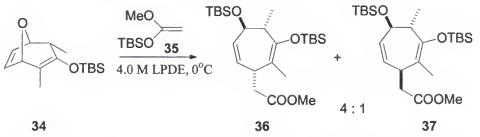

34 **36** **37**

Scheme 1-8. Ring opening of oxabicyclo[3.2.1] system with a silyl ketene acetal

Cycloheptadiene **36** was transformed into the C(19)-C(27) fragment **41** of Rifamycin S (Scheme 1-9). Grieco and Hunt also applied the protocol in the synthesis of the chiral C(19)-C(26) and C(27)-C(32) fragments of Scytophycin.[18]

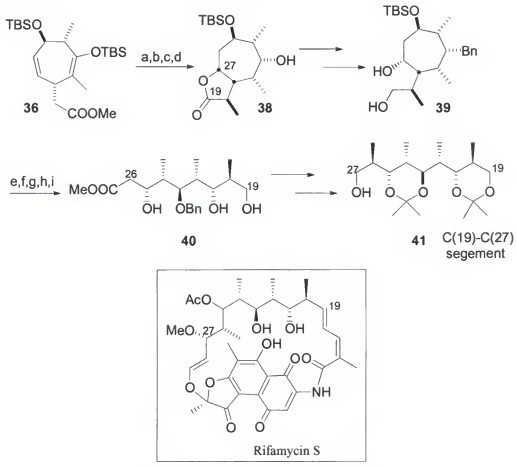

Scheme 1-9. Synthesis of C(19)-C(27) fragment of Rifamycin. a)TBAF,THF,HOAc b) $LiAl(OtBu)_3H$, THF, -20°C c) i. NaOH, THF, MeOH, H_2O ii. CO_2 iii. KI/I_2, 0°C d) Bu_3SnH, THF, AIBN, 60°C e) TESCl, 2,4,6-collidine, CH_2Cl_2, -78°C f) TPAP, NMO, CH_2Cl_2, 4h g) TBAF, HOAc, THF h) MCPBA, absolute EtOH i) K_2CO_3, MeOH, 0°C, 1h

Lautens[19] and Cha et al.[23-25]have also proven the utility of cleaving the carbon-oxygen bridgehead bond, C1-C2, of the oxabicyclo[3.2.1] system in the synthesis of natural products. Lautens and co-workers explored the reactivity of oxabicyclo[3.2.1] compounds toward nucleophilic addition, demonstrating that they can be opened with

reagents such as aluminum hydrides,[20] high order cuprates,[21] and organolithium[22] type-nucleophiles by an S_N2' mechanism. Examples are illustrated in Scheme 1-10.

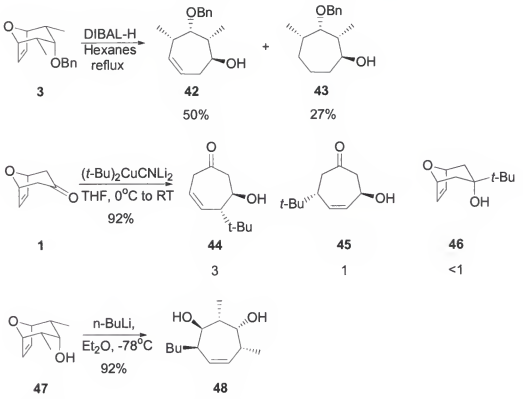

Scheme 1-10. Ring opening of oxabicyclo[3.2.1] compounds by nucleophilic additions.

Minor products derived from anti S_N2, such as **45** were also obtained when organocuprates were used as the nucleophile. Subsequent manipulations of cycloheptanol **42,** including ozonolytic cleavage, afforded the C(17)-C(23) unit of ionomycin (Scheme 1-11).

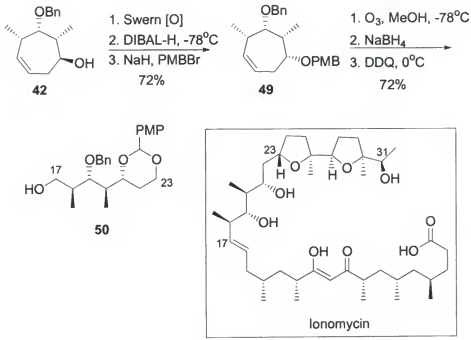

Scheme 1-11. Synthesis of the C(17)-C(27) segment of ionomycin

Cha et al. took advantage of the [4+3] cycloaddition to synthesize phorbol[26] and tropone-containing natural products, such as imerubrine[23], colchicine[24], and hinokitiol[25] from complex oxabicyclo[3.2.1] systems. Cha et al. employed Föhlish[27] and Mann[28] methods to cleave the carbon-oxygen ether bond of the oxabicyclic compounds. In his synthesis of the tropolone, hinokitiol, Moriarty's oxidation of cycloadduct **51** produced alcohol **52**, which was subjected to double elimination according to the procedures of Föhlish et al.[27] and Mann et al.[28] (Scheme 1-12).

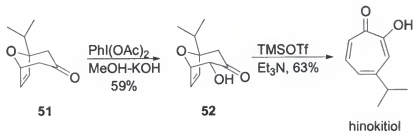

Scheme 1-12. Cha's synthesis of hinokitiol

The value of oxabicyclo[3.2.1] compounds in organic synthesis has been demonstrated by the examples presented above. This dissertation focuses on the use of olefin metathesis to cleave the unsaturated bond, C6-C7, of the 8-oxabicyclo[3.2.1]octene derivatives to generate a *cis*-2,6-disubstituted pyran moiety with two differentiated ends that can be useful to synthesize pyran-containing natural products.

Olefin Metathesis

Olefin metathesis[29] is a method that allows a redistribution of olefins. During the reaction two olefin partners are exchanged to give a new unsaturated carbon-carbon bond in the presence of a metal carbene complex. Since the discovery of the olefin metathesis in the mid 1950's, a large number of catalyst systems have been reported to initiate this reaction. However, it was not until the accepted metal carbene mechanism proposed by Chauvin that scientists were provided with a basis for the design and development of well-defined catalysts. Chauvin and Herisson[30] proposed a [2+2] cycloaddition between an olefin **53** and a metal alkylidine catalyst **54** to generate a metallocyclobutane intermediate **55**. The metallocyclobutane intermediate **55** undergoes cycloreversion resulting in a new olefin **56** and a new metal alkylidine **57**. A second [2+2] cycloaddition between **57** and **58**, followed by cycloreversion yields the metathesis product **60** and the turnover of the catalyst **61** (Scheme 1-13).

The development of well-defined catalysts promoted the steady increase of the olefin metathesis usage in organic and polymer chemistry. Some well-defined catalysts are presented in Figure 1-2.

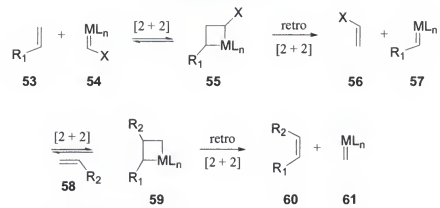

53 54 55 56 57

58 59 60 61

Scheme 1-13. Olefin metathesis mechanism

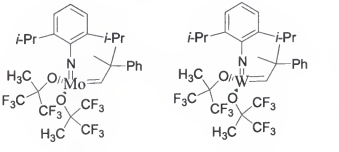

62 63 64

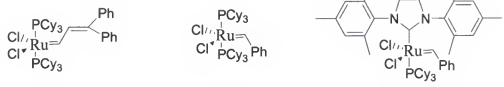

65 66 67

Figure 1-2. Selected olefin metathesis catalysts

Molybdenum and tungsten catalysts **62**, **63**, and **64** were proven to be very effective for this reaction. Basset and coworkers's catalyst **64** was tolerant to various functional groups such as silicon, phosphorous and tin; however, its efficiency varied according to the steric demand of the substrate.[31] Tungsten **62** and molybdenum **63** (Schrock's catalysts) presented high reactivity toward a broad range of substrates.[32] Catalyst **62** is a very useful catalyst for olefin metathesis; however, despite its high reactivity, **62** presents some drawbacks. These are extremely high sensitivity to air, and

moderate to poor functional group tolerance. Ruthenium catalysts **65-67** developed by Grubbs and coworkers[33-35] and co-workers overcame those problems. They were more tolerant to functional groups, reacting mainly with olefins in the presence of alcohols, aldehydes, amides and carboxylic acids. Metal alkylidine **65** was the first ruthenium catalyst developed by Grubbs et al.[33] Besides its stability and tolerance toward many functional groups, it was not as reactive as Schrock's molybdenum catalyst. Shortly after catalyst **65**, ruthenium catalyst **66** was reported to present a higher reactivity.[34] In the aim of finding a better catalyst, Grubbs et al. reported another ruthenium catalyst **67** in 1999.[35] Catalyst **67** exhibited higher reactivity, thermal stability and a lower rate of decomposition compared to metal alkylidine **66**. For this reason, **67** is commonly referred as "Super Grubbs" catalyst.[36] Today, metal alkylidines **62**, **66** and **67** are the most widely used catalysts for the olefin metathesis reaction. Our research involves mainly the usage of Grubbs catalyst **67**. Its mechanism of activity has been demonstrated to proceed by a "dissociative" pathway as depicted in scheme 1-14.[37]

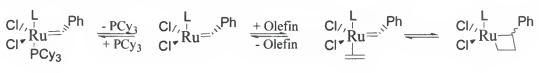

68 **69** **70** **71**

Scheme 1-14. Dissociative olefin metathesis mechanism

The 16-electron specie **68** generates a 14-electron complex **69** by the loss of a phosphine. This complex then associates with an olefin as in intermediate **70** that promotes the metallocyclobutane formation of **71** that will eventually generate the metathesis product and the catalyst turnover. One of the most fascinating aspects of the olefin metathesis is that several types of chemistry can be performed with the same catalyst depending on the reaction conditions and the nature of the substrate.

Types of Olefin Metathesis Reactions

There are five main variants on the olefin metathesis reaction. These are: a) ring-opening metathesis polymerization (ROMP) b) acyclic diene metathesis (ADMET) c) cross metathesis (CM) d) ring-closing metathesis (RCM) e) ring-opening cross metathesis (ROCM) (Scheme 1-15).

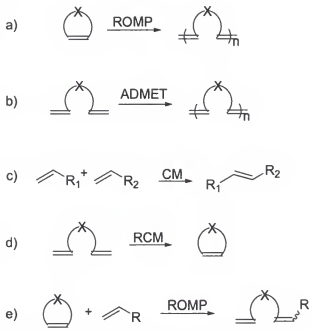

Scheme 1-15. Different types of olefin metathesis reactions

Ring-opening metathesis polymerization

Ring-opening metathesis polymerization (ROMP) marked the beginning of olefin metathesis, since olefin metathesis was discovered while examining the polymerization of olefins. In this reaction, driven by the release of ring strain, a monomer is opened by a metal alkylidine and the resulting intermediate reacts with another monomer initiating the propagation for polymerization. The success of this reaction has been described in several reviews.[38] The main advantage in the polymer chemistry is that well-defined catalysts allow for the realization of living polymerization. Thus, control of the

architecture and length of the polymer can be obtained.[39-40] This has many applications for the development of new materials.[41-42]

An area of research that has been growing in the last decade is the use of functionalized polymers as scaffolds for the delivery of drugs. ROMP provides a viable route to prepare polymeric scaffolds for the delivery of drugs by attaching the drug to a substrate that can undergo polymerization, such as norbornene. The anti-inflammatory and cancer preventive indomethacin **72** was attached to *exo*-5-norborneol **73** to form monomer **74** which can undergo polymerization (Scheme 1-16).[43]

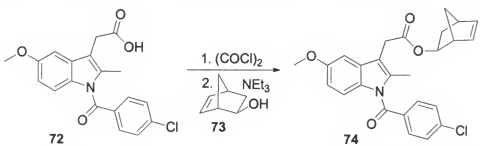

Scheme 1-16. Monomer preparation toward a functionalized polymeric scaffold for drug delivery

Acyclic diene metathesis

Acyclic diene metathesis (ADMET) is the acyclic cross metathesis of dienes or the acyclic version of ROMP. In this reaction the elimination of gaseous ethylene from the polymerization is believed to be the driving force of the reaction. In an example, biopolymers were created by Wagner and coworkers using ADMET in dienes that incorporated amino acid units in the backbone (Scheme 1-17).[44]

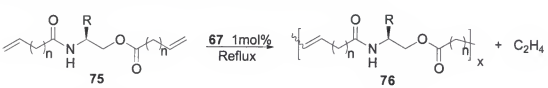

Scheme 1-17. Biopolymers from ADMET

Cross metathesis

Another type of olefin metathesis is the cross metathesis reaction (CM). In this reaction, the rearrangement of two olefins results in a new carbon-carbon double bond incorporating one carbon from each partner. The CM reaction is advantageous since it allows the synthesis of highly substituted olefins. One disadvantage, however, is the formation of unwanted self metathesis products. Another challenge is the control of geometry of the newly formed olefin (Scheme 1-18).

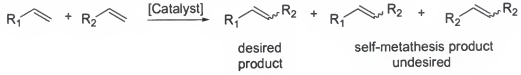

Scheme 1-18. Possible cross metathesis products

To overcome these problems it is necessary to determine a way to minimize self-metathesis, thus maximizing cross-coupling as well as improve the stereoselectivity of the reaction. Over the years researchers have worked on these problems. With the development of well-defined catalysts, cross metathesis has gained more attention as a viable tool in organic chemistry. In 1995, Crowe and coworkers showed the viability of acrylonitrile to undergo cross metathesis with a molybdenum based catalyst.[45] Although, the cross metathesis product was obtained in moderate yield, high *cis* selectivity was obtained and no self-metathesis product was observed (Scheme 1-19, entry 1). Crowe also showed that addition of steric bulk at the allylic position of the olefin promoted *trans* selectivity. This was demonstrated with a series of allyl silanes (Scheme 1-19, entries 2, 3).[46] Blechert et al. observed the same with substituted allylic amines, reporting the first example of exclusively trans selective CM (Scheme 1-19, entries 4, 5).[47] The homodimerization was controlled by the electronic and steric parameters of one of the

alkene partners in the CM reaction. Furthermore, the high reactivity and tolerance to functional groups allowed catalyst **67** to give CM products of disubstituted olefins (Scheme 1-19, entry 6)[48] and α,ß-unsaturated carbonyls[49] or acrylic amides[50] (Scheme 1-19, entries 7, 8). One important application of the CM reaction is that it allows for the preparation of reagents by providing different highly functionalize olefins. Products derived from CM of allyl silanes (Scheme 1-19, entries 2, 3) are useful for silane addition to carbonyl compounds (Sakurai reaction). Also, products from the CM reaction of vinyl boronates[51] with alkenes are useful for Suzuki couplings (Scheme 1-20, entries 1, 2), while CM of allyl boronates[52] with alkenes are analogous to allyl silane compounds, and can be added to aldehydes and ketones (Scheme 1-20, entries 3, 4).

Ring-closing metathesis

A well-recognized type of metathesis reaction is the ring-closing metathesis (RCM). RCM has found the widest application in synthesis, being a key step in various total syntheses. The release of volatile ethylene is believed to drive this reaction. Its value consists in being a reliable method for the formation of small, medium and large membered-rings. Examples of RCM abound in literature. RCM have been employed in the synthesis of carbohydrates,[53] numerous heterocycles, and peptides.[54] Perhaps, the major utility of this application has been found in the synthesis of natural products. RCM was used at the early stage of the synthesis of a marine natural product dysinosin A (Scheme 1-21).[55] Meyers and co-workers reported the first successful synthesis of (-)-griseoviridin using RCM strategy in a macrocyclization that led to the 20-membered ring antibiotic (Scheme 1-22).[56]

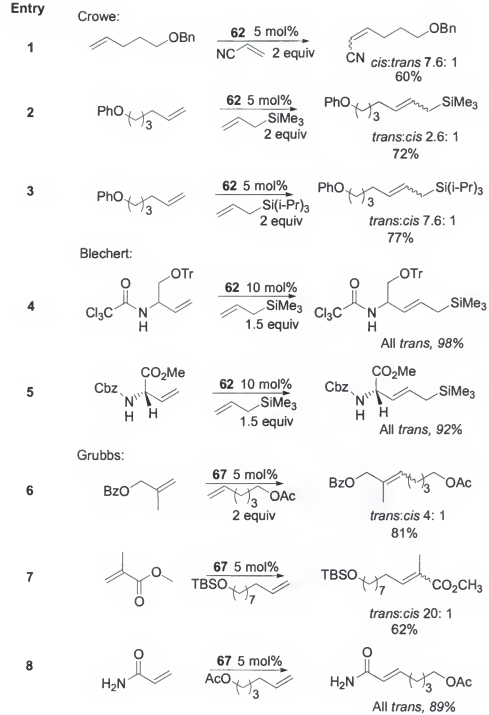

Scheme 1-19. Examples of intermolecular Cross Metathesis

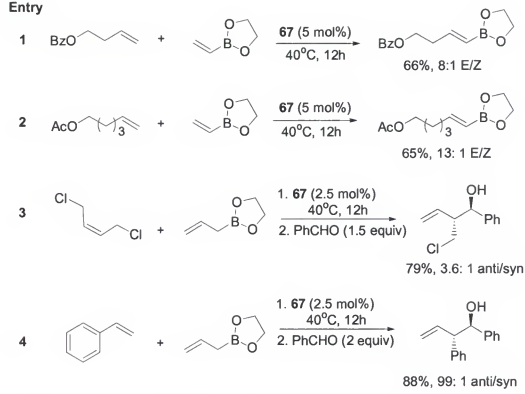

Scheme 1-20. Cross metathesis of vinyl and allyl boronates

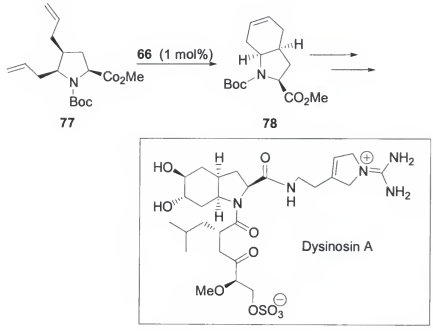

Scheme 1-21. Application of RCM in the synthesis of Dysinosin A

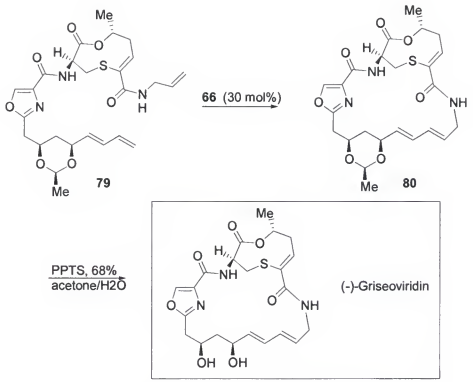

Scheme 1-22. Application of RCM in the synthesis of (-)-Griseoviridin

In addition, RCM involving alkynes has been reported. One example is presented in scheme 1-23. Pyroglutamic acid **81** was converted to the enyne **82**, which underwent RCM with ruthenium carbene **66**. Compound **83** was further elaborated to yield the alkaloid (-)-Stemoamide.[57]

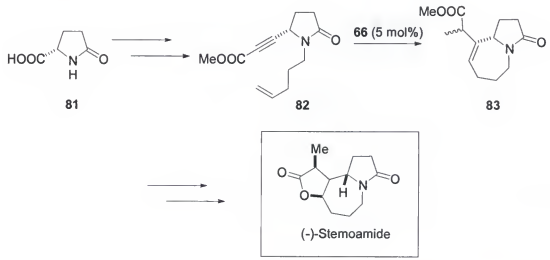

Scheme 1-23. RCM with an alkyne at the early stage of the synthesis of (-)-stemoamide

Ring-opening cross metathesis

Ring-opening cross metathesis (ROCM) is a variant of cross metathesis where one of the olefin partners is a cyclic olefin. In this type of metathesis, the release of ring strain drives the reaction. ROMP is avoided by performing the reaction under diluted conditions with excess of the acyclic olefin partner. This olefin metathesis variant has not received as much attention as the RCM. This is because it is necessary to have efficient control of the regio- and stereoselectivity in order to make this strategy synthetically useful. Therefore, ROCM has been limited to unsubstituted or symmetric cyclic olefins. Regiochemical issues arise when the starting cyclic olefin is not symmetrically substituted. For example, whereas ROCM of symmetric bicyclic alkene **84a** with a terminal alkene can produce only one product (**85 = 85'**, X = H), an unsymmetrical bicyclic alkene such as **84b** can produce two regioisomers **86** and **87** (X ≠ H) (Scheme 1-24).

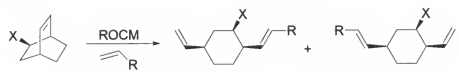

84a x = H
84b x ≠ H

85
86

85'
87

Scheme 1-24. Possible regioisomers from unsymmetrical bicyclic alkenes

Early successful examples using well-defined olefin metathesis catalyst were disclosed by Snapper et al. in 1995. He reported the ROCM of various cyclobutenes with a series of terminal alkenes, using vinylidene catalyst **65** (scheme 1-25).[58] His studies included the first examples of regioselectivity in the ROCM of unsymmetrical bicylic systems. Whereas symmetric cyclobutenes gave a ratio of stereoisomers favoring the Z-alkene, asymmetric cyclobutenes gave two regioisomers, where the more hindered alkene

was preferred (scheme 1-25, entry 2 and 3). Snapper explained that the products distribution was consistent with an alternating alkylidene mechanism, where the alkylidene **A,** generated from the reaction of the terminal olefin and the catalyst, was preferred over the methylidene **B** as the active catalyst in the reaction (path I was favored over Path II, scheme 1-26). In addition, Blechert et al.[59] and Arjona et al.[60] reported regioselective ROCM examples of bicyclic alkenes (Scheme 1-25, entries 4-6). In their studies, the less hindered alkenes were obtained. Furthermore, Szeimies and Feng disclosed a highly regioselective ROCM of various 1-arylcyclobutenes with allyltrimethylsilane and 1-octene. In this case, the less hindered regioisomer was obtained as the only product (Scheme 1-25, entries 7-8).[61]

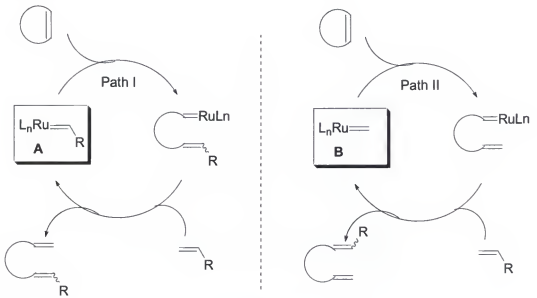

Scheme 1-26: A selective ROCM process based on the identity of the propagating alkylidene

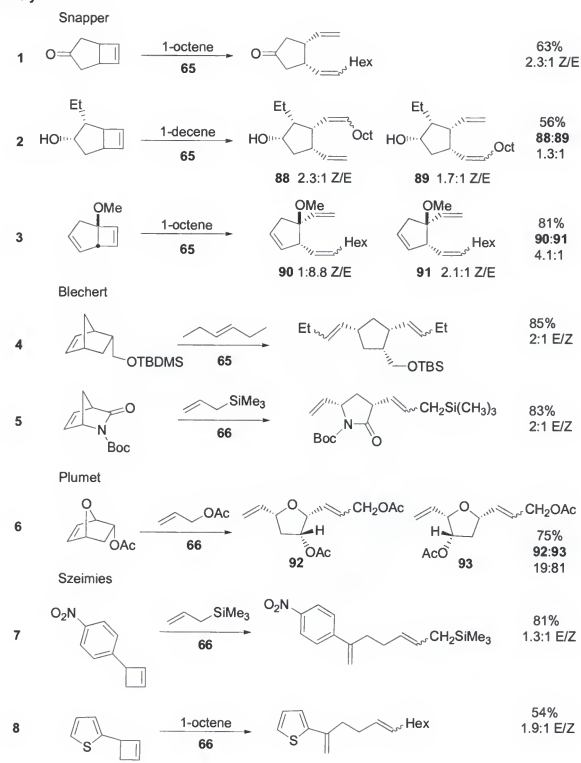

Scheme 1-25. Examples of ROCM reaction on symmetric and unsymmetrical bicyclic systems

Although regiochemical issues have limited the use of ROCM to symmetrical cyclic systems in organic synthesis, examples have demonstrated the possibility of obtaining good regioselectivity in the ROCM reactions. However, additional efforts are required to evaluate the steric and electronic influence of this issue.

Tandem Metathesis

Tandem or domino metathesis reactions involve more than one transformation in a sequential order in one pot. They are desired because they can provide complex structures in fewer steps. Tandem metathesis can be defined as the combination of two or more consecutive metathesis operations. The driving force for these consecutive operations is attributed to either the loss of ethylene or ring-strain release. These reactions need to be carried out at high dilution to promote intramolecular rearrangement over olygomer formation.

Grubbs et al. reported double ring-closing metathesis of dienynes, catalyzed by ruthenium metal complex **65,** producing fused bicyclic [n.m.0] rings.[62] In an example, reaction of compound **94** with catalyst **65** produces the metal alkylidine **95**, which undergoes RCM, forming a new metal alkylidine **96** which is able to undergo a second RCM yielding the fused ring **97** (Scheme 1-27). Bulky substituents at the triple bond can significantly slow down the reaction or cause no reaction to occur.

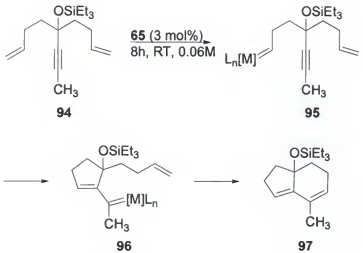

Scheme 1-27. Tandem metathesis with a dienyne

Blechert et al. reported the first total synthesis of (-)-halosaline using domino metathesis with ruthenium catalysts **66**.[63] Employing the combination of RCM/ROM/RCM operations, compound **101** was built in a single operation from **100** (Scheme 1-28).

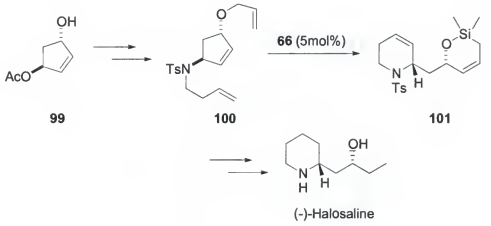

Scheme 1-28. Total synthesis of (-)-halosaline

In another example, Arjona and Plumet et al. reported the combination of ROM/RCM/CM with 2-azanorbornenones **103** toward the synthesis of 1-azabicyclic γ-lactam compounds **104** in modest yields 55-65% (Scheme 1-29).[64] The domino metathesis was catalyzed by ruthenium complex **66**.

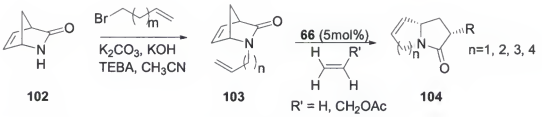

Scheme 1-29. Tandem ROM/RCM/CM of 2-azanorbornenones

Cyclized product **104** was observed with n = 2 or 3. With n = 1, 4 ROM/CM took place affording **110**. The distribution of the products is explained based on the mechanisms depicted in scheme 1-30.

There are two different pathways (A and B) that lead to either product **104** or **110**. If the initial metathesis occurs at the terminal olefin (path A), the formed metal alkylidine **105** undergoes intramolecular RCM followed by CM yielding the desired lactam **104**. On the other hand, if initial metathesis occurrs at the internal olefin, two regioisomers can be formed giving rise to alkylidines **109a** and **109b**. Alkylidine **109a** can not undergo RCM, but instead undergoes CM with a terminal alkene yielding **110**, whereas alkylidine **109b** can give rise to the lactam **104**. Nonetheless, compound **110** can be converted to **104** by a separate RCM reaction.

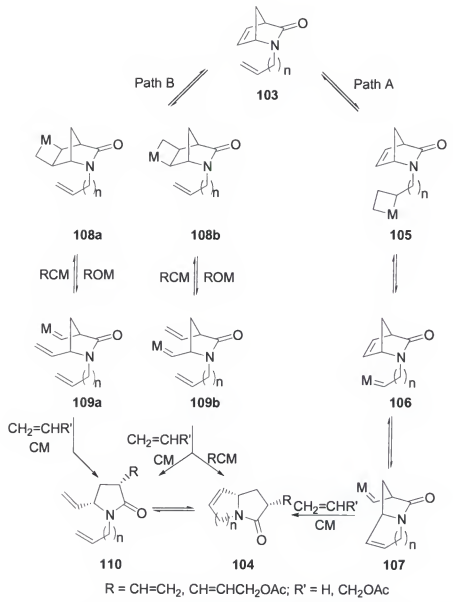

Scheme 1-30. Regioselctivity of ROM/CM of 2-substituted 2-azanorbornenones

Catalytic Asymmetric Olefin Metathesis

The latest achievement in olefin metathesis is the possibility of getting chiral molecules from racemic substrates with the development of chiral metathesis catalysts. The first chiral catalysts were derived from Schrock molybdenum alkylidene **62** (Figure 1-3).[65-67]

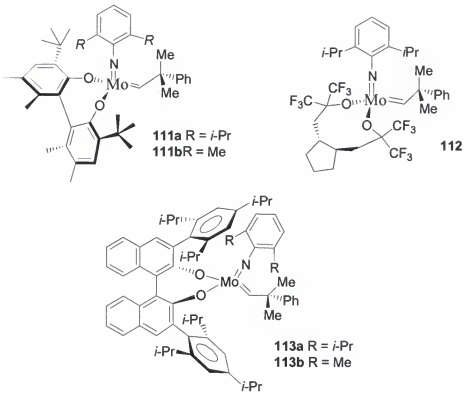

Figure 1-3. Some Asymmetric Olefin Metathesis Catalysts

In 1993, Schrock et al. reported the first asymmetric olefin metathesis catalyst **111a** for the synthesis of chiral polymers by ROMP.[65] In addition to that publication, reports on the use of asymmetric olefin metathesis catalysts concentrated on the asymmetric ring-closing metathesis (ARCM) reaction. The first report on ARCM was disclosed by Grubbs and Fujimura on the kinetic resolution of various dienes using asymmetric ruthenium catalyst **112**.[66] Poor enantioselectivity was observed by these workers; an example is presented in scheme 1-31, entry 1. Starting with the pioneer work presented by Grubbs, Hoveyda and Schrock studied a series of asymmetric molybdenum-based catalysts, **111** and **113**, in the kinetic resolution of dienes (Scheme 1-31, entries 2-5).[67]

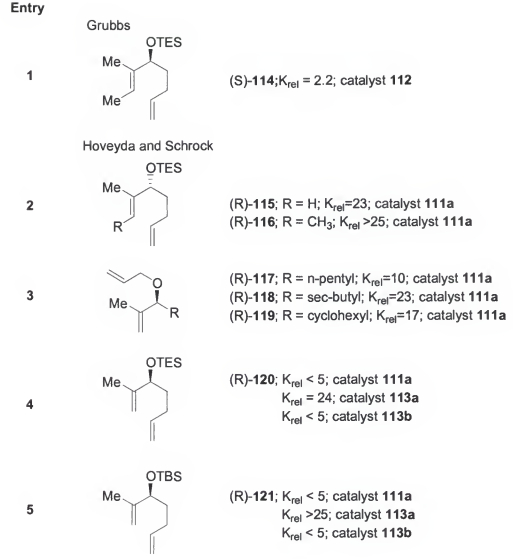

Scheme 1-31. Kinetic resolution of dienes with chiral Mo-based catalyst

Regardless of the good enantiocontrol observed with the chiral catalyst **111a**, they concluded that it was not possible to generalize which catalyst provide the best enantiocontrol. For compounds **120** and **121,** catalyst **113a** provided the highest enantioselection. Thus, they highlighted the importance of testing a set of chiral catalysts per substrate to decide which one gives the best enantiocontrol. The impact of ARCM in organic synthesis was observed in the desymmetrization of achiral molecules. Two examples are illustrated in scheme 1-32.

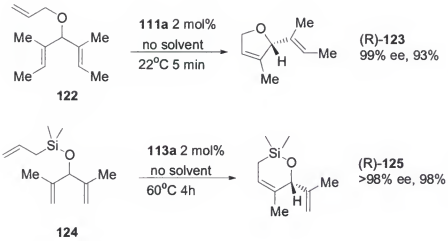

Scheme 1-32. Desymmetrization of achiral trienes

Thus, substrates **122** and **124** were transformed to optically enriched compounds **123** and **125** respectively without the need of solvent. The absence of homodimers when these reactions were performed neat indicates the high degree of catalyst-substrate specificity in these reactions.[68] The ARCM strategy was utilized in the enantioselective total synthesis of *endo*-brevicomin by the desymmetrization of achiral triene **126** employing chiral catalyst **111a** (Scheme 1-33).[69]

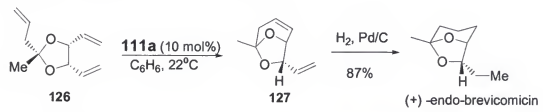

Scheme 1-33. Application of Mo-catalyzed ARCM to the synthesis of endo-brevicomin

In addition to the ARCM, several examples on the tandem AROM/CM were reported. Chiral catalyst **111a** gave excellent enantioselection (92-99% ee) in the tandem AROM/CM of various substrates. Two examples are illustrated in scheme 1-34.

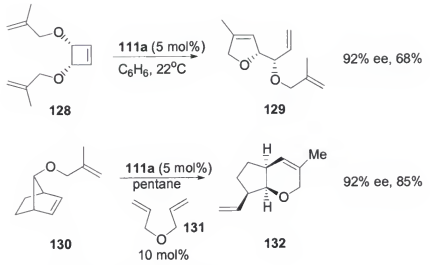

Scheme 1-34. Mo-catalyzed tandem AROM/RCM

The reaction of **128** with catalyst **111a** generates the heterocycle triene **129** in 92% ee and 68% yield.[70] To generate compound **132** from bicycle **130**, diallyl ether **131** was necessary.[71] Based on earlier mechanisms, Schrock explained that reaction of **131** with **111a** led to the formation of the chiral Mo-methylidene complex (vs Mo-neophylidene), which reacted with the sterically hindered norbornyl system **130** to initiate the catalytic cycle.

Tandem AROM/CM has also been explored with a series of norbornyl substrates. As depicted in scheme 1-35, chiral catalyst **111a** catalyzed the tandem AROM/CM reaction of norbornene systems with allyl silane or styrene. Although the yields were moderate, the enantioselectivity was high.[72]

To address the issue of a more practical and accessible chiral catalyst, in 2001 Hoveyda and Schrock et al. reported a new chiral molybdenum type catalyst **139** (scheme 1-36).[73]

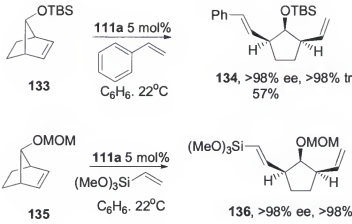

Scheme 1-35. Mo-catalyzed tandem AROM/CM toward enatioselective functionalized cyclopentanes

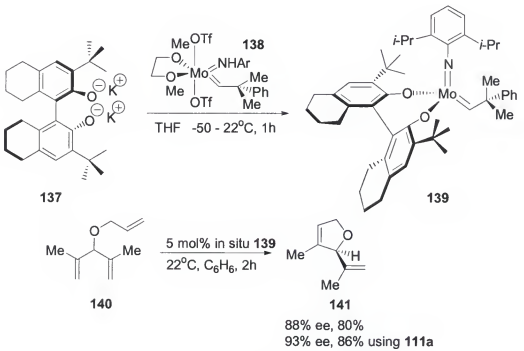

Scheme 1-36. In situ preparation and utility of chiral catalyst **139**

This catalyst exhibited the properties of a biphenolate-based complex such as **111** and binaphtholate system such as **113,** which were proven to be efficient earlier, thus leading to the expection that catalyst **139** would be more suitable for a wide range of substrates. The advantage of this catalyst relies on its easy preparation from commercially available reagents. The catalyst can be used in-situ without the need of

purification, and is air stable. They also reported a supported chiral Mo-catalyst for olefin metathesis that did not exhibit much activity.[74]

Chiral ruthenium-based olefin metathesis catalysts were also developed. Grubbs et al. reported the first chiral Ru-based catalyst **144**.[75] As in the previous reports, the enantioselection depended on the substrates. The highest ee reported in the study was 90% ee (scheme 1-37). They reported that the enantioselection was increased by the addition of NaI.

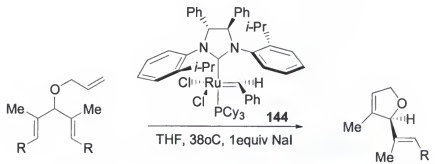

142a R = H
142b R = Me

143a 39% ee, 22%
143b 90% ee, 82%

Scheme 1-37. ARCM with Grubbs's Ru-based chiral catalyst

More recently, Hoveyda and coworkers developed a new ruthenium chiral catalyst **145**.[76] This new catalyst was reported to be air stable and recyclable besides promoting high enantioselectivity, up to 98% ee, (Scheme 1-38).

There is no doubt that the olefin metathesis will remain as an area of continuing interest with the development of more olefin metathesis catalysts.

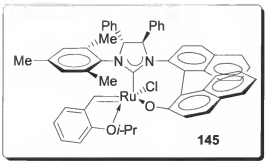

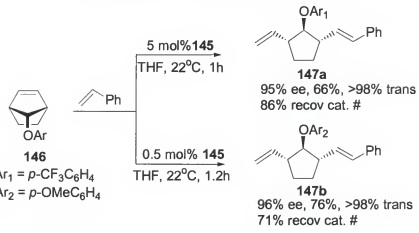

Scheme 1-38: Air stable Ru-based catalyst in tandem AROM/CM

Since latrunculin B was the target chosen to apply our methodology of ring-opening metathesis of 8-oxabicyclo[3.2.1] systems to generate pyrans, the next segment presents a brief history of the Latrunculins.

The Latrunculins

Two toxins, namely Latrunculin A and Latrunculin B, were isolated from the Red Sea sponge *Latrunculia Magnifica* (keller) by Kashman et al. in 1980.[77] The *Latrunculia Magnifica* is sponge that enjoys freedom from predation because it secrets a reddish fluid that causes fish to flee. Furthermore, squeezing this sponge in an aquarium is lethal to fish. The fluid causes them agitation, followed by hemorrhage, loss of balance and the death within 4 to 6 min.[78] The interesting biological activities of this sponge lead to the isolation, purification and characterization of the above mentioned toxins.

The structures of Latrunculin A and B were determined by spectroscopic methods and X-ray difraction.[77,79] The Latrunculins were the first marine macrolide known to possess 14 and 16 membered-rings and the first natural products found to contain a 2-thiazolidinone moiety. The biological interest of these molecules arises from the reversible changes in the cell morphology, disruption of the microfilament organization and inhibition of the cytoskeletal protein actin polymerization.[78a]

In 1985, Kashman et al. reported the first synthetic approach towards the synthesis of the Latrunculin synthon by the preparation of the bicyclic 2-thiazolidinone-tetrahydropyran **90** (Scheme 1-50), as well as isolation of two new toxins from the same sponge, Latrunculin C and Latrunculin D.[79] In 1989, he reported the isolation of another congener, Latrunculin M, and the preparation of Latrunculin C and M from Latrunculin B.[80] To date, two total syntheses of Latrunculin B as well as Latrunculin A have been reported. The first total synthesis of Latrunculin B was reported by Smith and coworkers in 1986.[81] The other total synthesis was elaborated by Fürstner and coworkers in 2003.[82] Latrunculin A total syntheses were independently completed by Smith[83] and White[84] in 1990.

Total Syntheses of Latrunculin B

Smith's total synthesis

Smith's synthesis was achieved in a convergent and stereocontrolled route of 14 steps in 2% overall yield.[81] Smith's retrosynthetic analysis is depicted in Scheme 1-39. Early in the synthesis, Smith connects the thiazolidinone moiety **152** to ortho ester **151** by an aldol reaction that generates **150**. An interesting structural reorganization occurs upon exposure of the new ortho ester **150**, to tosic acid which leads to the pyran **148**. According to Smith, the skeletal rearrangement involves hydrolysis of the ortho ester **150**

to give a hydroxy ester intermediate **153**, which in the presence of methanol forms the mixed methyl ketal **154** (Scheme 1-40). Completion of the synthesis is accomplished by reduction of ester **154** with DIBAL, a Wittig reaction that connects the advance intermediate **148** with the northern hemisphere of the molecule **149**, and an inverted Mitsunobu macrolactonization. The northern hemisphere of the molecule, the Wittig reagent **149**, was prepared in 5 steps in 54% overall yield (Scheme 1-41).

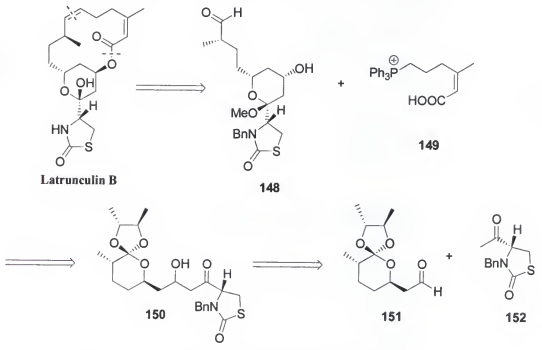

Scheme 1-39. Smith's retrosynthetic analysis of Latrunculin B

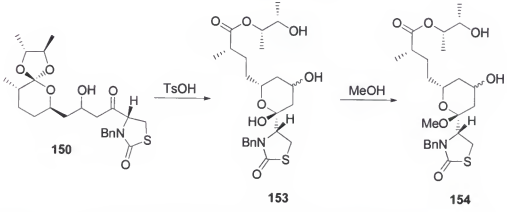

Scheme 1-40. Acid catalyzed formation of the pyran moiety in Smith's synthesis of Latrunculin B

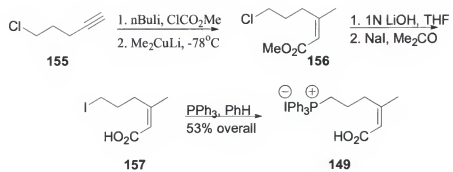

Scheme 1-41: Synthesis of the northen hemisphere of the Latrunculin B molecule.[7]

Fürstner's total synthesis

Fürstner assembled the molecule using aldol chemistry, esterification, ring-closing alkyne metathesis and Lindlar reduction as the key reactions. [82]

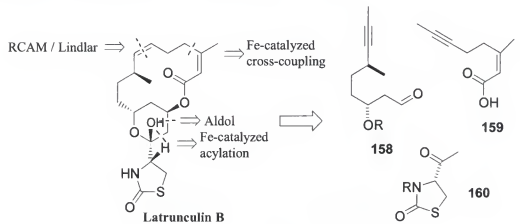

Scheme 1-42. Fürstner's retrosynthetic analysis of Latrunculin B

Reaction of building blocks **158** and **160** produces aldol product **161**, which under acid-catalyzed conditions rearranged to form pyran **162**. Compound **162** was then reacted with **159** to produce **163,** which upon alkyne metathesis, Lindlar reduction, and deprotection gave the target molecule, Latrunculin B (Scheme 1-43). The total synthesis which comprised 16 steps as the longest sequence was performed in 6% overall yield.

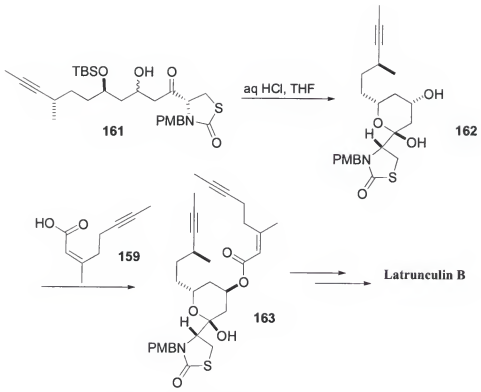

Scheme 1-43. Fürstner's synthesis of Latrunculin B

Total Syntheses of Latrunculin A

Smith's total synthesis

Smith's total synthesis of Latrunculin A involves the same common intermediate **150** previously used in his synthesis of Latrunculin B (Scheme 1-44).[83] However, the nitrogen atom had to be protected as a PMB (*para*-methoxybenzyl) rather than a benzyl group due to interference of the sensitive diene moiety not present in Latrunculin B at the time of its deprotection. Latrunculin A was then completed in an analogous manner to the synthesis of Latrunculin B by a Wittig reaction that connects the common intermediate **150** with the northern hemisphere of the molecule following the inverted Mitsonubu macrolactonization. The northern hemisphere of Latrunculin A and B is the differing point in these molecules. The preparation of the northern hemisphere of Latrunculin A (**164**) took 10 steps and was obtained in 34% overall yield (scheme 1-45).

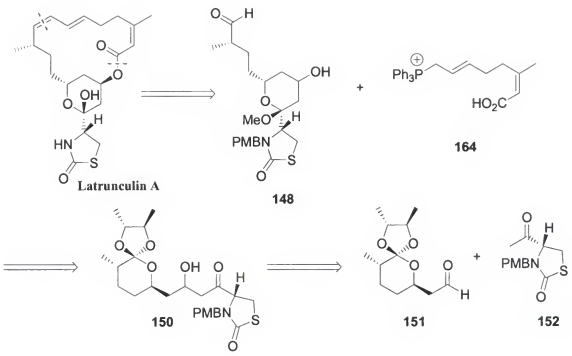

Scheme 1-44: Smith's retrosynthetic analysis of Latrunculin A

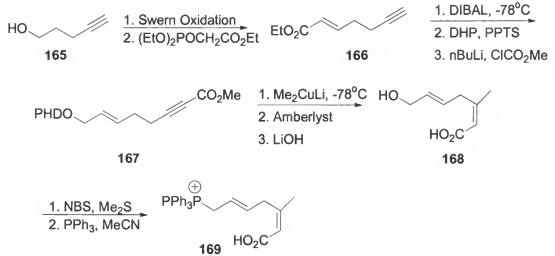

Scheme 1-45: Synthesis of the northern hemisphere of Latrunculin A molecule

White's total synthesis

White's total synthesis of Latrunculin A was designated to exemplify his methodology towards (E,Z)-1,3-dienes that involves tandem addition of an enolate

dianion to a dienylphosphonium salt following a Wittig reaction of its derivative with an aldehyde.[84] The target was sectioned in three principal subunits presented in scheme 1-46.

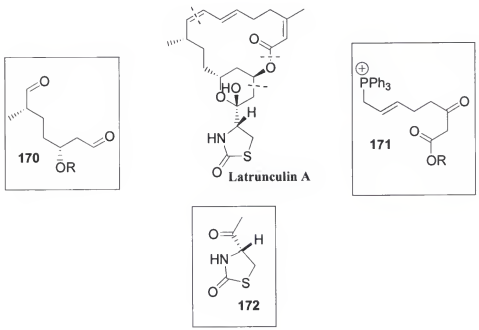

Scheme 1-46. Principal subunits in White's total synthesis of Latrunculin A

Fragment **170** was derived from the union of epoxide **173** and sulfone **174** (scheme 1-47). Aldehyde **176** was employed in his novel methodology to form **183** in scheme 1-48.

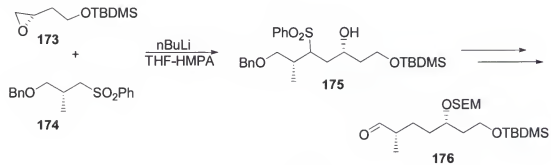

Scheme 1-47. Construction of segment **170** in White's total synthesis of Latrunculin A

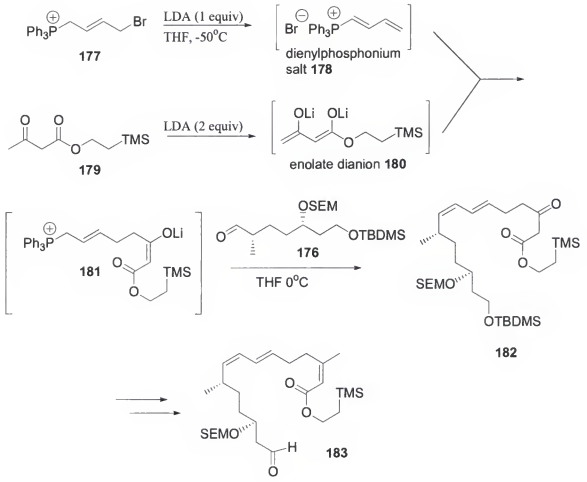

Scheme 1-48. Construction of segment 171 in White's total synthesis of Latrunculin A

Condensation of intermediate **183** with the (R)-4-acetyl-2-oxothiazolidine **172** proceeded without the need to protect the nitrogen atom. This condensation produced an epimeric mixture of the alcohols **184**. Selective deprotection of the SEM ether and exposure of the resulting diol to acidic methanol produced separable ketals **185** and **186** (Scheme 1-49). Cleavage of the ester of compound **185** followed by a Mitsonubu reaction, and hydrolysis afforded the natural compound Latrunculin A in 26 steps as the longer linear sequence in 0.9 % overall yield. In a parallel sequence, ketal **186** was converted to 15-epilatrunculin A.

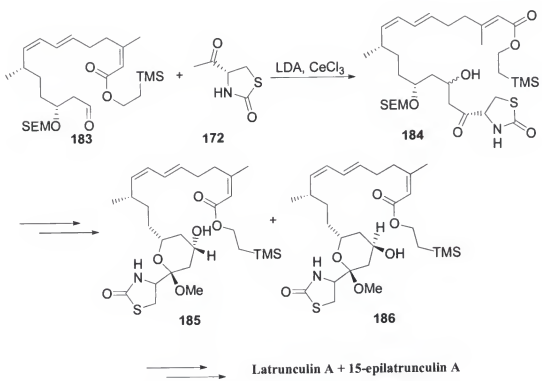

Scheme 1-49. Completion of White's total synthesis of Latrunculin A

Kashman's Approach to the Latrunculin Synthon[79]

Kashman's approach to the Latrunculin synthon started with L-cysteine **189**, which by reaction with phosgene afforded a thiazolidinone moiety. After protection of the thiazolidinone nitrogen atom by benzylation, the ester moiety was converted to an acid chloride with thionyl chloride affording **188**. Stille coupling of the acid chloride with the siloxy stannane yielded **189**, which produced the bicyclic 2-thiazolidinone-tetrahydropyran **190** after removal of the TBS protecting group and partial hydrogenation over Lindlar's catalyst (Scheme 1-50).

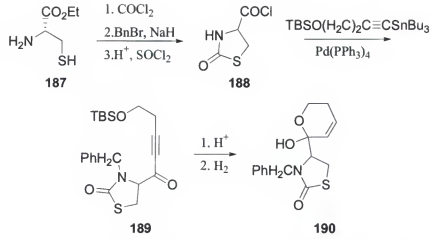

Scheme 1-50. Kashman's synthetic approach towards the Latrunculin synthon

Kashman's Synthesis of Latrunculin M and C[79,80]

From the same sponge from which Latrunculin A and B were isolated, three additional marine toxins were obtained by Kashman. These toxins are Latrunculin C, D and M, which are presented in Figure 1-4.

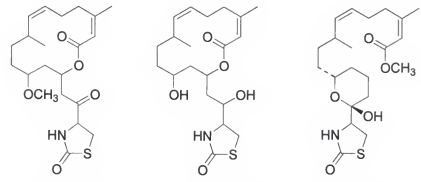

Latrunculin C[5,6] **Latrunculin D**[5] **Latrunculin M**[6]

Figure 1-4. Latrunculin C, D and M

Kashman et al. converted Latrunculin B to Latrunculin C and its 15-epilatrunculin C by reduction with sodium borohydride.[79] He also prepared Latrunculin M, a minor component of the *L. Magnifica* sponge, from Latrunculin B in a four step sequence (Scheme 1-51).

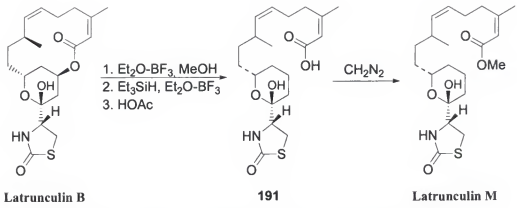

Latrunculin B **191** **Latrunculin M**

Scheme 1-51 Kashman's synthesis of Latrunculin M from Latrunculin B

CHAPTER 2
RESULTS/DISCUSSION

Intermolecular Ring-Opening Cross Metathesis (ROCM)

Our research focused on the synthesis of the tetrahydropyran moiety using ruthenium-based olefin metathesis on oxabicyclo[3.2.1]octene derivatives. Initial investigations centered on the study of the parent compound 8-oxabicyclo[3.2.1]oct-6-en-3-one[3] (**1**). The intermolecular ring-opening metathesis of **1** was explored with a series of electronically different terminal alkenes (Scheme 2-1).[85-87]

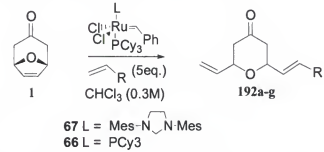

Scheme 2-1. ROCM of 8-oxabyciclo[3.2.1]oct-6-en-3-one 1 with terminal alkenes

Table 2-1. ROCM of 8-oxabyciclo[3.2.1]oct-6-en-3-one 1 with terminal alkenes[85,86]

Pyran	Alkene	-R	Catalyst	Yields (%)
192a	Styrene	-Ph	**67**	83
192b	2-bromostyrene	-*o*-BrPh	**67**	65
192c	1-hexene	$-(CH_2)_3CH_3$	**66**	89
192d	allyl bromide	$-CH_2Br$	**67**	71
192e	4-bromo-1-butene	$-CHCH_2Br$	**67**	72
192f	methylacrilate	-CO2Me	**67**	33
192g	acrylonitrile	-CN	**67**	10

The reaction was highly selective for the formation of the E-alkene and demonstrated the correlation between the alkene used and the reaction yields. The yields were better when electron rich alkenes were used rather than electron poor alkenes.

Literature reports support the limited reactivity of electron poor alkenes in cross metathesis.[46,88] Thus, electron rich alkenes afforded the highest yields.

Another observation was the increment of reactivity of the system when the hybridization of the carbonyl group was changed from sp^2 to sp^3.[85,86] This was revealed in attempts to improve the yield of the reaction. Though the yields were good (up to 83% with styrene as the donor alkene), the reactions were not reaching completion. Studies demonstrated that the reaction reached equilibrium after a certain amount of starting material was consumed. To drive the reaction to completion, the addition of a set of 1,3-diaxial interactions in the reaction intermediate (**194**) was proposed. This was done by placing a bulky group at C3 in the *endo* position (Scheme 2-2).[85,86] The idea consisted of creating unfavorable steric interactions between the bulky group and the two appendices of the opened intermediate, thereby driving the reaction to product, and avoiding reversibility.

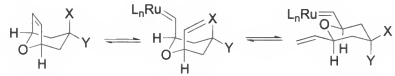

1 = X = Y = O
192 = X = OTBS, Y = H
193 = X = H, Y = OTBS

194a = X = Y = O
194b = X = OTBS, Y = H
194c = X = H, Y = OTBS

195a-c

Scheme 2-2. Reversibility of the ROCM reaction

As predicted, the consumption of the starting material was complete; however, the yields decreased dramatically (Table 2-2).[85,86] A competitive reaction was occurring, namely the ring-opening metathesis polymerization.

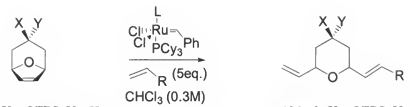

Scheme 2-3. ROCM of the reduced derivatives[85,86]

Table 2-2. ROCM of the reduced derivatives[85,86]

Pyran	Alkene	-R	Catalyst	Yields (%)
196a	Styrene	-Ph	**67**	60
196b	2-bromostyrene	-*o*-BrPh	**67**	18
196c	1-hexene	$-(CH_2)_3CH_3$	**66**	63
196d	allyl bromide	$-CH_2Br$	**67**	62
196e	4-bromo-1-butene	$-CHCH_2Br$	**67**	56
196f	methylacrilate	-CO2Me	**67**	0
197a	Styrene	-Ph	**67**	67
197b	1-hexene	$-(CH_2)_3CH_3$	**66**	75

Exo-silyl ether **193** showed that despite the absence of the large group in the axial position, the reactivity was enhanced. Thus, the *exo*-silyl ether gave results comparable to the *endo*-silyl ether using styrene and 1-hexene as the donor alkene in the metathesis reaction (Table 2-2, last two entries).

Based on these observations it was understood that a change in hybridization at C3, and not the position of the bulky silyl ether, was responsible for the change in reactivity. In an attempt to provide a rationale for whether the hybridization, steric hindrance or electronic effects were affecting the reactivity of the system, further studies were undertaken.

Kinetic Studies

Kinetic experiments were conducted with a series of 8-oxabicyclo[3.2.1]octene derivatives differing by the functional group placed at C3. The substituent placed at C3 varied according to three categories: oxygen in the *endo* position (ether **192**, alcohols **201**

and **202**, and ketal **203**), hydrogen in the *endo* position (ether **193**, methylene **204** and alcohol **205**), and sp^2 hybridization (ketone **1**, oxime **199** and exo-methylene **200**). The plan was to generate a relative trend of the reaction rate among the bicycle derivatives to have a general idea of the effects of the remote substituents in the reactivity of the system.

sp^2 hybridized:

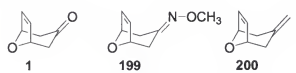

1 **199** **200**

sp^3 hybridized with electron rich oxygen in the *endo* position:

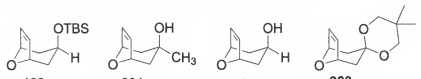

192 **201** **202** **203**

sp^3 hybridized with hydrogen in the *endo* position:

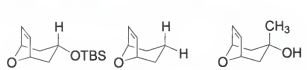

193 **204** **205**

Figure 2-1. Substrates considered for the kinetics studies.

The substrates were derived from ketone **1** (Scheme 2-4). Substrates **1**,[3] **192**,[89] **202**,[89] **203**,[90] and **193**[89] were known compounds and were prepared according to reported procedures in the literature. Oxime **199** was made in 81% yield by condensation of **1** with methoxylamine hydrochloride in the presence of molecular sieves. The exo-methylene **200** was prepared following a Peterson olefination protocol[91] of **1**, since Wittig conditions produced low yields. Wolf-Kishner[92] reaction of **1** afforded compound **204** in 68% yield. Grignard addition to ketone **1** in the presence of cerium chloride

yielded alcohol **201** in 74% yield; if cerium chloride was not present, aldol product was isolated. Epoxidation of **200** with *m*-CPBA produced epoxides **207-210**, and the opening of epoxide **208** with lithium aluminum hydride gave alcohol **205**.

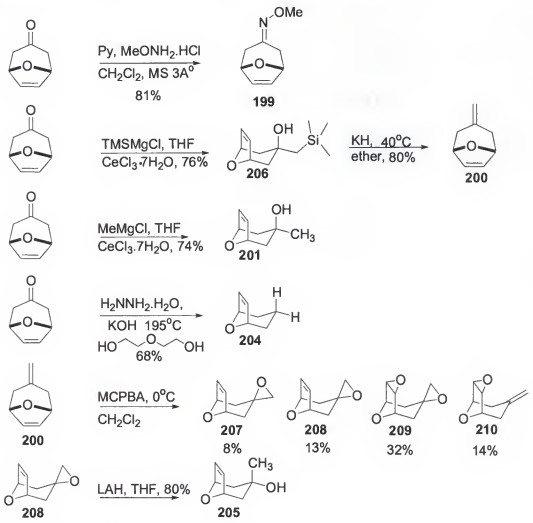

(Scheme 2-4). Synthesis of the some substrates employed in the kinetic studies

The substrates were compared with 4,10-dioxa-tricyclo[5.2.1.0 ^{2,6}]dec-8-ene-3,5-dione (**198**), namely the standard, in a ring-opening metathesis polymerization reaction (Scheme 2-5). The relative rate of the ring opening polymerization of the substrate versus the standard was determined using a Varian inova 500 MHz NMR. This particular standard was chosen because: (i) its alkene proton does not overlap with the alkene

proton of the substrates studied; (ii) the resulting polymer precipitates out of solution most of the time and when it does not, the signals of the resulting polymer do not interfere with the signals monitored; (iii) its reactivity in the ROMP reaction is comparable with the substrate's reactivity; (iv) it is easily obtained by a Diels-Alder reaction of furan and maleic anhydride. Thus, the standard (**198**) and each substrate were mixed at different relative concentration with an internal standard to normalize their integral area. These concentrations varied from 0.25 to 16 [standard/substrate] ratios. The variation in concentration was done to observe how the rate was affected by concentration. To the mixture, Grubbs' second generation catalyst (**67**) was added, and the consumption of the compounds versus time was monitored by proton NMR. Thus, spectra were acquired on automation (ca. 100 points for the course of the reaction), which varied from 10 minutes to 1.5 h, and the integrals of the alkene protons of the substrate and of the standard were normalized against the integral of a comparable amount of internal standard, benzene or residual TMS from the deuterated solvent. The normalized proton integral area was the concentration measurement during the course of the reactions. The plot of concentration versus time does not follow first order kinetics, displaying an induction period at the beginning of the reaction (Figure 2-2). Therefore individual rates for the reactions of the substrate and the standard could not be obtained. Thus, the data was obtained by plotting the natural logarithm of the substrate concentration against the natural logarithm of the standard (ln [substrate] vs. ln [standard]), which showed linearity. Figure 2-3 is a representative example of the linearity obtained and the generation of the data by the lineal regression equation.

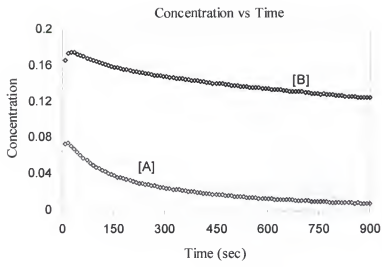

Figure 2-2. The evolution of the normalized concentrations of the substrate [A] and the standard [B]

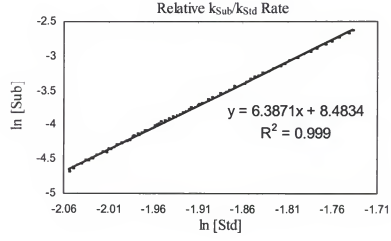

Figure 2-3. Representative example of the generation of the data with the linear regression equation of the ln[sub] vs ln[std]

This is consistent with the alkenes being consumed in a first order reaction, where the concentration of the catalyst is included in the rate constant as established by the following equations: $d[sub]/dt = k_{sub}[cat][sub]$, $d[std]/dt = k_{std}[cat][std]$, which leads to $\ln[sub] = \rho \ln[std] + const.$, where $\rho = k_{sub} / k_{std}$ and $const. = \ln[sub]_{init} - \rho \ln[std]_{init}$. In the

induction period, the active catalyst is formed, but by using the slope of ln[sub] *vs.* ln[std], the relative rates can be measured without considering the catalyst concentration. Relative rates measured at different ratios [std]/[sub] are given in Table 2-3.

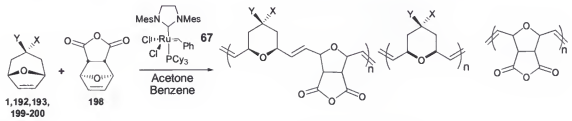

Scheme 2-5. Possible polymers from the ROMP of substrates and standard

Table 2-3. Relatives' rates k_{sub}/k_{std} of ring-opening metathesis polymerization of 8-oxabicyclic[3.2.1] octene derivatives

Substrate	X	Y	Ratio [Std/Sub]; *nm*=not meassured				
			0.25	1	4	8	16
1	X = Y = O		*nm*	0.21	0.29	0.34	0.42
192	OTBS	H	5.2	6.34	6.34	*nm*	*nm*
193	H	OTBS	1.46	1.38	1.55	*nm*	*nm*
199	X = Y = N-OCH_3		*nm*	0.34	0.49	0.56	0.55
200	X = Y = CH_2		1.56	1.05	1.15	1.29	*nm*
201	OH	CH_3	4.12	4.25	4.55	*nm*	*nm*
202	OH	H	6.03	6.17	5.39	*nm*	*nm*
203	X = Y = $OCH_2C(CH_3)_2CH_2O$		3.18	3.83	4.21	4.66	4.62
204	X = Y = H		2.38	2.22	1.91	*nm*	*nm*
205	CH_3	OH	3.92	4.28	3.38	*nm*	*nm*

The concern for the influence of the reagents ratio on the relative rates comes from the fact that there are four reactions by which the polymers grows:

(1) sub + std-poly ⟶ sub-std-poly (K1)

(2) std + std-poly ⟶ std-std-poly (K2)

(3) sub+sub-poly ⟶ sub-sub-poly (K3)

(4) std + sub-poly ⟶ std-sub-poly (K4)

where: sub = substrate
std = standard
poly = the growing polymer

sub-poly =  std-poly = 

Scheme 2-6. Possible pathways for the reagents consumption in the ring-opening metathesis polymerization

The substrate as a monomer can react with the living-growing polymer of the standard, path (1), or with its living-growing polymer, path (3). In the same way, the standard could react with its living-growing polymer, path (2), or via path (4), reacting with the living-growing polymer of the substrate.

The measured relative rate is $\rho = k_{sub} / k_{std} = (k1 + k3) / (k2 + k4)$. By eliminating the last two reactions, the rates in the reaction with the same polymer could be compared, meaning $\rho_{ideal} = \rho = k1 / k2$. This could be achieved by making k3 and k4 closer to 0 at high [std] / [sub] ratio. High [std] / [sub] ratio would make the substrate and the standard compete for the same living-growing polymer, thus k3 and k4 will approach to 0. However, ratios [std] / [sub] higher than 16 are impractical, because of the errors arising from a small ratio substrate / internal standard. The same errors can be observed towards the end of the reaction monitored period. Measurements become less precise as the concentrations of substrate or standard become too small compared to the internal standard, benzene or residual TMS, and a contiguous number of points at the end of the reaction were discarded in order to improve the precision. Comparisons can be seen in Figure 2-4.

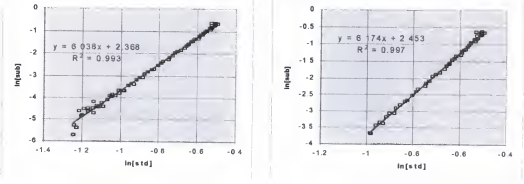

Figure 2-4. Comparison of selected data points: (a) left total of 76 points (b) right total of 50 points

Since the data obtained (Table 2-3) showed no correlation with the concentration, additional ρ values were taken for compounds **192,199, 202-204** at a ratio of [std]/[sub] = 1. Table 2-4 presents all the values measured, the average of these values and the 95% confidence interval.

Table 2-4. Relative rates k_{sub}/k_{std} and confidence interval (95%) from the ROMP of 8-oxabicyclic[3.2.1] octene derivatives

Substrate	X	Y	ρ								Mean ρ	Interval for 95% confidence	
1	X = Y = O		0.21	0.29	0.34	0.42					0.32	0.18	0.45
192	OTBS	H	5.20	6.34	6.34	6.81	7.11	6.6	7.09	7.09	6.5	5.96	7.03
193	H	OTBS	1.46	1.38	1.55						1.43	1.28	1.59
199	X = Y = N-OCH_3		0.34	0.49	0.56	0.55	0.78	0.40	0.75	0.76	0.58	0.44	0.72
200	X = Y = CH_2		1.56	1.05	1.15	1.29					1.26	0.90	1.61
201	OH	CH_3	4.12	4.25	4.55						4.31	3.76	4.86
202	OH	H	6.03	6.17	5.39	6.03	5.49	5.24	5.60	5.53	5.56	5.25	5.87
203	X = Y= $OCH_2C(CH_3)_2CH_2O$		3.18	3.83	4.21	4.66	4.62	3.83	3.77	3.69	3.97	3.54	4.39
204	X = Y = H		2.38	2.22	1.91	2.29	1.91	1.98	1.95	2.04	2.07	1.94	2.21
205	CH_3	OH	3.92	4.28	3.38						3.85	2.79	4.92

All ρ values given in Table 2-3 and Table 2-4 correspond to an R^2 greater than 0.98. For certain ratios, [std] / [sub], a R^2 values greater than 0.98 could not be achieved. This is because of an overlap between signals from polymer and signals from the substrate or because the difference between the signals compared was too large. Those cases were marked as *nm* (not measured) in table 2-3. Figure 2-5 presents a plot of the average relative rates k_{sub} / k_{std} and the 95% confidence interval for the substrates studied in a decreasing order of reactivity.

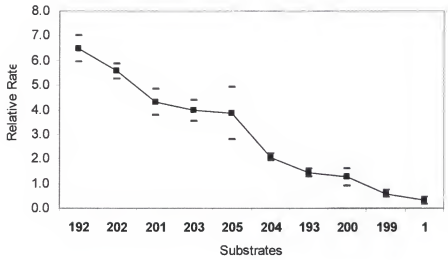

Figure 2-5. Plot of the average relative rates k_{sub} / k_{std} and the 95% confidence interval for the substrates studied in order of reactivity

Based on the results, the order of reactivity is depicted in Figure 2-6. Surprisingly, the results obtained do not show a large difference in the relative rate values among the substrates. The major difference was observed between ketone **1** and ether **192**. Nonetheless, whereas the *exo* silyl ether **193** demonstrated the same reactivity in the intermolecular reaction with styrene (Table 2-2), the results showed that it is less reactive than the corresponding *endo* silyl ether **192**. This is in agreement with the hypothesis that a bulky group in the *endo* position would make the oxabicyclic system more reactive toward ring-opening metathesis.

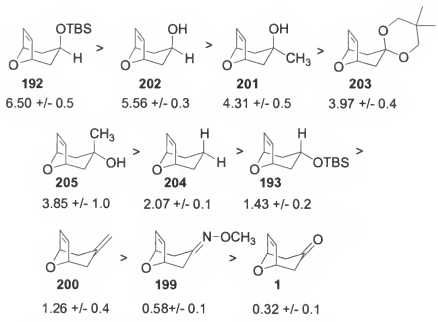

Figure 2-6. Substrates arranged based on their order of reactivity from average relative rates k_{sub} / k_{std} and the 95% confidence interval

Though it was considered that oxygen in the *endo* position of the bicyclic substrates would make the system more reactive from electrondensity donation to the double bond, other factor such as steric hindrance play an important role in the reactivity of the oxabicyclic compounds studied. This was exemplified by comparison of alcohols **201** and **205**. Because **201** has an oxygen in the *endo* position, it was expected to be more reactive than bicycle **205**. Nonetheless, the alcohols displayed similar reactivity pattern, indicating that sterics play a more important role than electronic, when the system is sp^3 hybridized. Thus, a bulky group in the *endo* position would make the system more reactive. On the other hand, the sp^2 hybridized substrates showed a correlation between electronegativity and reactivity. As a result, ketone **1** exhibited the lowest reactivity when compared with the other sp^2 hybridized derivatives **199** and **200**. Although the values obtained did not show a drastic difference among them, the knowledge obtained can help improve sluggish reactions by tuning the reactivity of the system as well as

manipulating the system to avoid polymerization and provide the ROCM product. Hence, the ROCM proceeds better (higher yield) with ketone **1** than with ether **192**, but if the interest is rather to obtain a polymer, ether **192** will be the preferred substrate for the reaction.

As an expansion of the methodology to the construction of more substituted pyrans, bridgehead substituted systems were studied. Though the olefin metathesis reaction has been studied for a long time, little is known about the regioselectivity of this reaction. Herein, our findings are reported on the intermolecular ROCM reactions of bridgehead substituted oxabicyclic systems.

Bridgehead Substituted 8-Oxabicyclo[3.2.1]Octene Derivatives

Having reported the success of the ring-opening cross metathesis of 8-oxabicyclo[3.2.1]octene derivatives to generate the pyran moiety,[85,86] it was decided to explore bridgehead substituted systems. As shown in scheme 2-7, two regioisomers are expected from this reaction. This outcome makes the reaction unpractical from a synthetic perspective. However, considering the impact of the olefin metathesis reaction in organic synthesis, this issue needed additional investigations.

Scheme 2-7: Attempted ring opening cross metathesis of substituted systems

In addition, interesting targets possess a substituent adjacent to the oxygen of the pyran moiety. For example, Forskolin possesses two neighboring methyl groups, and Latrunculin contains an adjacent alcohol (Figure 1- 1).

The reaction was first explored with 1-methyl-8- oxabicyclo[3.2.1]oct-6-en-3-one, **206a**. After subjecting **206a** to the reaction conditions that have proven favorable in the unsubstituted cases, no reaction was observed. Various reaction conditions were tried such as high catalyst loading (up to 10 mol %), elevated temperatures, and higher concentrations; however, only trace amounts of product were obtained. The system did not polymerize even at 110°C in 1M toluene. Ketones **206b** and **206c** also failed to react.

Considering the enhanced reactivity previously obtained by reduction/silylation of ketone **1** towards ring opening, ketone **206a** was reduced and converted to the corresponding ether **207a**. This dramatically increased the reactivity of the system under the reaction conditions, producing the expected regioisomers in 83% yield using 1.5 mol% of **67** and 4 equivalents of styrene. The regioisomers were obtained in a ratio of 6:1, where the major isomer placed the cross metathesized olefin on the more hindered side (Table 2-5). Initial attempt of this reaction using 5 mol % of **67** showed a decrease in regioselectivity to 3:1. Additional trials with unprotected alcohol **207c** gave surprising results. Though the yield of the reaction was similar to the yield obtained with the *endo* ether **207a**, the regioselectivity increased significantly from 6:1 (**208a**: **209a**) to 20:1 (**208c**: **209c**).

Additional substituted substrates, **207b** and **207d**, were prepared and studied in order to increase the regioselectivity by coordination of the oxygen with the catalyst; however, the regioselectivity did not improve, and the yields decreased.

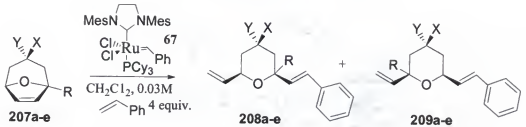

Scheme 2-8: Intermolecular cross-metathesis of reduced derivatives

Table 2-5: Intermolecular cross-metathesis of reduced derivatives

Alkene	R	X	Y	Yield [%]	Ratio (208:209)
207a	Me	OTBS	H	83	6:1
207b	CH_2OMe	OTBS	H	65	1.6:1
207c	Me	OH	H	85	20:1
207d	CH_2OMe	OH	H	66	20:1
207e	Me	H	OH	15	6:1

Efforts made to optimize the reaction yield with **207d** by increasing the temperature, lowered the regioselectivity to 3:1. To study the effect of the remote substituent stereochemistry, the *exo* alcohol **207e** was prepared by reduction of the corresponding ketone **206a** with samarium diiodide. The *exo* alcohol gave poor yield. Moreover, the regioselectivity decreased compared with the *endo* alcohol **207c** to equal the selectivity obtained with the ethers (6:1), again favoring the more hindered regioisomer. This regioselectivity preference for the more hindered alkene is in accordance with results obtained by Snapper[58] on ROCM reactions. Thus, the regioselectivity could be attributed to a high preference for the alkylidene formed with styrene over the methylidene as the active catalyst as Snapper findings (Scheme 1-26). Hence, the mechanism of the reaction could be as depicted in Scheme 2-9, where the styryl unit is placed first, forming the alkylidene **211**, which upon reaction with the

terminal alkene (styrene) produced the more substituted product. These reactions represent one of the few successes with regioselective ROCM of unsymmetrical bicyclic systems.[58-61]

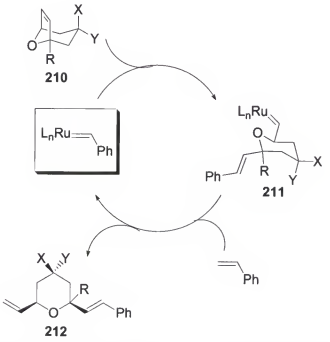

Scheme 2-9. Proposed mechanism for the high regioselective ROCM of 8-oxabicyclo[3.2.1]octene derivatives with styrene

In addition, two other systems were investigated: see scheme 2-10. A 1:1 mixture of *trans* and *cis* isomers of 1-methyl-8-oxa-bicyclo[3.2.1]oct-6-en-3-one-O-methyl-oxime (**213a, 213b**) was obtained by condensation of **206a** in refluxing dichloromethane with methoxylamine hydrochloride salt. This example was made to have an additional case of bridgehead substituted 8-oxabicyclo[3.2.1]octene derivative with sp^2 hybridization to study the system. The system has similar electronic properties to the ketone but differs in reactivity. When the mixture of isomers was subjected to the reaction conditions, no reaction was observed. Increased temperatures did not help promote the reaction.

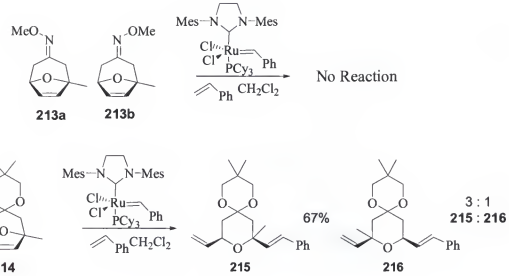

Scheme 2-10: Additional examples of ROCM of C1 substituted oxabicyclo derivatives

Ketal **214**, prepared from transketalization with tetramethyl dioxane and p-toluene sulfonic acid,[90] mimics the ketone functionality, possessing the same electronic properties of the parent ketone, but remaining sp^3 hybridized at C3. The ROCM of **214** produces a mixture of regioisomers in a 3:1 ratio and 67% yield. However, further investigation of this case demonstrated that the regioselectivity of the reaction is dependant on the reaction time; thus, at the early stage of the reaction, higher regioselectivity is observed (Table 2-7). This is attributed to the reversibility of the reaction. In fact, when the reaction was allowed to react for 1.5 hour one isomer was isolated in high yield, 90% (Scheme 2-11). Though, ketal **214** was the only case monitored carefully by GCMS, it is predictable that the substrates presented in Table 2-5, **207a-e**, could exhibit the same behavior and thus, high regioselectivity could be achieved if the reaction is allowed to react for a specific amount of time, though the starting material never will be consumed completely.

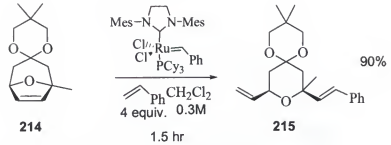

Scheme 2-11. The regioselectivity ratio is dependent on time

Table 2-7. The regioselectivity ratio is dependent on time

Time (hrs)	Regioselectivity Ratio (215:216)
1	>99:1
2	>99:1
3.5	16:1
24	3:1

Envisioning the synthesis of targets like Forskolin, a disubstituted bridgehead substrate **217** was also explored (Scheme 2-12). The substrate was prepared in the same fashion as the unsubstituted cases, using Föhlish's method.[3] No reaction was observed upon exposure of the substrate to the reaction conditions.

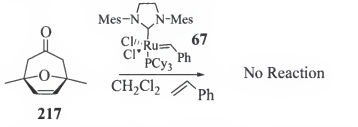

Scheme 2-12. Attempted ring opening cross metathesis of 1,5-dimethyl-8-oxabicyclo[3.2.1] oct-6-en-3-one.

Various sets of conditions were explored to make the reaction work. These conditions varied from increasing the amount of catalyst to using high temperatures. Despite our efforts, no reaction was observed. The reaction was also tried using the molybdenum-based catalyst (Schrock catalyst), which has been reported to be more reactive than Grubbs' catalyst;[92] however the substrate still resisted reaction. Considering the increment in the reactivity previously obtained converting the carbonyl

to the ether, the *endo* ether **218** was prepared from **217** and exposed to the same reaction conditions (Scheme 2-13). However, our expectation was not met as no reaction was observed. The disubstituted ether **218** did not undergo reaction or polymerization, even at elevated temperatures and high concentrations.

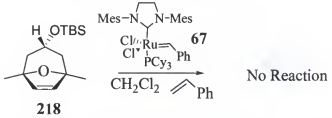

Scheme 2-13. Attempted ring-opening cross metathesis of the disubstituted ether **218**

As an expansion of the methodology to the construction of highly substituted pyrans an intramolecular process was attempted by tethering an alkene as a substituent in the bicycle.

Intramolecular Ring-Opening Cross Metathesis (ROCM)

In principle, there are three types of fused pyrans that can be synthesized from 8-oxabicyclo[3.2.1]octene derivatives by varying the place of a tethered alkene in the bicycle (Scheme 2-14).[93] A spiro-fused pyran is produced when it is placed at the bridgehead position, C1, of the oxabicyclic system. If the tethered alkene is located at C2, a linear-fused pyran is produced, while if the substituent is positioned at C3, a bridge-fused pyran is generated. Previous work in our group has demonstrated the viability of this domino metathesis toward fused pyrans.[86,93] In that area, spiro-fused pyrans were obtained in good yields and with high selectivity for the spiro-fused compound over oligomers or dimers.[86,93]

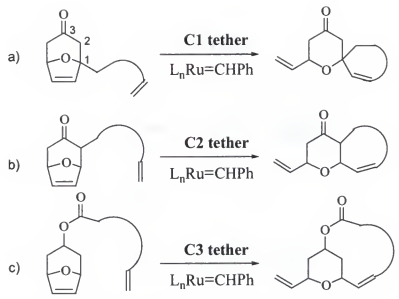

Scheme 2-14. Fused-pyrans from intramolecular ROCM reaction

The fact that the intermolecular reaction of **206c** with styrene did not generate product raised interesting mechanistic questions involving the intramolecular cross metathesis reaction in which the alkene is tethered at the C1 bridgehead position (type a, Scheme 2-14).[93] The unreactive **206c** is the saturated analog of **219**, an example of an oxabicyclic system with a tethered alkene at the bridgehead position that yielded a spiro-fused pyran **220** (Scheme 2-15).[93]

One plausible mechanism involves an initial reaction with the terminal alkene followed by cyclization (path A, scheme 2-16). An alternative path would involve a regioselective opening of the bridged olefin followed by cyclization (path B, scheme 2-16). The high regioselectivity and yields obtained for the spiro-fused pyrans support the former pathway.[93]

Scheme 2-15. Formation of a spiro-fused pyran from an oxabicyclic system with a tethered alkene at the bridgehead position

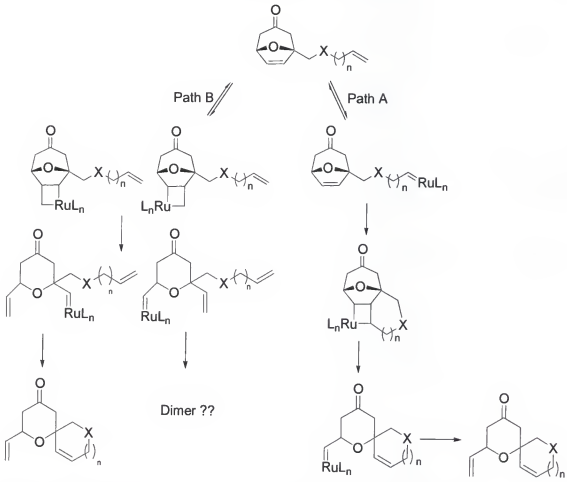

Scheme 2-16. Possible mechanism for an intramolecular ROCM reaction

This section presents our efforts toward the linear-fused pyrans by placement of a tethered alkene at the C2 position of the bicyclic system (type b, scheme 2-14). Two examples of C2 alkylated system were studied; they were prepared by Mann's alkylation protocol[94] (Scheme 2-17). The reaction produced the C2-carbon tethered substituted

intermediates in poor yield and as an epimeric mixture of the alkyl group at the C2 position. The ratios of epimers for **222** ranged from 100:1 to 70: 30, and the ratios of epimers for **223** ranged from 65: 35 to 50: 50 favoring the axial isomer in all cases. Nonetheless yields were reproducible and not higher than 38% and 20% for **222** and **223** respectively. Unfortunately, the epimeric mixture could not be separated after many trials. Consequently the intramolecular ROCM of compounds **222** and **223** to yield linear-fused pyrans was attempted with the mixture. However, no reaction occurred and the starting material was recovered unchanged for both cases.

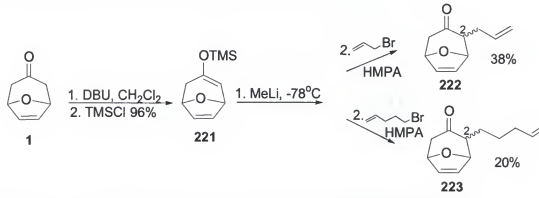

Scheme 2-17. Synthesis of the C2-carbon tethered substituted intermediates

To improve the reactivity of the system, as achieved earlier, and in an effort to separate the epimeric mixtures, ketones **222** and **223** were reduced with L-Selectride, to obtain their respective diasteromeric *endo* alcohols. The reduction proved to be more complicated because the placement of the alkyl group in the axial position afforded *exo* alcohol and *endo* alcohol from the reduction, thus making the mixture more difficult to separate (Scheme 2-18).

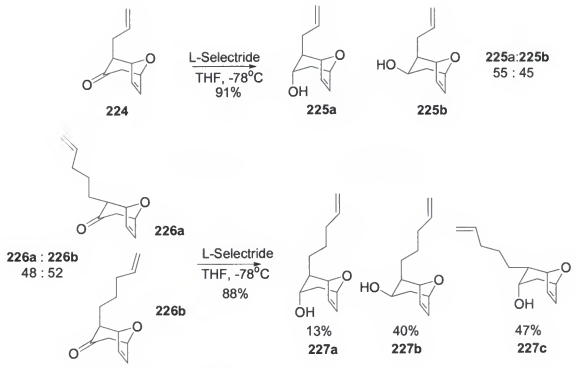

Scheme 2-18. Reduction of the C2-alkylated oxabicyclo[3.2.1]octene derivatives

When ketone **224**, obtained as a single isomer from the alkylation, was reduced with L-selectride alcohols **225a** and **225b** were produced. When a mixture of 48: 52 of the C2 epimeric ketones **226** were submitted to the reaction conditions (L-Selectride, THF, -78°C) afforded a mixture of alcohols **227a-c** was obtained. The *exo* alcohols **225b** and **227b** derived from ketones **224** and **226b** respectively were obtained from an *endo* attack of the hydride rather than the usual exo attack that provides the *endo* alcohols. This is due to steric hindrance provided by the tethered alkene in the axial position. The separation of alcohols **225a** and **225b** was possible. However, from the mixture generated from ketone **226a-b**, compound **227a** was isolated, while alcohols **227b-c** remained as a mixture. Nevertheless with the alcohols in hand, the intramolecular ROCM was attempted (Scheme 2-19).

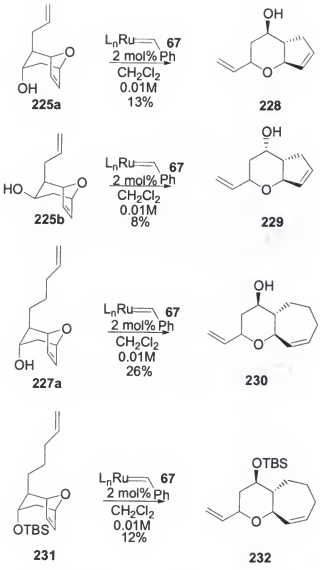

Scheme 2-19. Intramolecular ROCM of the reduced C2-tethered systems

The yields for the linear-fused pyran products were low. During the first minutes of reaction, the mixture becomes cloudy and all the starting material is consumed. After evaporation of the solvent, a white precipitate is left, presumably some polymer. In an attempt to improve the yield, the bulky silyl ether **231** was prepared from alcohol **227a**. Nonetheless, the system became more reactive toward polymerization and the yield dropped compared to the results obtained with the respective alcohol **227a**. Though the intramolecular ROCM of the reduced C2-tethered systems was not successful, the

hypothesis of being able to form linear-fused pyrans from that type of system was confirmed.

To prove the efficiency of the ROCM strategy of 8-oxabicyclo[3.2.1]octene derivatives in natural products synthesis, an approach to Latrunculin B was attempted.

Approaches Towards Latrunculin B from Ring-Opening Metathesis of 8-Oxabicyclo[3.2.1]Octene Derivatives

The marine macrolide Latrunculin B possesses interesting biological activity[78] and a pyran-skeleton that is amenable using a ROCM approach. It was foreseen that ROCM of an oxabicycle derivative would provide the differentiated cis-2,6-substituted pyran. The rest of the target was envisaged to be completed by chiral alkylation, Wittig olefination, where the formation of the *cis* olefin would be critical for the success of the synthesis, a macrolactonization, oxidative decarboxylation or allylic oxidation, depending on the substituent adjacent to the oxygen, and at the last stage of the synthesis, construction of the thiazolidinone moiety. This approach differs from previous syntheses in the initial formation of the pyran moiety from ROCM, and the last stage placement of the thiazolidinone moiety, allowing for the preparation of analogs at that center. A proposed fragmentation for a retrosynthetic analysis is presented in scheme 2-20.

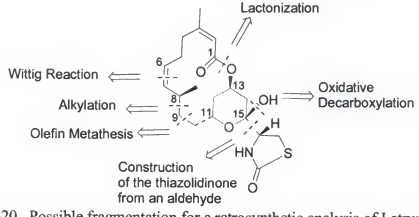

Scheme 2-20. Possible fragmentation for a retrosynthetic analysis of Latrunculin B

Although various methods were formulated to choose which oxabicycle system would lead to the desired pyran, two routes were tried to approach the target and thus will be presented in this section. All the approaches were done with racemic mixture to study the strategy.

Initial attempts to the target were based on the ROCM of methoxy bridgehead substituted oxabicyclo **237** (Scheme 2-21). This route permits easy access to the pyran moiety with the contiguous oxygen, protected as a methoxy acetal. This strategy presents interesting possibilities for other natural products possessing this acetal type pyran such as phorboxazole, callipeltosides and the bryostatins. However, this sequence presented some drawbacks, such as the low yields obtained for the starting material, methoxyketone **235**, and the poor efficiency of the intermolecular ROCM reaction. The low yield obtained for methoxyketone **235** (30% over two steps, cycloaddition and reduction) represents a problem due to the price of the 2-methoxyfuran, even though the reaction could be performed on large scales. Nonetheless, with the bridgehead substituted oxabicyclo **235** in hand, the ROCM with styrene was attempted. Surprisingly, the ketone yielded 20% of the trisubstituted pyran **236** as a single regioisomer. This gave us some basis to assume that the ROCM of the reduced derivative would provide a higher yield and high regioselectivity. However the ROCM of the reduced derivative **237** was not as successful as expected. The reaction was monitored by NMR to determine the time of completion with the highest regioselectivity. The regioselectivity was high, one isomer was observed by NMR, but the reaction proved to be highly reversible, favoring the starting material. Product was formed up to a maximum of 65% (9 hours of reaction) based on NMR. Prolonged reactions times favored the equilibrium to the starting

material, thus after 24 hours only traces of products were present along with the starting material. At that point, there was less amount of stylbene (reaction byproduct) present, probably taking part in the reversibility of the reaction.

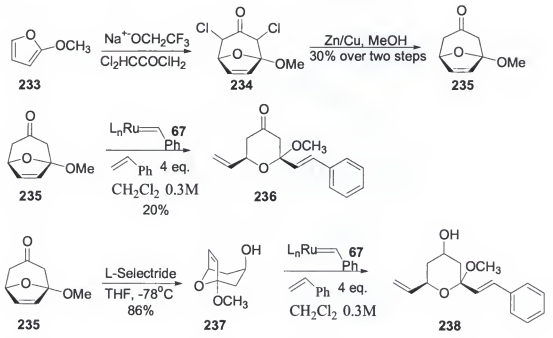

Scheme 2-21. Approach to the acetal type pyrans from the ROCM strategy

Consequently, another strategy was explored simultaneously. The new method started with the ROCM of alcohol **242** (Scheme 2-22). Ketone **241** can be obtained on large scale in good yield from the relatively cheap furfuryl alcohol **239**. Ketone **241** failed to undergo ROCM with styrene. On the other hand, *exo* alcohol **242**, which provides the desired stereochemistry at the C13 of latrunculin B, underwent ROCM; however the alcohol gave low yields and poor regioselectivity. Further, ROCM of the *endo* alcohol **245** gave a 79% yield of the more hindered alkene **246** as a single regioisomer. None of the other regioisomer was observed by NMR or GCMS. Nonetheless, high loads of styrene can provide the diphenyl cross metathesized product.

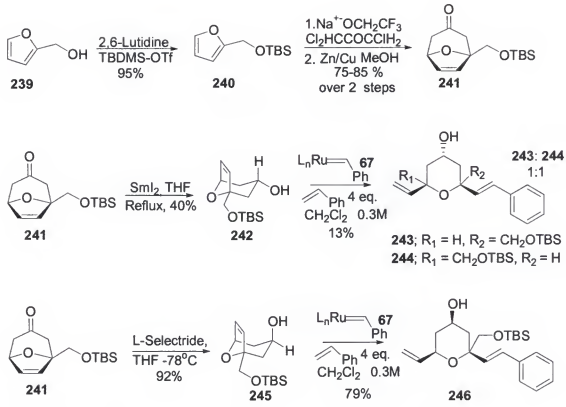

Scheme 2-22. Initial approach to latrunculin B: generation of the pyran.

With the pyran **246** in hand, functionalization of the skeleton started with protection of the free alcohol and hydroboration of the protected material; the two step sequence gave a 74% yield of alcohol **247**, which was then protected as a *tert*-butyl dimethyl silyl ether **249** (Scheme 2-23). The hydroboration selectively oxidized the less hindered alkene. The alcohol side chain was foreseen to be protected as a triflate to undergo alkylation with an Evan's oxazolidinone enolate to set the center at C8. Nonetheless, silyl ether **240** was used as a model compound to functionalize the pyran by studying the oxidative decarboxylation to generate the C15 alcohol, whose stereochemistry was supposed to be set by the anomeric effect.[95] After ozonolysis of styryl compound **249** and oxidation to acid **251** with sodium chlorite, attempts were done toward the oxidative decarboxylation of **251** (Scheme 2-23). It is interesting to mention

that acid **251** did not exhibit the characteristic OH stretch in the IR. Hence, an ester derivative (**263**) was made by treatment of diazomethane for further confirmation.

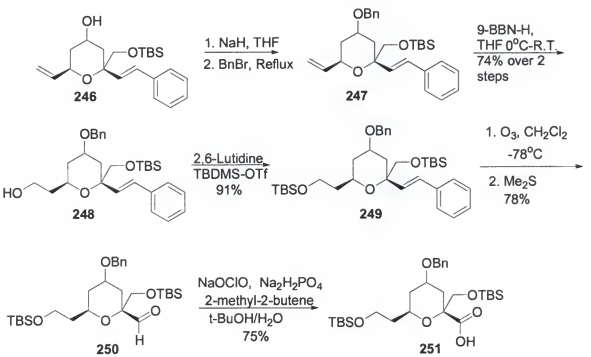

Scheme 2-23. Functionalization of the pyran intermediate to approach Latrunculin B

Various conditions were attempted in an effort to promote the oxidative decarboxylation of **251** as a strategy to install the C15 alcohol of the target (Scheme 2-24). The first thing tried was the use of lead tetraacetate ($Pb(OAc)_4$). Lead tetraacetate is commonly used for this type of transformation.[96] Exposure of **251** to $Pb(OAc)_4$ in refluxing benzene gave an undefined mixture of compounds, though the starting material was totally consumed. Presumably, the acetic acid present in the $Pb(OAc)_4$ may have deprotected the alcohols promoting further reactions with them that lead to a mixture of compounds. Another possibility is that the starting material **251** decomposed under those conditions. Another protocol, developed by Suarez et al. that was the simple oxidative decarboxylation using the hypervalent iodine, diacetate iodobenzene (DIB), which has been reported to react via a radical mechanism.[97] Based on the proposed mechanism

reported in the literature, compound **251** was expected to undergo oxidative decarboxylation as depicted in scheme 2-25.

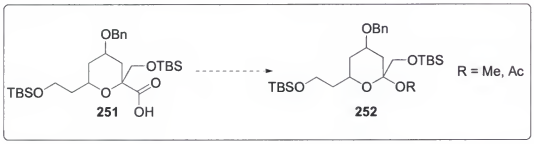

Scheme 2-25. Oxidative decarboxylation as depicted in the literature

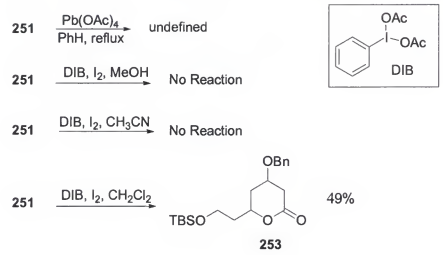

Scheme 2-24. Attempts of oxidative decarboxylation of the acid intermediate

The reaction of **251** with DIB was attempted in various solvents as reported in successful examples from the literature. The product from oxidative decarboxylation reaction was not observed in any of the cases. Interestingly, when dichloromethane was used as solvent, lactone **253** was isolated as the only product. Although the yield was moderate (49% yield), the reaction was clean: crude NMR showed only the new compound **253** and excess of the DIB reagent. A proposed mechanism for the lactone formation based on previous reported mechanism of this reagent with carboxylic acids is presented in scheme 2-26.

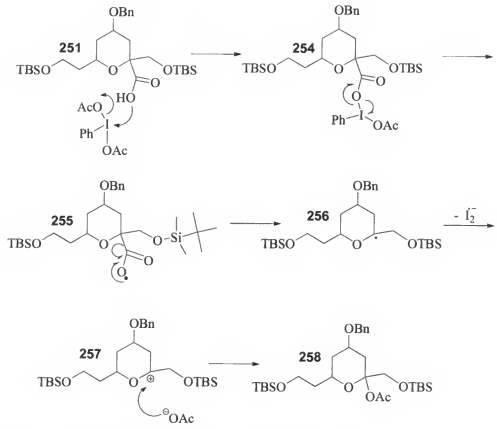

Scheme 2-25. Proposed mechanism based on literature reports

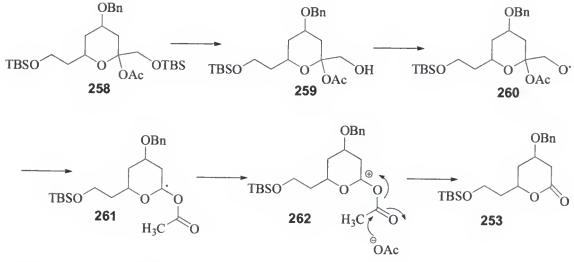

Scheme 2-26. Proposed mechanism for the lactone formation

It is proposed that compound **258** is a plausible intermediate for the lactone formation. Compound **258** is predicted to be formed based on the mechanism depicted in

scheme 2-25. Thus, reaction of the carboxylic acid with DIB generates intermediate **254**, which fragments to the radical intermediate **256** by loss of CO_2, then radical oxidation by the iodine gives carbocation **257**, which eventually is quenched by an acetate group to give **258**. It is supposed that deprotection of the silyl ether of **258** generates the alcohol **259** which could form radical **260** by reaction with DIB, then loss of formaldehyde could give rise to the new radical **261**, that gave lactone **253**.

Based on the results and the proposed mechanism for formation of lactone **253**, it was presumed that if compound **258** was formed, the reagent was performing the oxidative decarboxylation. Hence, compound **265**, would be able to form an oxygen radical and loss CO (Scheme 2-26), and form a carbocation intermediate **262** stabilized by an styryl unit that can lead to the C15 alcohol. However, compound **266** appears to be formed based on extensive NMR studies; this was not confirmed by mass spectrometry. This may imply that the proposed mechanism is not taking place or that addition of the iodine to the double bond, followed by cyclization is faster than the reaction of **265** with DIB.

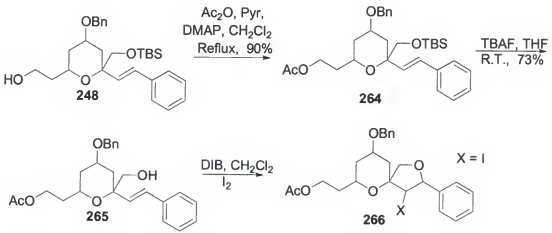

Scheme 2-27. An alternative attempt to form the acetal type pyran

Some future work that may provide the desired oxygen at C15 could be the use of the Hunsdiecker reaction, with subsequent quench of with methanol in the presence of catalytic acid. Nonetheless, preliminary results failed to give the desired alkyl halide. Furthermore, $Pb(OAc)_4$ could be tried with different protecting groups not as sensitive to acid as the silyl ether case studied, and electrochemical oxidation, another common procedure for the oxidative decarboxylation, should be also studied. In addition, if the lactone could be obtained in higher yields, careful Grignard addition to the lactone could provide the desired alcohol. Another route would be exploring the ROCM of other oxabicycle systems, for example, ROCM of **1** and further allylic oxidation. Nevertheless, ROCM has proven to be a useful strategy that may be employed in natural product synthesis.

CHAPTER 3
CONCLUSIONS AND FUTURE WORK

The studies performed have proven that ring-opening cross metathesis reactions of oxabicyclo[3.2.1]octene derivatives is a viable pathway toward the formation of highly-substituted pyrans. The presence of a bridgehead substituent decreased the reactivity of the system in the intermolecular ROCM. These findings disclosed mechanistic details in the intramolecular ROCM reaction, implying that the intramolecular ROCM reaction proceeds via initial reaction with the tethered vinyl group followed by cyclization rather than initial regioselective opening of the bridged olefin.

The lack of reactivity in bridgehead substituted systems can be manipulated by changes in remote substituents. The changes on remotes substituents can also affect the regioselectivity of these reactions. However, it was observed that the regioselectivity may depend on the reaction time. Thus, at the early stages of the reaction the regioselectivity is higher.

Unfortunately, disubstitution at the bridgehead position of the oxabicyclo leads to no reaction. Neither reduction/silylation had an effect on the reactivity of the system.

The kinetics studies performed on the unsubstituted oxabicyclic compounds lead to a new hypothesis of how remote substituents affect the reactivity of the system. Based on the results, it is suggested that the enhancement in reactivity is caused by the ability of the substituent at C3 to donate electron density to the double bond through space rather than by changes in hybridization as initially proposed.[85] In addition, steric factor plays a major role on the reactivity of the system. Although a small difference in the relative

rates was observed for the ROMP of the 8-oxabicyclo[3.2.1]octene derivatives, the differences manifest themselves in significant effects such as yield of ROCM products versus polymers.

Our investigations have contributed to the expansion of the methodology towards unsymmetrical cyclic compounds, as well as provided new insight into the factors that can affect the valuable metathesis reaction.

The Intramolecular ROCM of the C2-tethered alkene oxabicyclic substrates was sluggish, and rendering the direction of the reaction more to the production of polymer rather than the linear-fused pyran.

The ROCM of of 8-oxabicyclo[3.2.1]octene derivatives proved to be an effective way for the fast construction of the pyran moiety in Latrunculin B. Additional work needs to be done to further functionalization of the pyran skeleton and obtain the acetal type pyran.

In order for the ROCM 8-oxabicyclo[3.2.1]octene derivatives to be useful and appealing in synthesis, asymmetric intermediates need to be obtained. Thus it is important to study the ROCM of chiral oxabicycles, and observe the effect on the regioselectivity of asymmetric substituted bicycles. Another alternative is the asymmetric ROCM with a chiral catalyst.[98] Of interest could be the screening of various chiral catalysts with a series of oxabicycle to determine a trend on which chiral catalyst is better for specific functional groups and substitution of the system.

CHAPTER 4
EXPERIMENTAL PROCEDURES

General Methods. All the solvents used in the reactions were distilled prior to use, unless reported. Thin-layer chromatography was performed using silica gel 60 F_{24} precoated plates (250 μm thickness). Column chromatography was performed using 230-400 mesh silica gel 60. Melting points were obtained on a Thomas-Hoover Capillary Melting point apparatus, and reported uncorrected. IR spectra were obtained on a FT-IR spectrometer. NMR spectra were obtained on a Varian 300 MHz spectrometer; chemical shifts are reported in δ units relative to the tetramethylsilane (TMS) signal at 0.00 ppm. Coupling constants are reported in Hz. High-resolution mass spectroscopy was provided by the University of Florida Mass Spectroscopy Services.

Kinetic Studies. A 0.65 ml solution of acetone containing 4,10-dioxa-tricyclo[5.2.1.0 ^{2,6}]dec-8-ene-3,5-dione (standard, **198**), the substrate to be analyzed, oxabicyclo[3.2.1]octene derivatives (**1,192, 193, 199-200**), in different ratios (1: 1, 1: 4, 4:1, and 8:1, 16:1 in some cases) and a drop of benzene as the internal standard was prepared. To the mixture, 0.1 ml of a solution of 1.0 mg of Grubbs catalyst **67** in 1 ml of $CDCl_3$ was added. The reactions were monitored by ^{1}H NMR at 500 MHz on a Varian Inova spectrometer. The spectra were acquired on automation, ca. 100 points for the course of the reaction, which varied from 10 minutes to 1.5 h, and the integrals of the alkene protons of the substrate and of the standard were normalized against the integral of a comparable amount of benzene. The plot of ln[substrate] vs ln[standard] afforded a line, whose slope corresponded to the relative rate of the substrate versus the standard

(k_{sub}/k_{std}) with a typical R^2 of 0.98-0.99. In accordance with the following equations: $\ln(A_0/A) = kt$, where $k=[cat]*k_A$, the ratio of k_A/k_{std} is the slope of ln[A]/ln[Std], where [A] = [substrate] and [Std] = standard.

Figure 4-1. 8-Oxa-bicyclo[3.2.1]oct-6-en-3-one O-methyl-oxime **(199)**

8-oxa-bicyclo[3.2.1]oct-6-en-3-one **1** (0.100 g, 0.806 mmol) was dissolved in 2 ml of dry CH_2Cl_2 and mixed with methoxylamine hydrochloride (0.101 g, 1.210 mmol) and 3A° molecular sieves. Then 0.10 ml of pyridine was added, a condenser was fixed and the reaction mixture was allowed to reflux for 5 hours. Upon completion of the reaction by TLC, the reaction was diluted in CH_2Cl_2, the resulting powdering molecular sieves were filtered. The filtered liquid was washed with brine and dried over $MgSO_4$, filtered trough a small plug of silica gel, eluting with 85:15 hexanes: ether and concentrated to achieved a white solid (0.1003 g, 81%) of **199**. Rf = 0.33 (85: 15 hexane: ethyl acetate). Melting Point 55-56°C. ^{1}H NMR (300 MHz, $CDCL_3$): δ 6.23-6.18 (2H, m), 4.90(1H, dt, J = 4.7Hz, 1.2Hz), 4.85 (1H, dt, J = 4.7Hz, 1.2Hz), 3.78 (3H, s), 2.93 (1H, dd, J = 16.1Hz, 0.9Hz), 2.66 (1H, ddt, J = 15.2 Hz, 4.4Hz, 1.5 Hz), 2.36 (1H, ddt, J = 16.1Hz, 4.4Hz, 1.5Hz), 2.26 (1H,dd, J = 15.2Hz, 0.9Hz). ^{13}C NMR ($CDCl_3$): δ 153.4, 133.4, 132.4, 78.0, 76.8, 61.4, 34.5, 30.4. HRMS (EI) calcd for $C_8H_{11}NO_2$ $[M]^+$ 153.0790, found 153.07889. IR (film): 2956, 2925, 2853, 2360, 1464, 1259, 1048, 994, 843 cm^{-1}. CH calcd for $C_8H_{11}NO_2$: C, 62.73; H, 7.24; found: C,62.74; H, 7.27.

Figure 4-2. 3-Methylene-8-oxa-bicyclo[3.2.1]oct-6-ene **(200)**

A flame dry 2-neck 25 ml flask was charged with 0.70 g of $CeCl_3$ heptahydrate and stir bar. The solid was dried by heating at 140°C under vacuum for 3 hours. Then it was allowed to cool to room temperature and a suspension was made by the addition of THF (3 ml). The suspension was allowed to stir at room temperature for 2 hours, then it was cooled to -78°C and 1M trimethylsilylmethyl magnesium chloride was added (0.97 ml, 97 mmol). The yellow suspension stirred for 30 min and oxabicyclic ketone **1** (0.10 g, 0.81 mmol) was added. The mixture was allowed to stir overnight and reach room temperature slowly. The reaction was worked up by quenching with ice and adding a solution of ammonium chloride for the emulsion formed. The layers were separated and the aqueus layers were extracted with ether. The organic layers were dried with $MgSO_4$, filtered and concentrated to yield the crude alcohol in 84% yield as an orange oil. The crude was added to a suspension of 35% wt. KH (1.1 g) in 6 ml of THF at 0°C. The mixture was allowed to stir at room temperature for 3 hours and then it was quenched carefully with a saturated solution of ammonium chloride at -10°C. The aqueous layers were extracted with ether, dried with MgSO4 and concentrated in a rotary evaporator. The oil was purified by column chromatography eluting with 95: 5 (hexanes: ether) affording 60% overall yield of the volatile, colorless oil **200**. $Rf = 0.71$ (35: 65 ethyl acetate: hexane). ^1H NMR (300 MHz, $CDCL_3$): δ 6.10 (2H, s), 4.79 (2H, d, $J = 4.1$Hz), 4.74 (2H, t, $J = 2.2$Hz), 2.61-2.54 (2H, m), 2.05 (2H, d, $J = 14.6$ Hz). ^{13}C NMR (CDCl3): δ 141.3, 131.7, 113.7, 78.7, 37.2. HRMS (EI) calcd for $C_8H_{10}O$ $[M]^+$ 122.0732, found

122.0733. IR (film): 3072, 2951, 2897, 2820, 1645, 1418, 1342, 1045, 990, 890, 871cm^{-1}.

Figure 4-3. *endo*-3-Methyl-8-oxa-bicyclo[3.2.1]oct-6-en-3-ol **(201)**

In a 2 neck flask 3.84g of $CeCl_3.7H_2O$ were dried with stirring under vacuum at 140°C for 3 hours. The powdery white solid was cooled down under argon to room temperature. Then 8 ml of dry freshly distilled THF were added and stirring was maintained for two additional hours. The cloudy white suspension was cooled to –78°C and 2.8 ml, 3.84 mmol of 1.0 M solution of $MgBrCH_3$ were added, where upon addition the color of the suspension turned from white to a pale yellow color. After being kept at the same temperature for 30 min, a solution of 8-oxa-bicyclo[3.2.1]oct-6-en-3-one **1** (0.400 g, 3.2 mmol) in 4 ml of THF was added. The reaction mixture was allowed to reach room temperature and stir under argon for 24 hours. Upon completion of the reaction, it was quenched with ice and filtered through a pad of celite. The filtrated was extracted with ethyl acetate, dried with Na_2SO_4, filtered and the solvent was evaporated under reduced pressure. The dark orange residue was purified by silica gel chromatography eluting with 85:15 hexane:ethyl acetate (residue previously adsorbed on silica) producing **201** as a pale yellow oil (0.2500g, 56%) of 21. *Rf* = 0.14 (65: 35 hexane: ethyl acetate). ^{1}H NMR (300 MHz, $CDCL_3$): δ 6.48 (2H, s), 4.80 (2H, d, J = 4.3Hz), 3.44 (1H, bs), 2.07 (2H, dd, J=14.9Hz, 4.0Hz), 1.74 (2H, d, J= 14.5 Hz), 1.15 (3H, s). ^{13}CNMR ($CDCl_3$): δ 135.5, 77.8, 69.4, 41.6, 32.7. HRMS (EI) calcd for $C_8H_{12}O_2$ $[M]^+$ 140.0837, found 140.0836. IR(film): 3429, 2947,1647, 1348, 1165, 1101, 857 cm^{-1}.

Figure 4-4. 8-Oxa-bicyclo[3.2.1]oct-6-ene **(204)**

In a sealed tube KOH (1.3g, 22mmol) was dissolved at 55°C in diethylene glycol (9 ml). To the yellow orange viscous solution (0.9025 g, 7.25 mmol) of **1** were added followed by the addition of hydrazine monohydrate (0.9 ml, 18 mmol). Then the mixtured was sealed and allowed to reflux to 195°C. Upon completion by TLC the reaction was worked up by adding water and a little amount of 2% HCl solution. The aqueous layer was extracted 4 times with small portions of ether. The ether layers were dried with Na_2SO_4 and filtered. The solvent was removed by distillation. The residue was purify by chromatography eluding with a mixture of 95:5 petroleum ether:ether. The compound containing fractions were collected, and the solvent was removed by distillation to afford **204** as a volatile pale yellow oil (0.5475g, 69% yield) of pungent smell. $Rf = 0.29$ (95:5 hexane:ether). ^1H NMR (300 MHz, $CDCL_3$): δ 6.14 (2H, s) 4.67-4.71 (2H, m), 1.01-1.81 (6H,m). ^{13}C NMR ($CDCl_3$): δ 130.6, 79.5.8, 41.6, 25.2. HRMS (EI) calcd for $C_7H_{10}O$ $[M]^+$ 110.0732, found 110.0732. IR (film): 2930, 2854, 1029, 806, 701 cm^{-1}.

Figure 4-5. exo-3-Methyl-8-oxa-bicyclo[3.2.1]oct-6-en-3-ol **(205)**

To a suspension of $LiAlH_4$ (83mg, 2.18mmol) in THF (3 mL) was added epoxide **208** (40 mg, 0.29 mmol) as a solution in 2 ml of dry THF at 0°C. After the addition, the mixture was refluxed at 66°C for 3hrs. The mixture was allowed to reach room temperature and then was cooled to -10°C and quenched with 0.25 ml of water follow by

0.25 ml of 2 M NaOH. Additional 0.5 ml of water was added and the mixture was filtered. The aqueous layer was extracted with ethyl acetate, dried with MgSO4, and concentrated in a rotary evaporator. The residue was purified by silica gel chromatography and gave a colorless oil **205** (27 mg, 68%). R*f* = 0.18 (40:60 hexane: ethyl acetate). ^{1}H NMR (300 MHz, $CDCL_3$): δ 6.18 (1H, s), 4.82 (1H, d, *J* = 5.4 Hz), 2.05 (2H, d, *J* = 13.7 Hz), 1.69 (2H, d, *J* = 13.1 Hz), 1.27 (2H, s). ^{13}C NMR ($CDCl_3$): δ 133.2, 77.6, 69.4, 41.7, 33.6. IR (film): 3406, 2924, 2850, 1258, 1096, 1047, 711 cm^{-}1.

Figure 4-6. 3-endo-spiro epoxide bicycle[3.2.1]oct-6-ene **(208)**

To a solution of 3-Methylene-8-oxa-bicyclo[3.2.1]oct-6-ene **(200)** (0.4000g, 3.27 mmol) in methylene chloride (5 ml) was added $NaHCO_3$ (0.35g, 3.89 mmol) of and *m*-CPBA 77% (1.70g, 7.78 mmol) at 0°C by portions. The reaction was allowed to stir for 6hrs at 0oC then was allowed to reach room temperature and stir for additional 9hrs. Upon completion of the reaction based on TLC the reaction was worked up by diluting the mixture with water and washing it with 20% NaOH extracting with CH_2Cl_2. The organic layer was dried with $MgSO_4$, filtered and concentrated in a rotary evaporator. The residue was then purify by silica gel chromatography using gradient elution (50g silica gel: residue adsorbed on silica; 95:5 – 65:35 hexane: ethyl acetate) gave a white semisolid **208** (58 mg, 13%). R*f* = 0.34 (65:35 hexane: ethyl acetate). ^{1}H NMR (300 MHz, $CDCL_3$): δ 6.21 (1H, s), 4.87 (1H, d, *J* = 3.5 Hz), 2.5 (2H, s), 2.32 (2H, dd, *J* = 13.2, 3.8 Hz), 1.35 (2H, dt, *J* = 13.2, 1.2 Hz). ^{13}C NMR ($CDCl_3$): δ 132.4, 78.3, 58.5, 54.8, 36.4. IR (film): 2958, 2924, 1394, 1245, 1048, 993 cm^{-}1.

Other epoxides were isolated:

Figure 4-7. 3-exo-spiro epoxide bicycle[3.2.1]oct-6-ene **(207)**

R*f* = 0.25 (65:35 hexane : ethyl acetate). ^{1}H NMR (300 MHz, $CDCl_3$): δ 6.37 (2H, s), 4.84 (2H,d, *J* = 3.33Hz), 2.54 (1H, d, *J* = 3.8 Hz), 2.49 (1H, d, *J* = 3.8 Hz), 2.38 (2H, s), 1.24 (2H, d, *J* = 14.1 Hz). ^{13}C NMR ($CDCl_3$): δ 133.7, 78.3, 54.0, 48.1, 37.3. Pale yellow oil (35 mg, 8%).

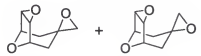

Figure 4-8. diepoxides **(209)**

R*f* = 0.13 (65:35 hexane: ethyl acetate). ^{1}H NMR (300 MHz, $CDCl_3$) **major**: δ 4.33 (2H, d, *J* = 4.09 Hz), 3.76 (1H, s), 2.57 (2H, s), 2.44 (2H, dd, *J* = 15.2, 4.4 Hz), 1.22 (2H, d, *J* = 15.2 Hz). **minor**: δ 4.38 (2H, d, *J* = 4.4 Hz), 3.62 (2H, s), 2.61 (2H, s), 2.30 (2H, dd, *J* = 14.0, 4.09 Hz), 1.38 (2H, d, *J* = 14.3 Hz). ^{13}C NMR ($CDCl_3$) **both**: δ 71.9, 71.5, 57.3, 53.6, 53.2, 53.1, 50.5, 34.5. HRMS (EI) calcd for $C_8H_{10}O_3$ $[M]^+$ 138.0630, found 154.0629. A yellow oil (0.16g, 32%).

Figure 4-9. 7-Methylene-3,9-dioxa-triciclo[3.3.$10^{2,4}$]nonane **(210)**

R*f* = 0.52 (65:35 hexane : ethyl acetate). ^{1}H NMR (300 MHz, $CDCl_3$): δ 4.79 (2H, t, *J* = 2.3 Hz), 4.26 (1H, d, *J* = 4.7 Hz), 3.5 (2H, s), 2.63-2.56 (2H, m), 2.23 (2H, d, *J* = 15.5 Hz). ^{13}C NMR ($CDCl_3$): δ 132.4, 78.3, 58.5, 54.8, 36.4. HRMS (EI) calcd for

$C_8H_{10}O_2$ $[M]^+$ 138.0696, found 138.0696. IR (film): 2960, 2902, 1650, 1054, 854, 695 cm^{-1}. Pale yellow oil (62 mg, 14%).

Figure 4-10. 1-methoxymethyl-8-oxa-bicyclo[3.2.1]oct-6-en-3-one **(206b)**

2-Methoxymethyl-furan prepared from furfuryl alcohol, sodium hydride and methyl iodide in THF (4.90g, 44 mmol) was placed in a 500 ml round bottom flask without purification and cooled to $0^{\circ}C$. Via two separate syringes, trichloroacetone (6.0 ml, 9.21g, 57 mmol) was added, followed by the slow addition of trifluoroethoxide (2M, 33 ml). Upon completion of the addition, the solution was allowed to warm to room temperature. The reaction was monitored by TLC using p-anisaldehyde as stain. After 12 hours, zinc/copper couple (8.8 g, 0.132 mmol) and a solution of methanol saturated with ammonium chloride (75 mol) were added, and the mixture was allowed to reflux for two days. Upon reaction completion, the mixture was filtered through celite washing with ethyl acetate to remove the zinc/copper couple. The filtrate was then evaporated, and the residue partitioned between dichloromethane and a saturated solution of EDTA. The aqueous layers were extracted with dichloromethane. The organic layers were combined and dried on $MgSO_4$, filtered, and the solvent removed in vacuo. The brown oil residue was then purified by chromatography using gradient elution (60: 1 silica gel: residue adsorbed on silica; (95: 5- 60: 40 hexanes: ethyl acetate) to give **206b** as a yellow oil (3.0g, 40 % over 3 steps). $Rf = 0.27$ (70: 30 hexanes: ethyl acetate). ^1H NMR (300 MHz, CDCl3) δ 6.27 (1H, d, $J = 5.9$), 6.10 (1H, d, $J = 5.9$), 5.11 (1H, d, $J = 4.5$), 3.62 (2H, s), 3.45 (3H, s), 2.77-2.68 (2H, m), 2.36 (1H, d, $J = 6.9$ Hz), 2.30 (1H, d, $J = 6.9$

Hz). ^{13}C NMR (300 MHz, CDCl3): δ 205.7, 134.2, 133.5, 86.0, 77.8, 74.6, 59.7, 47.8, 45.4. HRMS (EI) m/z calcd for $C_9H_{12}O_3$ $[M+H]^+$ 169.0865, found 169.0888. IR (film): 2923, 1716, 1455, 1406, 1343, 1183, 1108, 1020, 917, 854, 734 cm^{-1}.

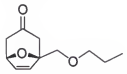

Figure 4-11. 1-Propoxymethyl-8-oxa-bicyclo[3.2.1]oct-6-en-3-one **(206c)**

2-Propoxymethyl-furan (1.005 g, 7.1 mmol) was placed in a dry 100 ml round bottom flask and cooled to 0°C. Via two separate syringes, solutions of trifluoroethoxide (2M, 15mL) and trichloroacetone (14.3 mmol, 1.5ml) in trifluoroethanol (7.5 ml) were added drop wise simultaneously, and the solution was allowed to warm to room temperature. The reaction was monitored by TLC using p-anisaldehyde as stain. Upon completion of the reaction an equal volume of water and dichloromethane was added, and the aqueous layers extracted 2 times with dichloromethane. The organic layers were combined and dried on MgSO4, filtered, and the solvent removed in vacuo. The crude dark orange/brown oil (7.39g) was placed in a 200 ml round bottom flask without purification. To the crude, zinc/copper couple (10.23 g) and a solution of methanol saturated with ammonium chloride (80 ml) were added, and the mixture was allowed to reflux for two days. The mixture was then filtered through celite, washing with ethyl acetate, to remove the zinc/copper couple. The filtrate was then evaporated, and the residue partitioned between dichloromethane and a saturated solution of EDTA. The aqueous layers were extracted with dichloromethane. The organic layers were combined and dried on MgSO4, filtered, and the solvent removed in vacuo. The brown residue was then purified by silica gel chromatography using gradient elution (60: 1 silica gel: residue

adsorbed on silica; (95: 5 - 3: 1 hexanes: ethyl acetate) to give **206c** as a dark yellow oil (1.271 g, 81 % over 2 steps). R*f* = 0.13 (85: 15 hexanes : ethyl acetate). ^{1}H NMR (300 MHz, CDCl3): δ 6.26 (1H,d, *J* = 5.8), 6.11 (1H, d, *J* = 5.8), 5.10 (1H,d, *J* = 4.4), 3.65 (2H, s), 3.52-3.46 (2H, m), 2.78-2.69 (2H,m), 2.33 (2H, t, *J* = 16.9 Hz), 1.62 (2H sextet, *J* = 7.0 Hz), 0.95 – 0.90 (3H,m).^{13}C NMR (300 MHz, CDCl3): δ 205.8, 134.0, 133.7, 86.0, 77.8, 73.6, 72.7, 47.9, 45.3, 22.6, 10.5. HRMS (EI) m/z calcd for $C_{11}H_{17}O_3$ $[M+H]^+$ 197.1178, found 197.1183. IR (film): 2963, 2876, 1716, 1341, 1113, 917, 854, 733 cm^{-1}.

Figure 4-12. *tert*-Butyl-dimethyl-(1-methyl-8-oxa-bicyclo[3.2.1]oct-6-en-3-yloxy)silane **(207a)**

1-Methyl-8-oxa-bicyclo[3.2.1]oct-6-en-3-ol **207c** (0.6044 g, 4.28 mmol) was dissolved in dichloromethane (4.3 ml). The solution was then cooled to 0°C and 2,6-lutidine (0.99 ml, 8.56 mmol) was added slowly, followed by the drop wise addition of tert-butyldimethylsilyltrifluoromethanesulfonate (1.5 ml, 6.422 mmol). The reaction was monitored by TLC. Upon completion of the reaction, the solvent was evaporated under reduced pressure and the residue was triturated with hexane. The hexane layers were combined and concentrated under reduced pressure. The residue was purified by silica gel chromatography, using gradient elution (60:1silica gel: residue; 100:0 – 98: 2 hexane: ethyl acetate) giving **207a** as a colorless oil (0.9838 g, 90%). R*f* = 0.43 (90: 10 hexane: ethyl acetate). ^{1}H NMR (300 MHz, CDCl3): δ 6.10 (1H, dd, *J* = 5.8 Hz, 1.2Hz), 5.92 (1H, d, *J* = 5.8), 4.72 (1H, s), 4.08-4.04 (1H,m), 2.10-2.02 (1H, m), 1.92 (1H, dd, *J* = 14.0 Hz, 5.3 Hz), 1.58 (1H, d, *J* = 14.0), 1.46 (1H, d, *J* = 14.0), 1.32 (3H,s), 0.84 (6H,

s), -0.04 (9H, s). ^{13}C NMR (300 MHz, CDCl3): δ 136.9, 133.8, 82.8, 79.1, 65.2, 42.7, 35.5, 25.9, 24.5, 17.9, -4.7. HRMS (EI) calcd for $C_{14}H_{26}O_2Si$ $[M]^+$ 254.1702, found 254.1695. IR (film): 3440, 2953, 2930, 2857, 1721, 1472, 1377, 1256, 1132, 1083, 1056, 859, 836, 774, 720, 682 cm^{-1}.

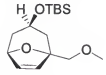

Figure 4-13. *tert*-Butyl-(1-methoxymethyl-8-oxa-bicyclo[3.2.1]oct-6-en-3-yloxy)-dimethyl-silane **(207b)**

1-Methoxymethyl-8-oxa-bicyclo[3.2.1]oct-6-en-3-ol **207d** (0.1335 g, 0.78 mmol) was dissolved in dichloromethane (0.79 ml). The solution was cooled to 0°C and 2,6-lutidine (0.18 ml, 1.58 mmol) was added slowly followed by the drop wise addition of tert-butyldimethylsilyltrifluoromethanesulfonate (0.27 ml, 1.18 mmol). The reaction was monitored by TLC. Upon completion of the reaction, the solvent was evaporated under reduced pressure and the residue was triturated with hexane. The hexane layers were combined and concentrated under reduced pressure. The residue was purified by silica gel chromatography using gradient elution (60:1 silica gel: residue; 100: 1 – 95: 5 hexane: ethyl acetate) gave **207b** as a colorless oil (0.1952 g, 88%). R_f = 0.13 (95: 5 hexane: ethyl acetate). ^1H NMR (300 MHz, CDCl3): δ 6.22 (1H, dd, J = 5.7, 0.9 Hz), 6.01 (1H, d, J = 5.7Hz), 4.819 (1H, s), 4.16-4.12 (1H, m), 3.50 (2H, AB quartet, J = 10.2 Hz), 3.44 (3H,s), 2.19-2.05 (2H, m), 1.56-1.50 (2H,m), 0.88 (9H, s), 0.00 (6H, s). ^{13}C NMR (300 MHz, CDCl3): δ 134.7, 133.7, 85.3, 79.1, 76.4, 64.8, 59.7, 37.4, 35.6, 25.8, 17.9, -4.8. HRMS (EI) calcd for $C_{15}H_{28}O_3Si$ $[M]^+$ 284.1823, found 284.1823. IR

(film): 2953, 2929, 1472, 1463, 1255, 1116, 1044, 836, 774, 727 cm^{-1}. Teoric CH calcd for $C_{15}H_{28}O_3Si$. C, 63.33; H, 9.92, found: C, 63.56, H, 10.05.

Figure 4-14. *endo*-1-Methyl-8-oxa-bicyclo[3.2.1]oct-6-en-3ol **(207c)**

A solution of oxabicyclic ketone **206a** (0.5150g, 3.7 mmol) in THF (4 ml) was cooled to –78°C. L-selectride (1 M in THF, 5.5 ml) was added drop wise. After 1 hour the reaction was allowed to reach room temperature. After 3 hours the reaction was cooled to 0°C and a solution of 2: 1, 20% NaOH and 30% H_2O_2 was added slowly. After 1 hour, the solution was neutralized with 2 M H_2SO_4. The aqueous layers were saturated with NaCl and extracted several times with ethyl acetate. The organic layers were combined, dried on $MgSO_4$, filtered, and concentrated under reduced pressure. The residue was purified by silica gel chromatography using gradient elution (50: 1silica gel; residue; 75:25 to 60: 40 hexane: ethyl acetate) gave **207c** as a colorless oil (0.4362 g, 83%). R*f* = 0.13 (65: 35 hexanes: ethyl acetate.^{1}H NMR (300 MHz, $CDCL_3$): δ 6.42 (1H,dd, *J* = 5.85Hz, 1.76Hz), 6.22 (1H, d, *J* = 5.84Hz), 4.81-4.80 (1H, m), 4.02-3.99 (1H, m), 2.30 (1H, bs), 1.37(3H,s). ^{13}C NMR (CDCl3): δ 138.8, 135.8, 82.8, 78.8, 65.7, 42.4, 35.3, 24.0. HRMS (EI) calcd for $C_8H_{12}O_2$ $[M-H]^+$ 139.0759, found 139.0765. IR (film): 3426, 2934, 1718, 1650, 1345, 1041, 917, 872, 815 cm-1.

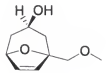

Figure 4-15. 1-Methoxymethyl-8-oxa-bicyclo[3.2.1]oct-6-en-3-ol **(207d)**

A solution of oxabicyclic ketone **206b** (0.4000 g, 2.4 mmol) in THF (2.4 ml) was cooled to –78°C. L-selectride (1M in THF, 3.1ml) was added drop wise. After 1 hour the reaction was allowed to reach room temperature. After 12 hours the reaction was cooled to 0°C and a solution of 2:1, 20% NaOH and 30% H_2O_2 was added slowly. After 1 hour, the solution was neutralized with 2M H_2SO_4. The aqueous layers were saturated with NaCl and extracted several times with ethyl acetate. The organic layers were combined, dried on $MgSO_4$, filtered, and concentrated under reduced pressure. The residue was purified by silica gel chromatography using gradient elution (50:1silica gel; residue; 90:10 to 50: 50 ethyl hexane: ethyl acetate) gave **207d** as a pale yellow oil (0.3763 g, 93%). R*f* = 0.13 (60: 40 ethyl acetate: hexane). ^{1}H NMR (300 MHz, CDCl3): δ 6.44 (1H, d, *J* = 5.9), 6.25 (1H, d, *J* = 5.9), 4.82 (1H,d, *J* = 1.9), 4.04-4.01 (1H, m), 3.51-3.43 (2H, ABquartet, *J* = 10.22 Hz), 3.38 (3H, d, *J* = 0.5), 2.40-2.08 (3H, m), 1.74-1.65 (2H, m). ^{13}C NMR (CDCl3): δ 136.1, 135.4, 85.1, 78.6, 75.6, 64.9, 59.5, 37.1, 35.1. HRMS (EI) calcd for $C_9H_{14}O_3$ $[M+H]^+$ 171.1055, found 170.1054. IR (film): 3437, 2923, 1651, 1455, 1348, 1193, 1107, 1035, 975, 870, 736, 696 cm-1.

Figure 4-16. *exo*-1-Methyl-8-oxa-bicyclo[3.2.1]oct-6-en-3ol **(207e)**

In a flame dry 3neck flask **206a** (0.3153g, 2.28mmol) were mixed with 0.2 ml (2.28 mmol) of isopropanol. A condenser was fitted and the mixture was degassed. Then

46 ml (4.56 mmol) of 0.1 M solution of SmI_2 in THF was added under an argon atmosphere. The deep blue solution was allowed to reflux for 5 hours. Upon completion the reaction turned yellow color. The reaction was worked up by adding a small amount of water, and then the solvent was evaporated under reduced pressure to almost completion. To the residue ethyl acetate and brine solution was added. The mixture was then filtered trough celite. The filtered was extracted with ethyl acetate, dried with magnesium sulfate, filtered and concentrated under reduced pressure to give a dark yellow oil that was purify by silica gel chromatography using gradient elution (75: 25–60:40 hexane: ethyl acetate; residue adsorbed on silica) gave 11e as a pale yellow color (0.1659g, 57%). R*f* = 0.20 (65:35 hexane: ethyl acetate). ^{1}H NMR (300 MHz, $CDCl_3$): δ 6.04 (1H, dd, *J* = 5.84Hz, 1.75Hz), 5.88 (1H, d, *J* = 6.14Hz), 4.82-4.81 (1H, m), 3.87-3.76 (1H, m), 2.99(1H, s), 1.99-1.87 (2H, m), 1.58-1.37(2H, m), 1.40 (3H, s). ^{13}C NMR (CDCl3): δ 134.8, 131.1, 83.6, 78.7, 65.3, 42.0, 34.8, 23.9. HRMS (EI) calcd for $C_8H_{12}O_2$ $[M]^+$ 140.0837, found 140.0837. IR (film): 3393, 2969, 2847, 1650, 1453, 1378, 1063, 869, 820 cm^{-}1.

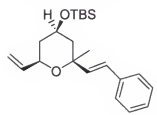

Figure 4-17. *tert*-Butyl-dimethyl-(2-methyl-2-styryl-6-vinyl-tetrahydro-pyran-4-yloxy)-silane **(208a)**

A solution of tert-Butyl-dimethyl- (1-methyl-8-oxa-bicyclo[3.2.1]oct-6-en-3-yloxy)-silane **207a** (0.4031g, 1.57 mmol) in dichloromethane (5 ml) was prepared. Styrene (0.72 ml, 6.29 mmol) was added followed by the addition of a solution of Grubbs catalyst **67** (18 mg, 0.021 mmol) in dichloromethane (0.2 ml). The reaction was

monitored by TLC, after 2 hours, the reaction reached equilibrium. After 12 hours, the solvent was evaporated under reduced pressure and the residue purified by silica gel chromatography using gradient elution (100: 1 silica gel: residue adsorbed on silica; 100: 0 – 98: 2 hexane: ethyl acetate) gave an inseparable mixture of **208a** and **208a** in a ratio of 6:1 as determined by GC/MS as a bright yellow oil (0.4690 g, 83%). R*f* = 0.25 (95: 5 hexane: ethyl acetate). ^{1}H NMR (300 MHz, $CDCL_3$): δ 7.175-7.395 (5H, m), 6.58 (1H, d, *J* = 16.2), 6.29 (1H, d, *J* = 16.2), 5.91 (1H, ddd, J= 17.2 Hz, 10.5 Hz, 5.9 Hz), 5.30 (1H, d, *J* = 17.2 Hz), 5.13 (1H, d, *J* = 10.5 Hz), 4.20-4.00 (2H, m), 1.93-1.84 (2H,m), 1.59-1.26 (2H,m), 1.40 (3H,s), 0.90 (9H, s), 0.09 (6 H, s). ^{13}C NMR ($CDCl_3$): δ 139.6, 137.6, 130.8, 128.9, 127.7, 126.8. HRMS (EI) calcd for $C_{22}H_{24}SiO_2$ $[M]^+$ 358.2328, found 358.2335. IR (film): 2952, 2929, 2857, 1601, 1495, 1472, 1463, 1449, 1377, 1255, 1082, 967, 862, 837, 776, 747, 693 cm^{1}.

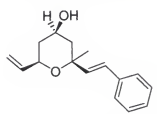

Figure 4-18. 2-Methyl-2-styryl-6-vinyl-tetrahydro-pyran-4-ol **(208c)**

In a 5 ml round bottom flask a solution of 1-Methyl-8-oxa-bicyclo[3.2.1]oct-6-en-3-ol **207c** (0.1135 g, 0.809 mmol) in dichloromethane (2.2 ml) was prepared. To that solution styrene (0.24 ml, 2.14 mmol) was added, followed by the addition of a solution of Grubbs catalyst **67** (10 mg, 0.011 mmol) in dichloromethane (0.2 ml). The resulted solution was allowed to stir under argon at room temperature. The reaction was monitored by TLC, after 5 hours an extra volume of styrene (0.07 ml, 0.610 mmol) was added. The reaction was monitored by TLC. After 8 hours no further reaction occurred.

After 12 hours, the solvent was evaporated under reduced pressure and the residue purified by silica gel chromatography using gradient elution (100: 1 silica gel; residue adsorbed on silica; 95:5 – 85: 15 hexane: ethyl acetate) gave an inseparable mixture of **208c** and **209c** in a ratio of 20:1 as determined by GC/MS as a white solid (0.1677 g, 85%). Major: R*f* = 0.43 (6: 4 Hexane: ethyl acetate). m.p. = (98-101) °C. ^{1}H NMR (300 MHz, $CDCl_3$): δ 7.40-7.19 (5H, m), 6.60 (1H, d, *J* = 16.2), 6.31 (1H, d, *J* = 16.2), 5.93 (1H, ddd, *J* = 17.4 Hz, 10.5 Hz, 5.7 Hz), 5.32 (1H, dd, *J* = 17.4 Hz, 1.2Hz), 5.16 (1H, dd, *J* = 10.5 Hz, 1.2 Hz), 4.22-4.04 (2H, m), 2.09-2.00 (2H, m), 1.58 (1H,bs), 1.40 (3H,s), 1.49-1.21 (2H, m), ^{13}C NMR ($CDCl_3$): δ 139.0, 137.26, 137.0, 128.7, 127.6, 126.9, 126.7, 115.4, 75.2, 70.7, 65.7, 44.5, 41.6, 22.3. HRMS (EI) m/z calcd for $C_{16}H_{20}O_2$ $[M]^+$ 244.1463, found 244.1459. IR (film): 3373, 2944, 1448, 1373, 1062, 1026, 968, 922, 748, 694 cm^{-1}. Theoretical CH calcd for $C_{16}H_{20}O_2$: C, 78.65; H, 8.25; found: C 78.32; H 8.32.

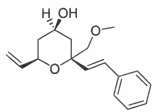

Figure 4-19. 2-Methoxymethyl-2-styryl-6-vinyl-tetrahydro-pyran-4-ol **(208d)**

A solution of 1-Methoxymethyl-8-oxa-bicyclo[3.2.1]oct-6-en-3-ol **207d** (0.0925g, 0.543 mmol) in dichloromethane (1.4 ml) was prepared. Styrene (0.19 mL, 1.629 mmol) was added, followed by the addition of a solution of Grubbs catalyst **67** (6.9mg, 0.0081mmol) in dichloromethane (0.2 ml). After 5 hours an extra volume of styrene (0.08mL, 0.698 mmol) was added. The reaction was monitored by TLC and it reached equilibrium after 8 hours. After 12 hours, the solvent was evaporated under reduced

pressure and the residue purified by silica gel chromatography using gradient elution (100: 1 silica gel: residue adsorbed on silica; gradient, 98: 2 – 3: 1 hexane: ethyl acetate) gave an inseparable mixture of **208d** and **209d** in a ratio of 20:1 as determined by GC/MS as a semi-solid (0.0985 g, 66%). Unreacted starting material **207d** (21mg) was recovered. R*f* = 0.33 (60:40 hexane: ethyl acetate). ^{1}H NMR (300 MHz, $CDCL_3$): δ 7.40-7.17 (5H, m), 6.67 (1H, d, *J* = 16.1), 6.32 (1H, d, *J* = 16.1), 5.91 (1H, ddd, *J* = 17.23 Hz, 10.52 Hz, 5.55 Hz), 5.31 (1H, d, *J* = 17.23 Hz), 5.14 (1H, d, *J* = 10.52 Hz), 4.27 (1H,dd, *J* = 10.8 Hz, 4.7 Hz), 4.14-4.07 (1H, m), 3.52 (2H, s), 3.34 (3H, s), 2.30-2.24(1H, m), 2.07-2.01 (1H, m), 1.807 (1H,bs), 1.43-1.21 (2 H, m). ^{13}C NMR (CDCl3): δ 138.8, 137.1, 133.6, 128.5, 128.0, 127.5, 126.6, 115.3, 76.8, 75.2, 71.7, 65.1, 59.6, 41.0, 40.7. HRMS (EI) calcd for $C_{17}H_{22}O_3$ $[M]^+$ 274.1569, found 274.1524. IR (film): 3391, 2924, 1496, 1449, 1368, 1106, 1063, 1026, 969, 923, 750, 695.

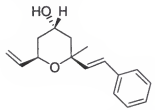

Figure 4-20. 2-Methyl-2-styryl-6-vinyl-tetrahydro-pyran-4-ol **(208e)**

exo-1-Methyl-8-oxa-bicyclo[3.2.1]oct-6-en-3-ol **207e** (0.070 g,0.499 mmol) in dichloromethane (0.62 ml) was prepared. Styrene (0.17 ml, 1.50 mmol) was added followed by the addition of a solution of Grubbs catalyst **67** (6.4 mg, 0.008 mmol) in dichloromethane (0.3 ml). The reaction was monitored by TLC, after 5 hours an extra volume of styrene (0.05 ml, 0.436 mmol) was added. After 12 hours, the reaction did not reach completion. The reaction solvent was evaporated under reduced pressure and the residue purified by silica gel chromatography using gradient elution (150: 1 silica gel:

residue adsorbed on silica; 100: 0 – 3: 1 hexane: ethyl acetate) gave an inseparable mixture of **208e** and **209e** in a ratio of 6:1 as determined by GC/MS as a semi-solid (0.0182 g, 15%). Unreacted starting material **207e** (50 mg) was recovered. R*f* = 0.11 (2: 8 ethyl acetate: hexane). ^{1}H NMR (300 MHz, $CDCL_3$): δ 7.40-7.18 (5H, m), 6.55 (1H, d, *J* = 16.2), 6.28 (1H, d, *J* = 16.2), 5.95 (1H, ddd, *J* = 17.2 Hz, 10.5 Hz, 5.9 Hz), 5.33 (1H, ddd, *J* = 17.2 Hz, 3.1 Hz, 1.1 Hz), 5.14 (1H, ddd, *J* = 10.5 Hz, 2.82 Hz, 1.28Hz), 4.63-4.57 (1H, m), 4.34-4.31 (1H, m), 1.83-1.65 (7 H, m), ^{13}C NMR (CDCl3): δ 139.8, 138.2, 137.5, 128.7, 127.4, 126.6, 126.4, 115.2, 73.6, 67.0, 65.1, 41.1, 38.4, 24.8. HRMS (EI) calcd for $C_{16}H_{20}O_2$ $[M]^+$ 244.1463, found 244.1459. IR (film): 3433, 2923, 1722, 1494, 1448, 1277, 1050, 988, 968, 923, 747, 693 cm^{-1}.

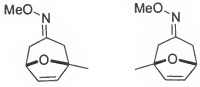

Figure 4-21. *cis* and *trans* 1-Methyl-8-oxa-bicyclo[3.2.1]oct-6-en-3-one O-methyl-oxime **(213a, 213b)**

1-Methyl-8-oxa-bicyclo[3.2.1]oct-6-en-3-one **206a** (0.5120, 3.70 mmol) was dissolved in 12mL of dry CH_2Cl_2 and, mixed with methoxylamine hydrochloride (0.6301, 7.5 mmol) and 3A° molecular sieves. Then 0.62 ml of pyridine was added, a condenser was fixed and the reaction mixture was allowed to reflux for two days. Upon completion of the reaction by TLC, the reaction was diluted in CH_2Cl_2; the resulting powdering molecular sieves were filtered. The filtered liquid was washed with brine and dried over $MgSO_4$, filtered trough a small plug of silica gel and concentrated to achieve pale yellow oil (0.4530g, 73%) of 1:1 ratio of **213a** and **213b**. The isomers were separated by chromatography using gradient elution of (98:2 – 95:5 ether: hexanes).

trans-1-Methyl-8-oxa-bicyclo[3.2.1]oct-6-en-3-one O-methyl-oxime (**213a**)

R*f* = 0.61 (65: 35 hexane: ethyl acetate). ^{1}H NMR (300 MHz, $CDCL_3$): δ 6.11 (1H, dd, *J* = 5.9Hz, 1.7Hz), 5.98 (1H, d, *J* = 5.9Hz), δ 4.88 (1H, dt, *J* = 4.8Hz, 1.2Hz), 3.78 (3H, s), 2.89 (1H, d, *J* = 16.2 Hz), 2.41 (1H, d, *J* = 15.2 Hz), 2.32 (1H, d, *J* = 15.0Hz), 2.29 (1H,ddt, *J* =16.2Hz, 4,8Hz, 1.2Hz), 1.45 (3H, s). ^{13}C NMR (CDCl3): δ 154.6, 135.7, 133.3, 83.8, 77.7, 61.4, 40.5, 29.4, 23.4. HRMS (EI) calcd for $C_9H_{13}NO_2$ $[M]^+$ 167.0946, found 167.0949. IR (film): 2919, 2850, 2360, 2359, 1463, 1264, 1050, 745 cm^{-1}.

cis-1-Methyl-8-oxa-bicyclo[3.2.1]oct-6-en-3-one O-methyl-oxime (**213b**)

R*f* = 0.55 (65: 35 hexane: ethyl acetate). ^{1}H NMR (300 MHz, $CDCL_3$): δ 6.13 (1H, dd, *J* = 6.0Hz, 1.4Hz), 5.98 (1H, d, *J* = 6.0Hz), 4.92 (1H, d, *J* = 4.3Hz), 3.78 (3H, s), 3.02 (1H, d, *J* = 16.2 Hz), 2.60 (1H, dd, *J* = 15.5 Hz, 4.5 Hz), 2.22 (1H, d, *J* = 15.5 Hz), 2.11 (1H, d, *J* = 16.2 Hz). ^{13}C NMR (CDCl3): δ 154.6, 136.5, 132.4, 82.6, 78.7, 61.3, 36.2, 33.5, 23.2. HRMS (EI) calcd for $C_9H_{13}NO_2$ $[M]^+$ 167.0946, found 167.0942. IR (film): 2964, 2908, 2820, 1379, 1073, 1054, 1024, 951, 942, 865 cm^{-1}.

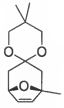

Figure 4-22. 1-Methyl-8-oxa-bicyclo[3.2.1]oct-6-en-3-(2,2-dimethyldioxane) ketal (**214**)

In a 2-neck flask, **206a** (0.8085g, 5.86mmol) was dissolved in 6ml of 2,2,5,5-tetramethyl-1,3-dioxane. *p*-TsOH·H_2O (0.0444g, 0.234mmol, 0.04 equiv.) was added. The flask was connected to a reduced pressure vacuum regulated to 28mmHg to remove the liberated acetone. The colorless solution started to turn pale pink-orange color to a dark pink-orange color. The reaction was allowed to stir under reduced pressure

overnight. After no further reaction was observed it was quenched with Et_3N (36µl, 0.0237 g, 0.234 mmol). Then the solvent was evaporated under reduced pressure and the residue was purify by silica gel chromatography using gradient elution (100:1 silica gel; residue; 98: 2 to 70: 30 hexane: ethyl acetate) gave **214** as a colorless oil (0.4365g, 33%). Some starting material was recovered, the rest decomposed. R*f* = 0.243 (60: 40 hexanes: ether). ^{1}H NMR (300 MHz, $CDCL_3$): δ 6.06 (1H, dd, *J* = 5.8Hz, 1.8Hz), 5.91 (1H, d, *J* = 5.8Hz), 4.82-4.81 (1H, m), 3.43 (4H, d, *J* = 3.2Hz), 2.24 (1H, d, *J* = 14.2 Hz), 2.19 (1H, d, *J* = 13.2 Hz), 1.91(1H, dd, *J* = 13.9Hz, 4.7Hz), 1.77 (1H, d, *J* = 14.0Hz), 1.39 (3H, s), 0.93 (6H, d, *J* = 9.6Hz). ^{13}C NMR (CDCl3): δ 135.8, 132.5, 97.2, 82.5, 78.0, 69.8, 69.7, 43.2, 35.5, 29.9, 24.0, 22.82, 22.76. HRMS (EI) calcd for $C_{13}H_{20}O_3$ $[M]^+$ 224.1412, found 224.1430. IR (film): 3078, 2953, 2930, 2868, 1602, 1471, 1344, 1099 cm^{-1}. Theoretical CH calcd for $C_{13}H_{20}O_3$: C, 69.61; H, 8.99, found: C, 69.19; H, 9.02.

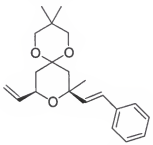

Figure 4-23. 3,3,8-Trimethyl-8-styryl-10-vinyl-1,5,9-trioxa-spiro[5.5]undecane **(215)**

A solution of 1-methyl-8-oxa-bicyclo[3.2.1]oct-6-en-3-(2,2-dimethyldioxane) ketal **214** (0.049 g, 0.22 mmol) in dichloromethane (0.53 ml) was prepared. Styrene (0.1 ml, 0.88 mmol) was added followed by the addition of a solution of Grubbs catalyst **67** (3 mg, 0.003 mmol) in dichloromethane (0.1 ml). The reaction was monitored by TLC, using p-anisaldehyde as stain. After 50 min, the solvent was evaporated under reduced

pressure and the residue purified by silica gel chromatography using gradient elution (100: 1 silica gel: residue adsorbed on silica; 100:0 – 95:5 hexane: ethyl acetate) gave a white semisolid (66 mg, 90%). R*f* = 0.68 (65:35 hexane : ethyl acetate). ^{1}H NMR (300 MHz, $CDCL_3$): δ 7.18-7.40 (5H, m), 6.58 (1H, d, *J* = 16.1), 6.27 (1H, d, *J* = 16.1), 5.93 (1H, ddd, *J* = 17.2 Hz, 10.5 Hz, 5.8 Hz), 5.34 (1H, dt, *J* = 17.2, 1.5 Hz), 5.16 (1H, dt, *J* = 10.5, 1.5 Hz), 4.35-4.41 (1H, m), 3.65-3.43 (4H, m), 2.46 (1H, dd, J=14.0, 2.6 Hz), 2.13 (1H, dt, *J* = 13.4, 2.3 Hz), 1.58-1.43 (2H, m), 1.50 (3H, s), 1.08 (3H, s), 0.91 (3H,s). ^{13}C NMR ($CDCl_3$): δ 139.0, 137.7, 137.3, 128.7, 127.4, 126.6, 126.6, 115.5, 96.7, 74.6, 70.5, 70.1, 69.2, 40.5, 39.0, 30.4, 23.2, 22.7, 22.2. HRMS (EI) calcd for $C_{21}H_{28}O_3$ $[M]^+$ 328.2038, found 328.2033. IR (film): 2960, 2934, 2865, 1090, 913, 745, 694 cm^{-1}.

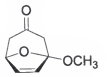

Figure 4-24. 1-Methoxy-8-oxa-bicyclo[3.2.1]oct-6-en-3-one **(235)**

2-Methoxyfuran **233** (1.25 g, 12.7 mmol) was placed in a 3-neck round bottom flask and cooled to 0°C. Via two separate addition funnels, solutions of trifluoroethoxide (2M, 12.7 ml) and trichloroacetone (19.1 mmol, 2.0 ml) in trifluoroethanol were added dropwise simultaneously. After the addition was completed, the solution was allowed to warm to room temperature. The reaction was monitored by TLC using p-anisaldehyde as stain. Upon completion of the reaction, an equal volume of water and dichloromethane was added, and the aqueous layers extracted twice with dichloromethane. The organic layers were combined and dried on $MgSO_4$, filtered, and the solvent removed *in vacuo*. The crude dark orange/brown oil is filtered through a bed of silica gel, eluding with 70: 30 hexanes: ethyl acetate. The filtered was concentrated under reduced pressure in a

rotary evaporator. The pale yellow solid was diluted with methanol, and zinc/copper couple (2.51 g) was added. The mixture was allowed to reflux for 4 hours. The mixture was then filtered through celite, eluding with ethyl acetate, to remove the zinc/copper couple. The filtrate was then evaporated to almost completion. Then the residue is adsorbed on silica and purified by silica gel chromatography using gradient elution (40: 1 silica gel; 90: 10 - 80: 25 hexanes: ethyl acetate) to give pale yellow oil (0.74 g, 37 % over 2 steps). R*f* = 0.57 (40: 60 hexanes: diethyl ether). ^{1}H NMR (300 MHz, CDCl3): δ 6.35 (1H, dd, *J* = 6.0, 2.5 Hz), 6.12 (1H, dd, *J* = 5.8, 0.6 Hz), 5.08-5.06 (1H, m), 3.43 (3H, s), 2.75-2.59 (3H, m), 2.28 (1H, dt, *J* = 16.4, 1.5 Hz). ^{13}C NMR (300 MHz, CDCl3): δ 205.4, 136.7, 132.6, 109.9, 74.8, 51.9, 51.8, 44.2. HRMS (EI) m/z calcd for $C_8H_{10}O_3$ $[M]^+$ 154.0630, found 154.0623. IR (film): 2976, 2913, 2838, 1718, 1338, 1172, 1043, 851, 728 cm^{-1}.

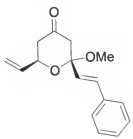

Figure 4-25. *endo*-1-Methyl-8-oxa-bicyclo[3.2.1]oct-6-en-3ol **(236)**

In an NMR tube, a solution of oxabicycle ketone **235** (33 mg, 0.21 mmol) and styrene (0.1 ml, 0.84 mmol) in deuterated chloroform (0.5 ml) was prepared. To the solution, grubbs catalyst **67** (3 mg, 0.0031 mmol) in deuterated chloroform (0.1 ml) was added. The resulted solution was allowed to stir under argon at room temperature for 5 days. The solvent was evaporated under reduced pressure and the residue purified by silica gel chromatography using gradient elution of ethyl acetate and hexane mixture,

affording **236** as a colorless oil (11 mg, 20 %). Starting material **235** was also recovered. ^{1}H NMR (300 MHz, $CDCL_3$): δ 7.45-7.26 (5H, m), 6.87 (1H, d, J = 16.2 Hz), 6.13 (1H, d, J = 16.2 Hz), 6.02 (1H, ddd, J = 17.0, 10.5, 5.9 Hz), 5.42 (1H, dt, J = 17.2, 1.3 Hz), 5.28 (1H, dt, J = 10.5, 1.3 Hz), 4.49-4.43 (1H, m), 3.19 (3H, s), 2.70-2.37 (4H, m). ^{13}C NMR ($CDCl_3$): δ 204.5, 137.1, 135.9, 132.8, 128.9, 128.5, 127.8, 127.0, 116.7, 101.5, 70.9, 51.8, 49.6, 46.6. HRMS (EI) m/z calcd for $C_{16}H_{18}O_3$ $[M]^+$ 258.1256, found 258.1250.

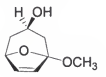

Figure 4-26. *endo*-1-Methyl-8-oxa-bicyclo[3.2.1]oct-6-en-3ol **(237)**

A solution of oxabicyclic ketone **235** (0.30 g, 1.95 mmol) in THF (2 ml) was cooled to –78°C. L-selectride (1M in THF, 2.35 ml) was added drop wise. After 1 hour the reaction was allowed to reach room temperature. After 3 hours the reaction was cooled to 0°C and a solution of 2: 1, 20% NaOH and 30% H_2O_2 was added slowly. After 1 hour, the solution was neutralized with 2M H_2SO_4. The aqueous layers were saturated with NaCl and extracted several times with ethyl acetate. The organic layers were combined, dried on $MgSO^4$, filtered, and concentrated under reduced pressure. The residue was purified by silica gel chromatography using gradient elution (30: 1silica gel; residue; 90:10 to 70: 30 hexane: ethyl acetate) gave **237** as a pale yellow oil (0.26 g, 86%). Rf = 0.18 (40: 60 hexanes: ethyl acetate. ^{1}H NMR (300 MHz, $CDCL_3$): δ 6.54 (1H, dd, J = 5.9 Hz, 2.04 Hz), 6.25 (1H, d, J = 5.9 Hz), 4.90-4.87 (1H, m), 4.17-4.13 (1H, m), 3.37 (3H, s), 2.35-2.15 (1H, m), 2.15 (1H, d, J = 6.1 Hz), 1.98 (1H, d, J = 14.1 Hz), 1.65 (1H, dd, J = 14.6 Hz, 1.2 Hz). ^{13}C NMR (CDCl3): δ 138.9, 134.6, 109.4, 78.1, 66.1,

50.9, 41.1, 35.4. HRMS (EI) calcd for $C_8H_{13}O_3$ $[M+H]^+$ 157.0864, found 157.0869. IR (film): 3432, 2929, 1667, 1342, 1174, 1108, 1018, 816 cm^{-1}.

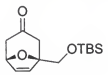

Figure 4-27. 1-(*tert*-Butyl-dimethyl-silanyloxymethyl)-8-oxa-bicyclo[3.2.1]oct-6-en-3-one **(241)**

tert-Butyl-(furan-2-ylmethoxy)-dimethyl-silane **240** (7.8243g, 36.9mmol) was placed in a 3-neck round bottom flask and cooled to 0°C. Via two separate addition funnels, solutions of trifluoroethoxide (2 M, 221.4 ml) and trichloroacetone (442.8 mmol, 23.42 ml) in trifluoroethanol (190.0 ml) were added dropwise simultaneously. After the addition was completed, the solution was allowed to warm to room temperature. The reaction was monitored by TLC using p-anisaldehyde as stain. Upon completion of the reaction an equal volume of water and dichloromethane was added, and the aqueous layers extracted 2 times with dichloromethane. The organic layers were combined and dried on $MgSO_4$, filtered, and the solvent removed in vacuo. The crude dark orange/brown oil was placed in a 500 ml round bottom flask without purification. To the crude, zinc/copper couple (58 g) and a solution of methanol saturated with ammonium chloride (250 ml) were added, and the mixture was allowed to reflux for two days. The mixture was then filtered through celite, eluding with ethyl acetate, to remove the zinc/copper couple. The filtrate was then evaporated to almost completion. Then the residue is adsorbed on silica and purified by silica gel chromatography using gradient elution (40: 1 silica gel; 90: 10 - 75: 25 hexanes: ethyl acetate) to give yellow oil (9.0 g, 90 % over 2 steps). $Rf = 0.21$ (85: 15 hexanes: diethyl ether). ^1H NMR (300 MHz, CDCl3): δ 6.23 (1H,dd, $J = 5.9, 1.5$ Hz), 6.11 (1H, d, $J = 5.9$ Hz), 5.08 (1H, d, $J = 5.1$

Hz), 3.81 (2H, d, J = 1.8 Hz), 2.72 (1H, dd, J = 16.4, 5.1 Hz), 2.68 (1H, d, J = 15.9 Hz), 2.41 (1H, d, J = 16.4 Hz), 2.30 (1H, d, J = 16.4 Hz), 0.90 (9H, s), 0.08 (6H, s). ^{13}C NMR (300 MHz, CDCl3): δ 206.5, 134.0, 133.9, 86.9, 77.9, 66.1, 48.2, 45.6, 26.0, 18.5, -5.2. HRMS (EI) m/z calcd for $C_{10}H_{15}O_3$ $[M-C_4H_9]^+$ 211.0790, found 211.0781. IR (film): 2955, 2929, 2857, 1717, 1103, 839, 778 cm^{-1}.

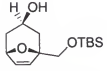

Figure 4-28. exo-1-(*tert*-Butyl-dimethyl-silanyloxymethyl)-8-oxa-bicyclo[3.2.1]oct-6-en-3-ol **(242)**

In a flame dry 2neck flask **241** (0.5000 g, 1.86 mmol) were mixed with 0.3 ml (3.73 mmol) of isopropanol. A condenser was fitted and the mixture was degassed. Then 40 ml (4.0 mmol) of 0.1 M solution of SmI_2 in THF was added under an argon atmosphere. The deep blue solution was allowed to reflux overnight. The reaction was worked up by adding a small amount of water, and then the solvent was evaporated under reduced pressure to almost completion. To the residue, ethyl acetate and brine solution were added. The mixture was then filtered trough celite. The filtered was extracted with ethyl acetate, dried with magnesium sulfate, filtered and concentrated under reduced pressure to give a dark yellow oil that was purify by silica gel chromatography, yielding **242** as a pale yellow color (0.20g, 40%). Rf = 0.10 (70:30 hexane: ethyl acetate). ^{1}H NMR (300 MHz, $CDCL_3$): δ 6.06 (1H, dd, J = 5.9Hz, 1.7Hz), 5.98 (1H, d, J = 5.9Hz), 4.83-4.82 (1H, m), 3. 88-3.77 (1H, m), 3.69 (2H, s), 2.30 (1H, bs), 2.04 (1H, dd, J =12.7, 6.1 Hz), 1.89 (1H, dd, J = 12.8, 6.4 Hz), 1.61-1.52 (1H, m), 1.41 (1H, dd, J = 12.7, 9.8 Hz), 0.91 (9H, s), 0.07 (6H, s). ^{13}C NMR ($CDCl_3$) : δ 132.2, 131.2, 86.9, 78.9, 67.0, 65.0, 37.1, 35.0, 26.0, 18.5, -5.3. HRMS (FAB) calcd for $C_{14}H_{26}O_3Si$ $[M]^+$ 271.1729,

found 271.1723. IR (film): 3388, 2952, 2928, 2857, 1471, 1462, 1253, 1103, 1052, 838, 779, 725 cm^{-1}.

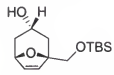

Figure 4-29. 1-(*tert*-Butyl-dimethyl-silanyloxymethyl)-8-oxabicyclo[3.2.1]oct-6-en-3-ol (**245**)

To a solution of **241** (1.0 g, 3.7 mmol) in THF (5.0 ml) at –78°C, L-selectride (1M in THF, 4.8 ml) was added drop wise. After 1 hour the reaction was allowed to reach room temperature. After 3 hours the reaction was cooled to 0°C and a solution of 2:1, 20% NaOH and 30% H_2O_2 was added slowly. After 0.5 hour, the solution was neutralized with 2M H_2SO_4. The aqueous layers were saturated with NaCl and extracted several times with ethyl acetate. The organic layers were combined, dried on $MgSO_4$, filtered, and concentrated under reduced pressure. The residue was purified by silica gel chromatography using gradient elution (40:1silica gel; residue; 90:10 to 85: 15 ethyl hexane: ethyl acetate) gave **245** as a pasty colorless oil (0.9194 g, 90%). R_f = 0.42 (60: 40 ethyl acetate: hexane). ^{1}H NMR (300 MHz, CDCl3): δ 6.45 (1H, dd, J = 6.6, 1.8 Hz), 6.33 (1H, d, J = 5.9), 4.84-4.81 (1H, m), 4.09-4.02 (1H, m), 3.67 (2H, s), 2.22 (1H, dd, J = 14.8, 1.5 Hz), 2.22 (1H, dd, J = 14.9, 9.9 Hz), 1.87 (1H, d, J =14.6 Hz), 1.71 (1H, dd, J = 14.6, 1.17 Hz). ^{13}C NMR (300 MHz, CDCl3): δ 136.7, 136.3, 86.3, 79.0, 67.2, 65.9, 38.1, 26.1, 18.6, -5.1. HRMS (EI) calcd for $C_{14}H_{26}O_3Si$ $[M-C_4H_9]^+$ 213.0947, found 213.0930. IR (film): 3436, 2956, 2938, 2864, 1478, 1282, 1260, 1170, 1096, 846, 778, 696 cm^{-1}.

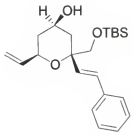

Figure 4-30. 2-(tert-Butyl-dimethyl-silanyloxymethyl)-2-styryl-6-vinyl-tetrahydro-pyran-4-ol **(246)**

In a 25 ml round bottom flask, a solution of *endo*-1-(tert-Butyl-dimethyl-silanyloxymethyl)-8-oxabicyclo[3.2.1]oct-6-en-3-ol **245**, (1.04 g, 3.85 mmol) and styrene (0.24 ml, 2.14 mmol) in dichloromethane (11.0 ml) was prepared. To the solution, Grubbs catalyst **67** (65 mg, 0.08 mmol) in dichloromethane (1.0 ml) was added. The resulted solution was allowed to stir under argon at room temperature for 10 hours. The solvent was evaporated under reduced pressure and the residue purified by silica gel chromatography using gradient elution (40: 1 silica gel; residue adsorbed on silica; 100:0 – 85: 15 hexane: ethyl acetate) gave **246** as a viscous colorless oil (1.13 g, 78%) and 81 mg of starting material **245** were recovered. R*f* = 0.19 (80: 20 Hexane: ethyl acetate). ^{1}H NMR (300 MHz, $CDCL_3$): δ 7.30-7.18 (5H, m), 6.65 (1H, d, *J* = 16.4 Hz), 6.33 (1H, d, *J* = 16.4 Hz), 5.91 (1H, ddd, *J* = 17.2, 10.5, 5.8 Hz), 5.32 (1H, dt, *J* = 17.2, 1.5 Hz), 5.15 (1H, dt, *J* = 10.5, 1.5 Hz), 4.35-4.30 (1H, m), 4.23-4.12 (1H, m), 3.86 (1H, d, *J* = 10.2 Hz), 3.59 (1H, d, *J* = 9.6 Hz), 2.43 (1H, ddd, *J* = 12.6, 4.7, 2.0 Hz), 2.04 (1H, dq, J = 12.3, 2.3 Hz), 1.57 (1H, bs), 1.37-1.26 (2H,m), 0.90 (9H,s), 0.46 (6H, d, J = 3.6 Hz). ^{13}C NMR ($CDCl_3$): δ 139.2, 137.4, 134.0, 128.7, 128.6, 128.0, 127.4, 126.6, 115.3, 104.8, 72.0, 66.1, 65.4, 41.3, 40.0, 26.1, 18.4, -5.2. HRMS (EI) m/z calcd for $C_{22}H_{34}O_3Si$ $[M]^+$ 374.2277, found 374.2290. IR (film): 3362, 2952, 2928, 2856, 1495, 1471, 1463, 1449, 1389, 1302, 1254, 1098, 1027, 838, 777, 747, 693 cm^{-1}.

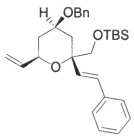

Figure 4-31. (4-Benzyloxy-2-styryl-6-vinyl-tetrahydro-pyran-2-ylmethoxy)-tert-butyl-dimethyl-silane **(247)**

In a flame dry 10 ml round bottom flask, 32mg of NaH, 60% dispersion in mineral oil, were washed twice with 0.6ml of pentane. A suspension of NaH in THF was prepared by adding 0.3mL of dry THF. A solution of compound **246** (0.072 g, 0.19 mmol) in 0.6 ml THF was added slowly to the white suspension at room temperature. After 10 min of the alcohol addition, benzene bromide was added (50mg, 0.29mmol). Then the mixture was allowed to reflux for 1.5 hours. The reaction was worked up by quenching with water and extracting with ethyl acetate. The solvent was evaporated under reduced pressure and the residue purified by silica gel chromatography producing **247** as a colorless oil (0.13 g, 68%). R*f* = 0.59 (80: 20 hexane: ethyl acetate). ^{1}H NMR (300 MHz, $CDCL_3$): δ 7.42-7.17 (5H, m), 6.65 (1H, d, *J* = 16.4 Hz), 6.33 (1H, d, *J* = 16.0), 5.91 (1H, ddd, *J* = 17.2, 10.5, 5.8 Hz), 5.31 (1H, dt, *J* = 17.2, 1.5Hz), 5.14 (1H, dt, *J* = 10.5, 1.5 Hz), 4.60 (2H, d, *J* = 0.87 Hz), 4.35-4.30 (1H, m), 3.99-3.89(1H, m), 3.84 (1H, d, *J* = 9.9 Hz), 3.55 (1H, d, *J* = 9.6 Hz), 2.54 (1H, ddd, *J* = , 12.8, 4.4, 2.0 Hz), 2.12 (1H, dq, *J* = 12.6, 2.3 Hz), 1.43 (1H, d, *J* = 11.4 Hz), 1.35 (1H,d, *J* = 11.4 Hz), 0.89 (9H,s), 0.02 (6H, d, *J* = 3.2 Hz). ^{13}C NMR ($CDCl_3$): δ 157.4, 139.3, 137.5, 134.1, 128.6, 128.0, 127.7, 127.4, 126.6, 115.2, 77.7, 72.2, 71.9, 69.8, 66.2, 38.3, 36.9, 26.1, 18.4, -5.3, -5.2. HRMS (EI) m/z calcd for $C_{29}H_{40}O_3Si$ $[M\text{-}C_4H_9]^+$ 407.2042, found 407.2041. IR

(film): 3090, 3061, 3030, 2956, 2930, 2856, 1498, 1470, 1448, 1361, 1253, 1096, 1072, 838, 777, 746, 694 cm^{-1}.

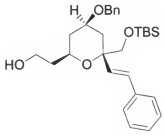

Figure 4-32. 2-[4-Benzyloxy-6-(tert-butyl-dimethyl-silanyloxymethyl)-6-styryl-tetrahydro-pyran-2-yl]-ethanol **(248)**

To a solution of ether **247** in 0.3 ml THF, 0.22 ml of 0.5 M soln of 9-BBN-H were added at 0^0C. After the addition the mixture was allowed to reach room temperature slowly. The reaction was allowed to stir for 12 hours. Then it was quenched with 0.6ml of 2:1, 30 % H_2O_2: 6 M NaOH and refluxed for 1 hour. The aqueous layers were saturated with K_2CO_3 and extracted with ether. The ether layers were dried with MgSO4, filtered and concentrated under reduced pressure. The residue was purified by silica gel chromatography using gradient elution (90: 5-80:10 Hexanes: Ether) yielding **248** as a colorless oil (39mg, 74%). R*f* = 0.27 (80: 20 Hexane: ethyl acetate). ^{1}H NMR (300 MHz, $CDCL_3$): δ 7.37-7.19 (10H, m), 6.59 (1H, d, *J* = 16.0 Hz), 6.24 (1H, d, *J* = 16.0 Hz), 4.58 (2H, s), 4.03-3,74 (5H, m), 3.64 (1H, d, *J* = 10.2 Hz), 2.34 (1H, dd, *J* = 12.3, 4.3 Hz), 2.09-2.03 (1H, m), 1.92-1.70 (2H, m), 1.50 (1H, d, *J* = 11.7 Hz), 1.37 (1H, d, *J* = 11.7 Hz), 0.88 (9H, s), 0.02 (6H, s). ^{13}C NMR ($CDCl_3$): δ 138.7, 137.2, 133.8, 128.7, 128.6, 128.3, 127.8, 127.7, 127.6, 126.6, 77.7, 72.0, 70.4, 69.9, 65.0, 61.4, 38.3, 38.2, 37.2, 26.0, 18.5, -5.3, -5.2. HRMS (EI) m/z calcd for $C_{25}H_{33}O_3Si$ $[M-C_4H_9]^+$ 425.21482, found 425.2100. IR (film): 3464, 3060, 2951, 2927, 2857, 1495, 1470, 1453, 1360, 1254, 1089, 1027, 969, 838, 746, cm^{-1}.

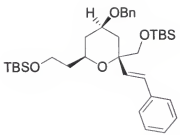

Figure 4-33. 4-Benzyloxy-6-[2-tert-butyl-dimethyl-silanyloxy)-ethyl]-2-(tert-butyl-dimethyl-silanyloxymethyl)-2-styryl-tetrahydro-pyran **(249)**

Alcohol **248** (0.25 g, 0.52 mmol) was dissolved in dichloromethane (1.0 ml) and added to an heterogeneous solution of tert-butyldimethylsilyl chloride (0.200 g, 0.73 mmol) and imidazole (53 mg, 0.78 mmol in methylene chloride (1ml). The mixture was allowed to stir at room temperature for two hours then the solvent was evaporated under reduce pressure. The residue was triturated with n-pentane and the solid formed was removed by filtration. The filtered solution was concentrated and purified by silica gel chromatography eluding with 5 % Et_2O / Hexanes that produced **249** as a viscous colorless oil (0.1560 g, 84 %). R*f* = 0.44 (85: 15 hexane: ethyl acetate). ^{1}H NMR (300 MHz, $CDCl_3$): δ 7.38-7.17 (10H, m), 6.61 (1H, d, *J* = 16.2 Hz), 6.32 (1H, d, *J* = 16.2), 4.62 (1H, d, *J* = 11.8 Hz), 4.57 (1H, d, *J* = 12.0 Hz), 3.94-3.72 (5H, m), 3.47 (1H, d, *J* = 9.8 Hz), 2.54 (1H, ddd, *J* = 12.5, 4.5, 1.8 Hz), 2.06 (1H, dt, *J* = 12.3, 2.3 Hz), 1.86-1.66 (2H, m), 1.38-1.18 (1H, m), 0.91 (9H, s), 0.89 (9H,s), 0.07 (6H, s), 0.00 (6H, s). ^{13}C NMR ($CDCl_3$): δ 138.9, 137.6, 134.5, 128.6, 127.8, 127.5, 127.3, 126.6, 77.2, 72.2, 69.8, 67.4, 65.2, 59.8, 40.1, 38.5, 36.6, 26.2, 26.1, 18.5, 18.4, -5.05, -5.02, -5.3, -5.2. HRMS (FAB) m/z calcd for $C_{35}H_{57}O_4Si_2$ $[M-H]^+$ 597.3795, found 597.3742. IR (film): 3064, 3027, 2956, 2934, 2860, 1498, 1474, 1360, 1258, 1096, 840, 778, 745, 692 cm^{-1}.

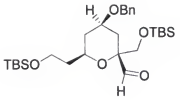

Figure 4-34. 4-Benxyloxy-6-[2-(*tert*-butyl-dimethyl-silanyloxy)-ethyl]-2-(*tert*-butyl-dimethyl-silanyloxymethyl)-tetrahydro-pyran-2-carbaldehyde **(250)**

A solution of compound **249** (0.22 g 0.35 mmol) in methylene chloride (1.2 ml) at -78°C underwent ozonolysis with Welsbach Ozonator T-408 for 8 min, until colorless solution turned light blue. Then excess of CH_3SCH_3 were added. The mixture was allowed to reach room temperature and water was added. Then the layers were separated and aqueous layers were extracted with small portions of methylene chloride. The organic layers were dried with $MgSO_4$, filtered and concentrated. The residue was purified by silica gel chromatography using gradient elution of (100 hexanes – 90:10 hexanes/ethyl acetate) yielding **250** as a colorless oil (0.174 g, 94 %). R*f* = 0.44 (85: 15 hexane: ethyl acetate). ^{1}H NMR (300 MHz, CDCL3): δ 9.50 (1H, s), 7.37-7.26 (5H, m), 4.57 (1H, d, J = 11.8 Hz), 4.51 (1H, d, J = 11.8 Hz), 3.89-3.68 (6H, m), 2.16 (1H, dd, J = 13.5, 4.5 Hz), 2.07 (1H, dt, J = 12.0, 2.1 Hz), 1.91-1.65 (2H, m), 1.39-1.21 (2H, m), 0.90 (9H, s), 0.86 (9H,s), 0.05 (6H, s), 0.016 (6H, d, *J* = 2.1 Hz). ^{13}C NMR ($CDCl_3$): δ 202.9, 138.5, 130.3, 128.7, 128.6, 127.8, 127.8, 127.7, 82.0, 71.6, 69.9, 68.1, 63.0, 59.9, 39.7, 38.2, 32.2, 26.2, 26.0, 18.5, 18.3, -5.06, -5.07, -5.4, -5.5. HRMS (FAB) m/z calcd for $C_{28}H_{51}O_5Si_2$ $[M+H]^+$ 523.3275, found 523.3266. IR (film):2958, 2934, 2890, 2857, 1714, 1471, 1255, 1093, 837, 777cm^{-1}.

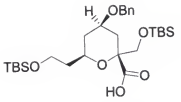

Figure 4-35. 4-Benxyloxy-6-[2-(*tert*-butyl-dimethyl-silanyloxy)-ethyl]-2-(*tert*-butyl-dimethyl-silanyloxymethyl)-tetrahydro-pyran-2-carboxylic acid **(251)**

To a solution of aldehyde **250** (80 mg, 0.15 mmol) in 2-methyl-2-butene (0.6 ml) was added a mixture of 1:1 *t*-BuOH: H_2O (1.4 ml), NaH_2PO_4 and sodium chlorite at 0°C. The mixture was allowed to stir at 0°C for 3 hours then allowed to warm to room temperature and stir for another 20 hours. The mixture was partitioned between ethyl acetate and water (4 ml). Then the aqueous layers were extracted with ethyl acetate. The ethyl acetate layers were dried with $MgSO_4$ and concentrated. The residue was purified by silica gel chromatography using gradient elution (90: 10-65: 35 hexanes: ether) yielding (60 mg, 74 %). Some starting material, aldehyde **250**, was recovered. ^{1}H NMR (300 MHz, $CDCl_3$): δ 7.37-7.26 (5H, m), 4.58 (1H, d, J = 11.8 Hz), 4.50 (1H, d, J = 11.8 Hz), 3.94-3.70 (6H, m), 2.34 (1H, dd, J = 13.3, 3.2 Hz), 2.09 (1H, dt, J = 9.3, 1.8 Hz), 1.95-1.71 (2H, m), 1.32 (1H, d, J = 11.4 Hz), 0.89 (9H, s), 0.86 (9H,s), 0.05 (6H, s), 0.03 (6H, s). ^{13}C NMR ($CDCl_3$): δ 173.3, 138.3, 128.6, 127.8, 127.7, 80.7, 71.3, 70.1, 69.3, 63.3, 59.9, 39.4, 37.6, 34.3, 26.2, 25.9, 18.5, 18.3, -5.07, -5.1, -5.3, -5.5. HRMS (FAB) m/z calcd for $C_{28}H_{51}O_6Si_2$ $[M+H]^+$ 539.3224, found 539.3250. IR (film):2956, 2930, 2888, 2857, 1780, 1734, 1100, 837, 780 cm^{-1}.

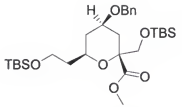

Figure 4-36. 4-Benxyloxy-6-[2-(*tert*-butyl-dimethyl-silanyloxy)-ethyl]-2-(*tert*-butyl-dimethyl-silanyloxymethyl)-tetrahydro-pyran-2-carboxylic acid methyl ester **(263)**

Acid **251** (29 mg, 0.05 mmol) was reacted with excess of freshly prepared diazomethane at 10°C. The mixture was allowed to stir for 6 hours then the solvent was removed under reduced pressure yielding a quantitative amount of ester **263**. ^{1}H NMR (300 MHz, $CDCL_3$): δ 7.36-7.28 (5H, m), 4.60 (1H, d, J = 11.7 Hz), 4.55 (1H, d, J = 11.7 Hz), 3.98-3.67 (6H, m), 3.73 (3H, s), 2.46 (1H, ddd, J = 13.1, 4.8, 2.1 Hz), 2.06 (1H, dt, J = 12.6, 2.1 Hz), 1.94-1.81 (1H, m), 1.73-1.23 (3H, m), 0.90 (9H, s), 0.86 (9H,s), 0.05 (6H, s), 0.01 (6H, s). ^{13}C NMR ($CDCl_3$): δ 172.6, 138.6, 128.6, 127.8, 127.7, 80.7, 71.7, 69.8, 68.3, 63.5, 59.7, 57.3, 52.4, 39.5, 37.9, 34.0, 26.2, 25.9, 18.5, 18.3, -5.08, -5.1, -5.3, -5.4. HRMS (FAB) m/z calcd for $C_{29}H_{53}O_6Si_2$ $[M+H]^+$ 553.3380, found 553.3357. IR (film): 2952, 2856, 1747, 1452, 1256, 1106, 837, 777 cm^{-1}.

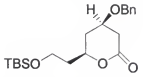

Figure 4-37. 4-Benxyloxy-6-[2-(*tert*-butyl-dimethyl-silanyloxy)-ethyl]-tetrahydro-pyran-2-one **(253)**

To a solution of acid **251** (35 mg, 0.065 mmol) in CH_2Cl_2 (2.6 ml) was added diacetoxyiodo benzene (DIB) (55 mg, 0.16 mmol) and iodine (10 mg, 0.039 mmol) as solids. After 3 hours the reaction was worked up by adding a saturated aqueous solution of sodium thiosulfate and extracting the aqueous layers with methylene chloride. After

silica gel chromatography, 10mg of **253** were recovered yielding 48%. R*f* = 0.41 (70: 30 Hexane: ethyl acetate). ^{1}H NMR (300 MHz, $CDCL_3$): δ 7.39-7.28 (5H, m), 4.56 (2H, s), 4.43-4.33 (1H,m), 3.96 (1H, ddt, *J* = 8.9, 7.1, 5.8 Hz), 3.86-3.70 (2H, m), 2.88 (1H, ddd, *J* = 17.2, 5.9, 1.0 Hz), 2.60 (1H, dd, *J* = 17.2, 7.2 Hz), 2.35 (1H, dddd, *J* = 13.9, 5.6, 3.0, 1.1 Hz), 1.93 (1H, ddt, *J* = 14.1, 8.2, 4.9 Hz), 1.81 (1H, dddd, *J* = 13.9, 8.4, 5.4, 4.5 Hz), 1.66 (1H, ddd, J = 13.9, 11.9, 9.0 Hz), 0.89 (9H, s), 0.05 (6H, s). ^{13}C NMR ($CDCl_3$): δ170.5, 137.9, 128.7, 128.1, 127.8, 74.2, 70.5, 58.8, 38.8, 37.0, 35.7, 29.2, 26.1, 18.5, -5.2. HRMS (CI) m/z calcd for $C_{20}H_{33}O_4Si$ $[M+H]^+$ 365.2148, found 365.2164. IR (film): 2954, 2928, 2856, 1744, 1253, 1093, 836, 777 cm^{-1}.

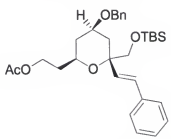

Figure 4-38. Acetic acid 2-[4-benzyloxy-6-[tert-butyl-dimethyl-silanyloxymethyl)-6-styryl-tetrahydro-pyran-2-yl]ethyl ester **(264)**

Alcohol **248** (0.100g, 0.025 mmol) was diluted in 0.4 ml of CH_2Cl_2 with 4-dimethylamino pyridine (DMAP) (<1 mg) and pyridine (25mg, 0.31 mmol). After 10 min, acetic anhydride (30 µl, 0.029 mmol) and the mixture was refluxed for 2 hours. The solvent was removed under reduced pressure and the residue was purified by silica gel chromatograpy using gradient elution (98: 2 - 85: 15 hexanes: ether). The reaction gave **264** (95 mg, 87%). R*f* = 0.59 (70: 30 hexane: ethyl acetate). ^{1}H NMR (300 MHz, $CDCL_3$): δ 7.34-7.16 (10H, m), 6.59 (1H, d, *J* = 16.2 Hz), 6.26 (1H, d, *J* = 16.2 Hz), 4.59 (1H, d, *J* = 13.3), 4.55 (1H, d, *J* = 13.3), 4.26-4.21 (1H, m), 3.93-3.85 (2H, m), 3.74 (1H, d, *J* = 9.7Hz), 3.52 (1H, d, *J* = 9.7 Hz), 2.51-2.44 (1H, m), 2.03 (3H, s), 1.96-1.78 (3H,

m), 1.42-1.20 (2H, m), 0.87 (9H,s), 0.00 (6H, s). ^{13}C NMR ($CDCl_3$): δ 171.3, 138.9, 137.5, 134.1, 128.7, 127.9, 127.4, 126.6, 77.4, 72.1, 69.9, 67.9, 66.2, 61.7, 38.4, 31.1, 36.0, 26.0, 21.2, 18.3, -5.3, -5.4. HRMS (FAB) m/z calcd for $C_{31}H_{45}O_5Si$ $[M+H]^+$ 525.3036, found 525.2991. IR (film): 2953, 2856, 1738, 1249, 1090, 838 cm^{-1}.

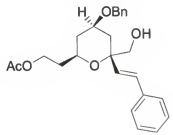

Figure 4-39. Acetic acid 2-(4-benzyloxy-6-hydroxymethyl-6-styryl-tetrahydro-pyran-2-yl)-ethyl ester **(265)**

To a solution of ether **264** (90 mg, 0.17 mmol) in THF (0.5 ml) was added tetrabuthyl ammonium fluoride (Bu_4NF) (0.7 ml of 1 M solution, 0.7 mmol) at room temperature. The solution was allowed to stir for 3 hours. The mixture was worked up by adding a saturated solution of sodium bicarbonate. The aqueous layers were extracted with ether, and the ether layers were dried over $MgSO_4$ and concentrated under reduced pressure. The residue was purified by silica gel chromatography using gradient elution (90: 10 – 75: 25 hexanes: ethyl acetate) affording **265** (50 mg, 71%). R*f* = 0.17 (70: 30 Hexane: ethyl acetate). ^{1}H NMR (300 MHz, $CDCL_3$): δ 7.40-7.20 (10H, m), 6.67 (1H, d, *J* = 16.2 Hz), 6.22 (1H, d, *J* = 16.2 Hz), 4.57 (2H, s), 4.45-4.37 (1H, m), 4.29-4.22 (1H, m), 3.95 (1H, d, *J* = 11.7 Hz), 3.81-3.70 (2H, m), 3.48-3.42 (1H, m), 2.18-2.05 (3H, m), 2.06 (3H,s), 1.97-1.86 (2H, m), 1.558 (1H, t, *J* = 12.2 Hz). ^{13}C NMR ($CDCl_3$): δ 171.6, 138.5, 136.9, 132.9, 128.7, 128.6, 127.9, 127.8, 127.7, 126.7, 77.8, 71.9, 70.0, 66.6, 63.0, 61.2, 38.3, 37.8, 35.8, 21.2. HRMS (CI) m/z calcd for $C_{25}H_{31}O_5$ $[M+H]^+$

411.2171, found 411.2150. IR (film): 3480, 3064, 3030, 2948, 2924, 2878, 1738, 1495, 1364, 1244, 1067, 969, 749, 696 cm^{-1}.

APPENDIX A
SELECTED SPECTRA

A

199

B

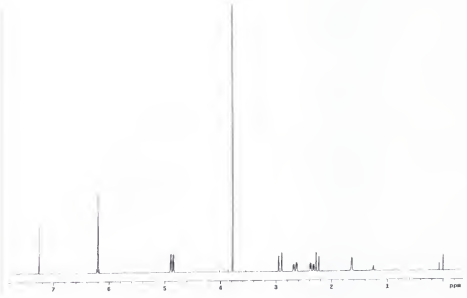

C

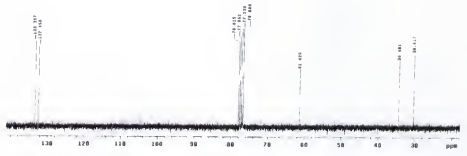

Figure A-1. Spectroscopy data for **199**. A) Structure B) ^{1}H spectrum C) ^{13}C spectrum

A

200

B

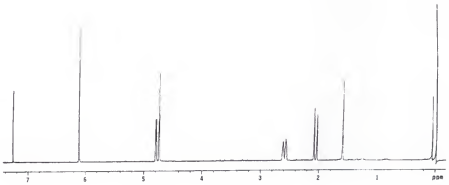

C

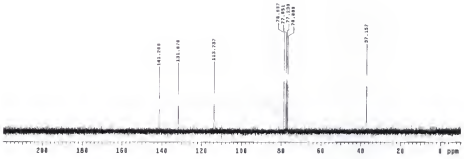

Figure A-2. Spectroscopy data for **200**. A) Structure B) ^{1}H spectrum C) ^{13}C spectrum

A

201

B

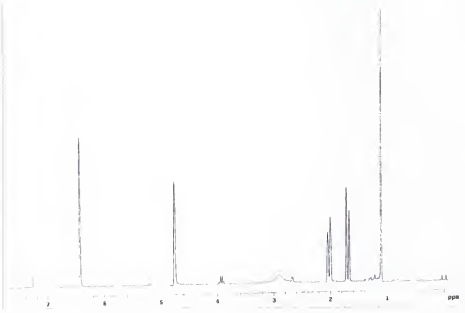

C

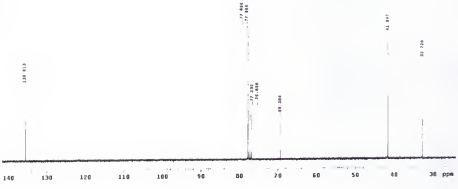

Figure A-3. Spectroscopy data for **201**. A) Structure B) ^{1}H spectrum C) ^{13}C spectrum

A

205

B

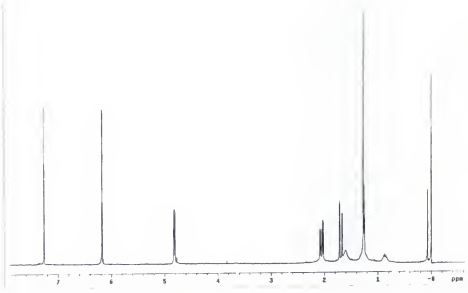

C

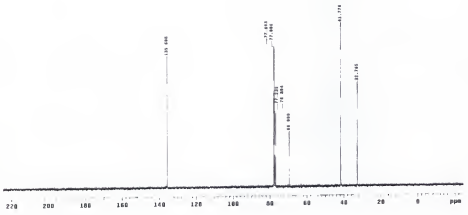

Figure A-4. Spectroscopy data for **205**. A) Structure B) ^{1}H spectrum C) ^{13}C spectrum

A

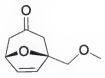

206b

B

C

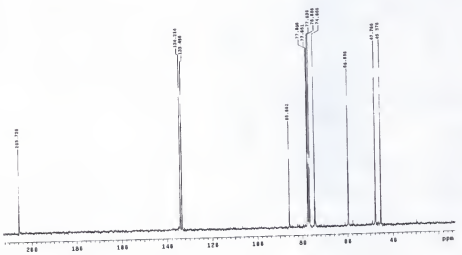

Figure A-5. Spectroscopy data for **206b**. A) Structure B) ^{1}H spectrum C) ^{13}C spectrum

A

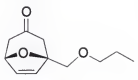

206c

B

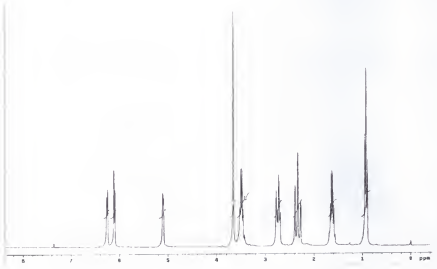

C

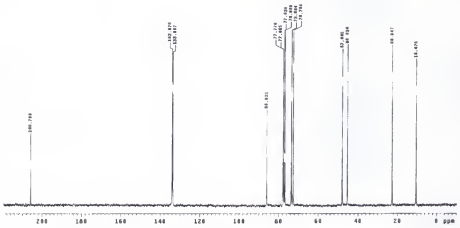

Figure A-6. Spectroscopy data for **206c**. A) Structure B) ^{1}H spectrum C) ^{13}C spectrum

A

207a

B

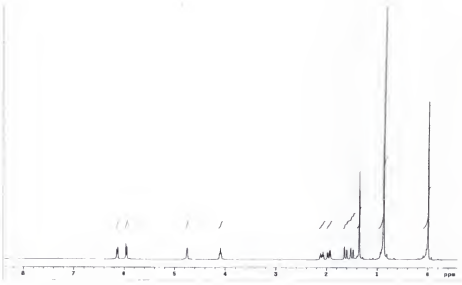

C

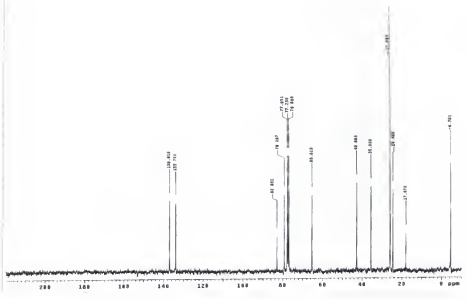

Figure A-7. Spectroscopy data for **207a**. A) Structure B) ^{1}H spectrum C) ^{13}C spectrum

A

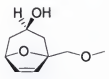

207d

B

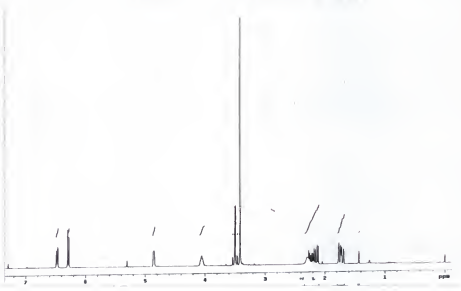

C

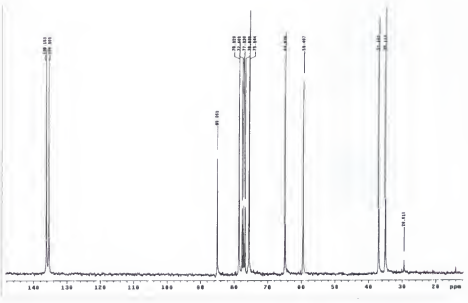

Figure A-8. Spectroscopy data for **207d**. A) Structure B) ^{1}H spectrum C) ^{13}C spectrum

A

207e

B

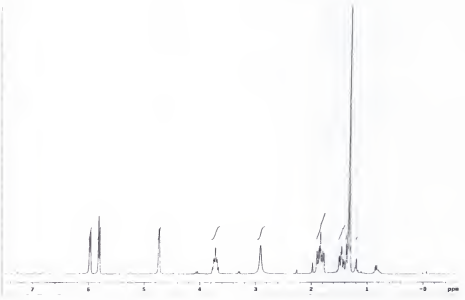

C

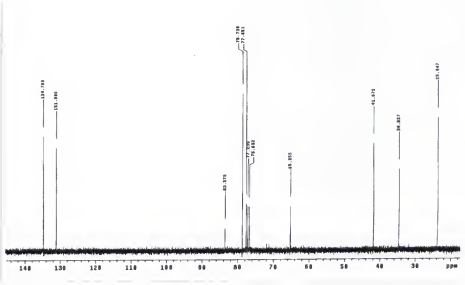

Figure A-9. Spectroscopy data for **207e**. A) Structure B) ^{1}H spectrum C) ^{13}C spectrum

A

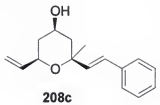

208c

B

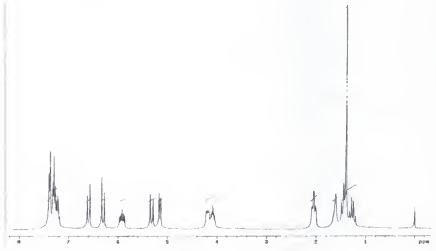

C

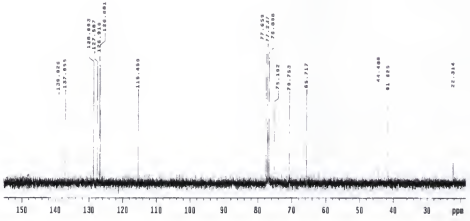

Figure A-10. Spectroscopy data for **208c**. A) Structure B) ^{1}H spectrum C) ^{13}C spectrum

A

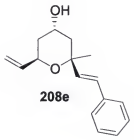

B

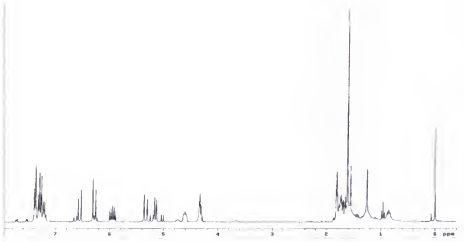

C

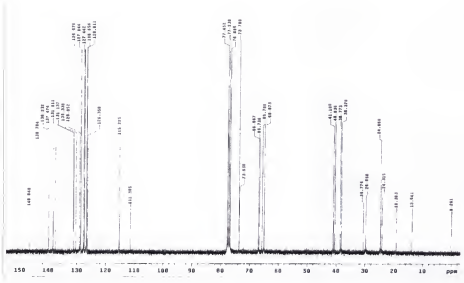

Figure A-11. Spectroscopy data for **208e**. A) Structure B) ^{1}H spectrum C) ^{13}C spectrum

A

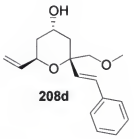

B

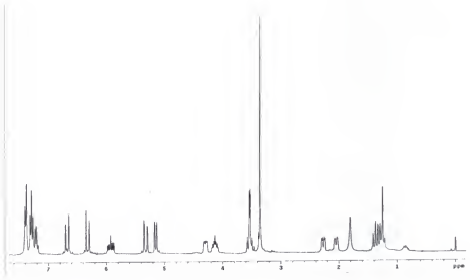

C

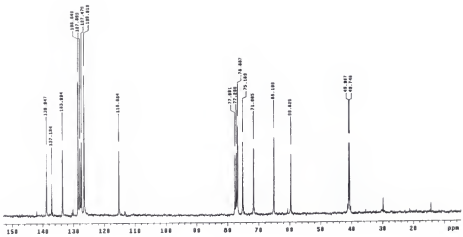

Figure A-12. Spectroscopy data for **208d**. A) Structure B) ^{1}H spectrum C) ^{13}C spectrum

A

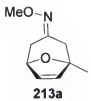

213a

B

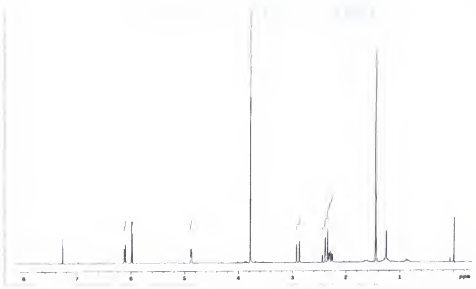

C

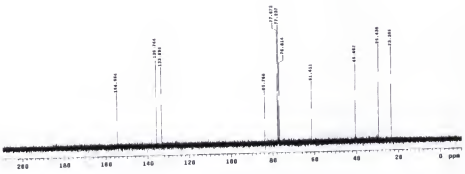

Figure A-13. Spectroscopy data for **213a**. A) Structure B) ^{1}H spectrum C) ^{13}C spectrum

A

213b

B

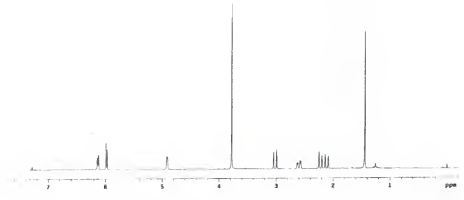

C

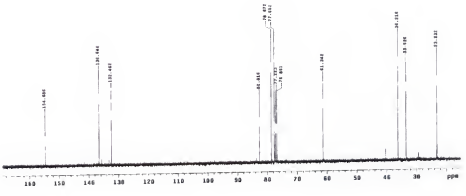

Figure A-14. Spectroscopy data for **213b**. A) Structure B) ^{1}H spectrum C) ^{13}C spectrum

A

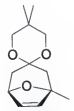

214

B

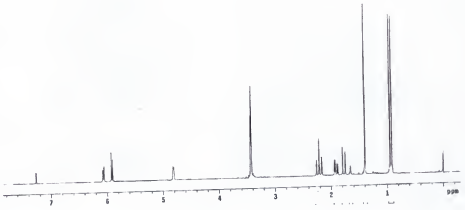

C

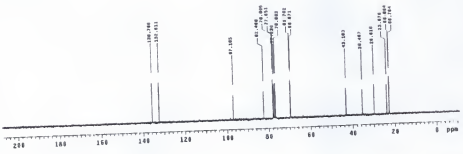

Figure A-15. Spectroscopy data for **214**. A) Structure B) ^{1}H spectrum C) ^{13}C spectrum

A

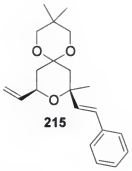

B

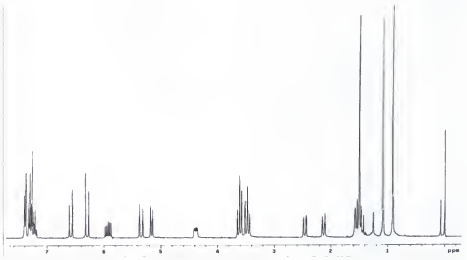

C

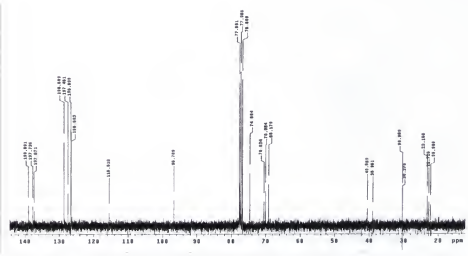

Figure A-16. Spectroscopy data for **215**. A) Structure B) ^{1}H spectrum C) ^{13}C spectrum

A

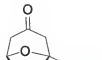

235

B

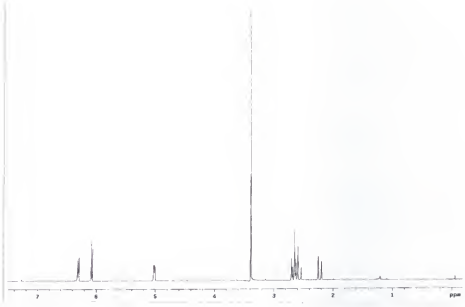

C

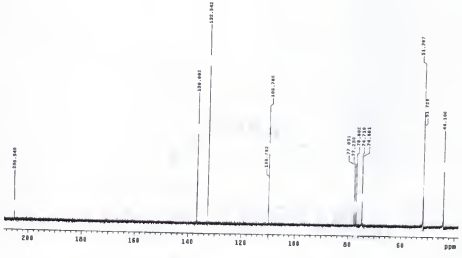

Figure A-17. Spectroscopy data for **235**. A) Structure B) ^{1}H spectrum C) ^{13}C spectrum

A

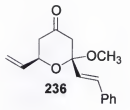

B

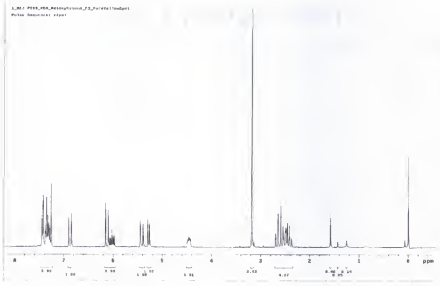

C

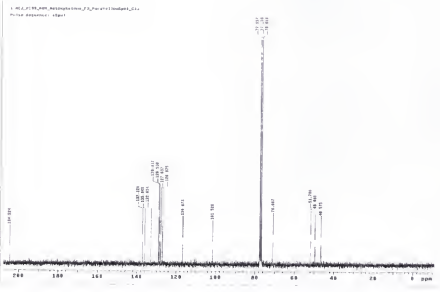

Figure A-18. Spectroscopy data for **236**. A) Structure B) ^{1}H spectrum C) ^{13}C spectrum

A

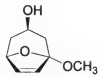

237

B

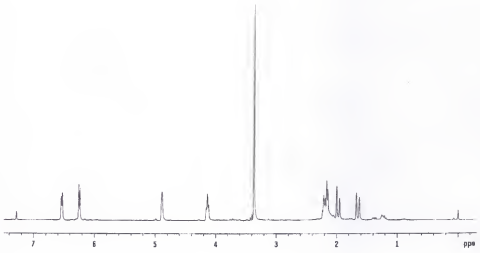

C

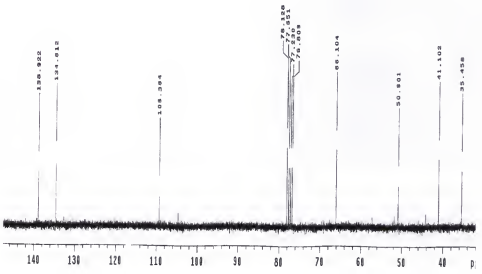

Figure A-19. Spectroscopy data for **237**. A) Structure B) ^{1}H spectrum C) ^{13}C spectrum

A

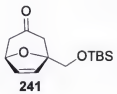

241

B

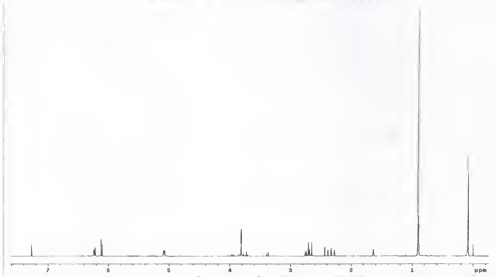

C

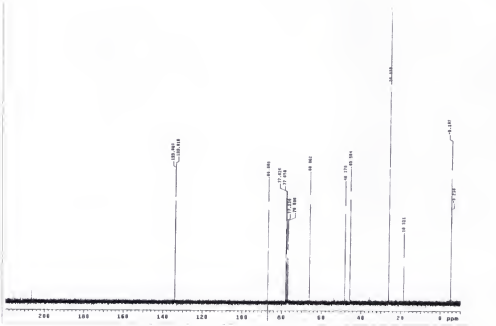

Figure A-20. Spectroscopy data for **241**. A) Structure B) ^{1}H spectrum C) ^{13}C spectrum

A

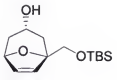

242

B

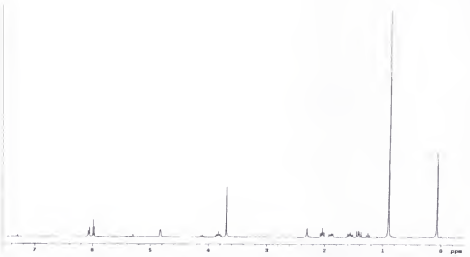

C

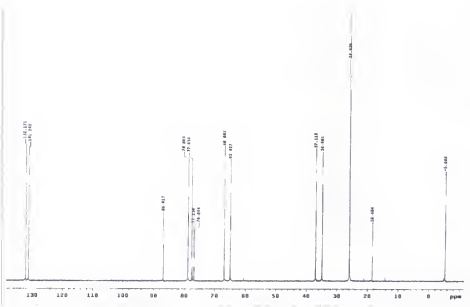

Figure A-21. Spectroscopy data for **242**. A) Structure B) ^{1}H spectrum C) ^{13}C spectrum

A

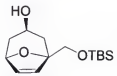

245

B

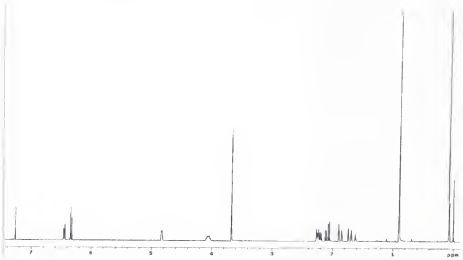

C

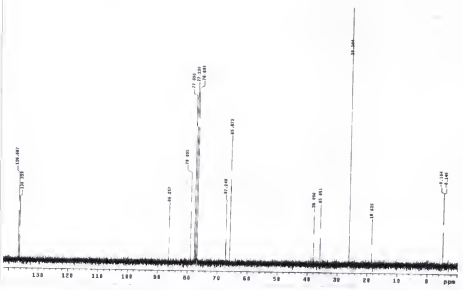

Figure A-22. Spectroscopy data for **245**. A) Structure B) ^{1}H spectrum C) ^{13}C spectrum

A

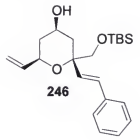

B

C

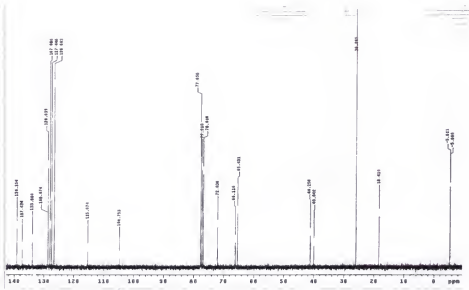

Figure A-23. Spectroscopy data for **246**. A) Structure B) 1H spectrum C) 13C spectrum

A

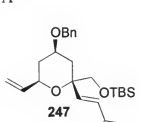

B

C

Figure A-24. Spectroscopy data for **247**. A) Structure B) ^{1}H spectrum C) ^{13}C spectrum

A

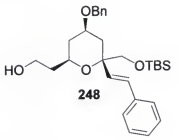

B

C

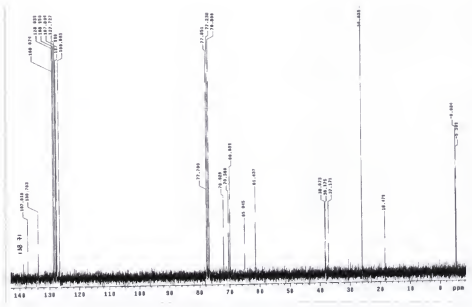

Figure A-25. Spectroscopy data for **248**. A) Structure B) ^{1}H spectrum C) ^{13}C spectrum

A

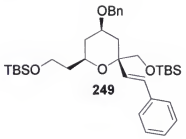

B

C

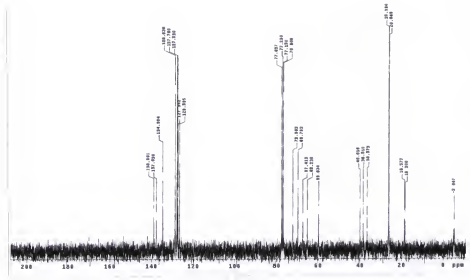

Figure A-26. Spectroscopy data for **249**. A) Structure B) ^{1}H spectrum C) ^{13}C spectrum

A

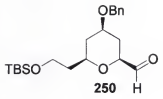

B

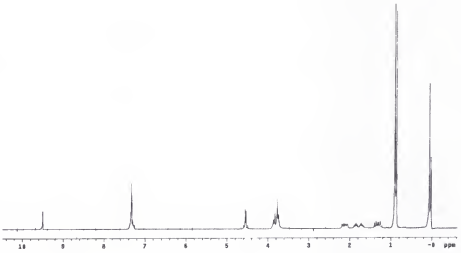

C

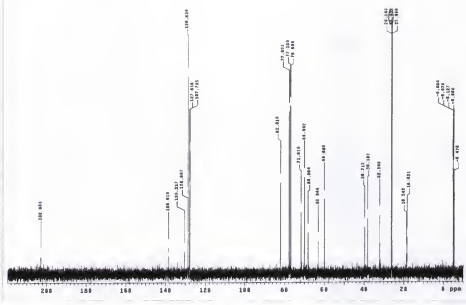

Figure A-27. Spectroscopy data for **250**. A) Structure B) 1H spectrum C) 13C spectrum

A

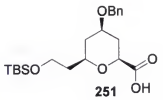

B

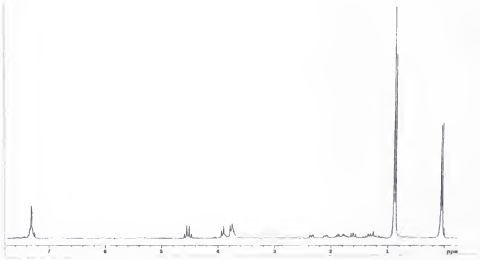

C

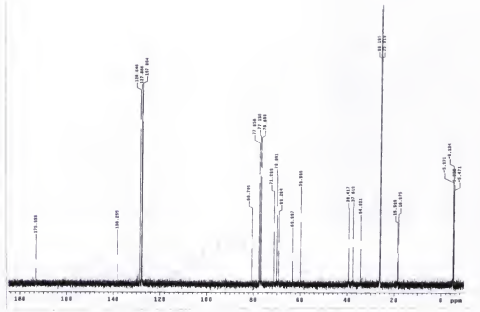

Figure A-28. Spectroscopy data for **251**. A) Structure B) ^{1}H spectrum C) ^{13}C spectrum

A

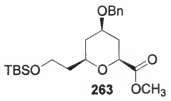

263

B

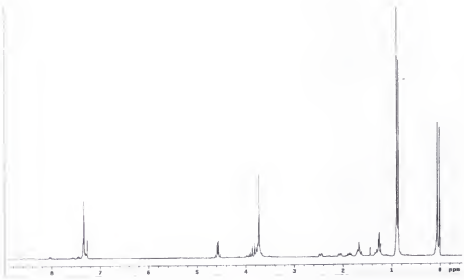

C

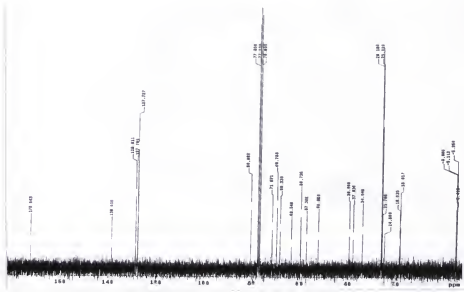

Figure A-29. Spectroscopy data for **263**. A) Structure B) ^{1}H spectrum C) ^{13}C spectrum

A

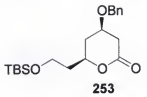

253

B

C

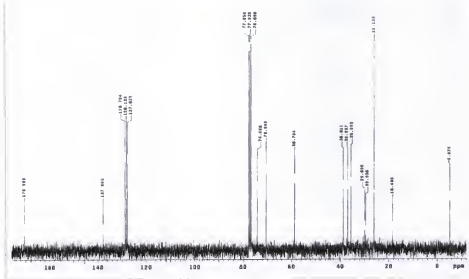

Figure A-30. Spectroscopy data for **253**. A) Structure B) ^{1}H spectrum C) ^{13}C spectrum

A

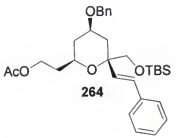

B

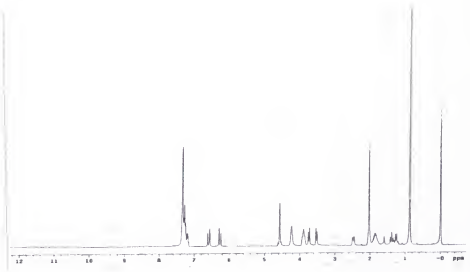

C

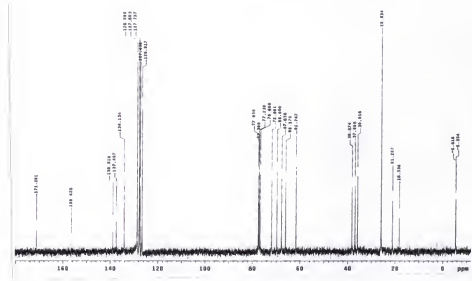

Figure A-31. Spectroscopy data for **264**. A) Structure B) ^{1}H spectrum C) ^{13}C spectrum

A

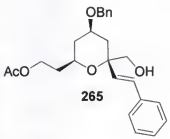

265

B

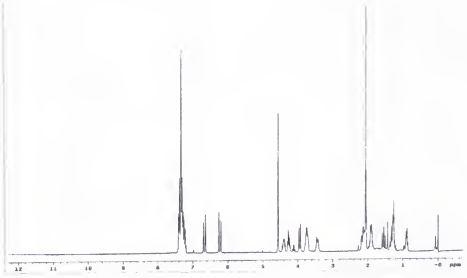

C

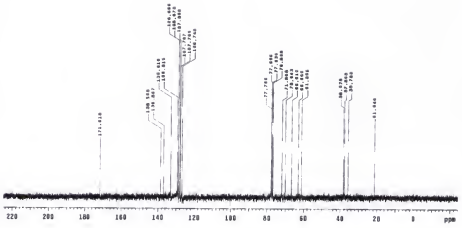

Figure A-32. Spectroscopy data for **265**. A) Structure B) ^{1}H spectrum C) ^{13}C spectrum

APPENDIX B
LIST OF TABLES FOR KINETIC STUDIES

The tables presented in this appendix are representative examples of the data generated by proton NMR used to calculated the relative rates of the ring opening metathesis polymerization of 8-Oxabicyclo[3.2.1]octene derivatives. The first column, time, refers to the second intervals at which each spectrum was collected. The second column, C_6H_6, is the integral area of benzene collected per second interval during the reaction. Benzene was used as an internal standard to normalize the integral area. The third column, standard, refers to the integral area of standard collected per second interval during the reaction. The forth column represents the measurement of the integral area used as a concentration measure of the substrate during the reaction. The fifth and sixth column represents the integral area normalized for standard and substrate respectively by dividing the individual respective integral area over the benzene integral area. The last two columns, shadow areas, are the natural logarithm of column fifth and sixth respectively, where the first one is placed in the x axe and the second one is placed in the y axe of the graphs presented in appendix C. The tables presented here corresponds to graphs 5, 4, 13, 24 and 32 respectively.

Table B-1(5). Data generated measuring integral area vs. time for [std/alkene **200**] = 0.25

Time (s)	Benzene	standard	alkene	std/C_6H_6	sub/C_6H_6	ln[std/C6H6]	ln[sub/C6H6]
45	0.318	0.1121	0.342	0.35252	1.07547	-1.04266	0.07276
54	0.3205	0.1119	0.3384	0.34914	1.05585	-1.05228	0.05435
63	0.3224	0.1115	0.3352	0.34584	1.03970	-1.06177	0.03893
72	0.3253	0.111	0.331	0.34122	1.01752	-1.07522	0.01737
81	0.3273	0.1106	0.3275	0.33792	1.00061	-1.08496	0.00061
90	0.3297	0.1102	0.3239	0.33424	0.98241	-1.09589	-0.01775
99	0.3325	0.1094	0.3201	0.32902	0.96271	-1.11163	-0.03801
108	0.3352	0.1091	0.3158	0.32548	0.94212	-1.12246	-0.05962
117	0.3373	0.1086	0.3124	0.32197	0.92618	-1.13330	-0.07669
126	0.3399	0.1081	0.3086	0.31803	0.90791	-1.14559	-0.09661
135	0.3424	0.1075	0.3049	0.31396	0.89048	-1.15849	-0.11600
144	0.345	0.1071	0.3008	0.31043	0.87188	-1.16978	-0.13710
153	0.347	0.1065	0.2974	0.30692	0.85706	-1.18118	-0.15425
162	0.3498	0.1059	0.2935	0.30274	0.83905	-1.19487	-0.17548
171	0.352	0.1051	0.2902	0.29858	0.82443	-1.20872	-0.19306
180	0.3549	0.1046	0.2861	0.29473	0.80614	-1.22169	-0.21549
189	0.3575	0.104	0.2825	0.29091	0.79021	-1.23474	-0.23546
198	0.3598	0.1035	0.2787	0.28766	0.77460	-1.24598	-0.25541
207	0.3621	0.1027	0.2753	0.28362	0.76029	-1.26011	-0.27406
216	0.3643	0.1023	0.2717	0.28081	0.74581	-1.27007	-0.29328
225	0.3669	0.1015	0.2679	0.27664	0.73017	-1.28503	-0.31448
234	0.3689	0.1008	0.2652	0.27324	0.71889	-1.29739	-0.33004
243	0.3715	0.1005	0.2615	0.27052	0.70390	-1.30739	-0.35111
252	0.3738	0.0995	0.2581	0.26619	0.69048	-1.32356	-0.37037
261	0.3765	0.099	0.2546	0.26295	0.67623	-1.33580	-0.39122
270	0.3785	0.0982	0.2515	0.25945	0.66446	-1.34921	-0.40877
279	0.3806	0.0976	0.2483	0.25644	0.65239	-1.36087	-0.42711
288	0.3828	0.097	0.2451	0.25340	0.64028	-1.37280	-0.44585

Table B-2(4). Data generated measuring integral area vs. time at [std/exo-OTBS **193**] = 0.25

Time (s)	Benzene	[Standard]	[exo-OTBS]	[std/C_6H_6]	[sub/C_6H_6]	ln[std/C_6H_6]	ln[sub/C_6H_6]
45	0.1104	0.0834	0.2377	0.75543	2.15308	-0.28046	0.76690
54	0.1114	0.0817	0.23	0.73339	2.06463	-0.31007	0.72495
63	0.1127	0.0807	0.2225	0.71606	1.97427	-0.33399	0.68020
72	0.1142	0.0792	0.2152	0.69352	1.88441	-0.36597	0.63362
81	0.1156	0.078	0.2073	0.67474	1.79325	-0.39343	0.58403
90	0.1173	0.0765	0.1994	0.65217	1.69991	-0.42744	0.53058
99	0.1187	0.0746	0.1918	0.62848	1.61584	-0.46446	0.47985
108	0.1203	0.0728	0.1855	0.60515	1.54198	-0.50227	0.43307
117	0.1216	0.0715	0.1781	0.58799	1.46464	-0.53104	0.38161
126	0.1226	0.0697	0.1709	0.56852	1.39396	-0.56473	0.33215
135	0.124	0.0683	0.1649	0.55081	1.32984	-0.59637	0.28506
144	0.1256	0.0672	0.1576	0.53503	1.25478	-0.62543	0.22696
153	0.1265	0.0647	0.1515	0.51146	1.19763	-0.67048	0.18034
162	0.1278	0.0634	0.1456	0.49609	1.13928	-0.70100	0.13040
171	0.1301	0.0623	0.1395	0.47886	1.07225	-0.73634	0.06976
180	0.1303	0.0614	0.134	0.47122	1.02840	-0.75243	0.02800
189	0.1314	0.0595	0.1284	0.45282	0.97717	-0.79227	-0.02310
198	0.1326	0.0574	0.1235	0.43288	0.93137	-0.83729	-0.07110
207	0.1334	0.0564	0.1182	0.42279	0.88606	-0.86088	-0.12097
216	0.1356	0.0532	0.1134	0.39233	0.83628	-0.93565	-0.17879
225	0.1362	0.0525	0.1091	0.38546	0.80103	-0.95331	-0.22186
234	0.137	0.0516	0.1037	0.37664	0.75693	-0.97646	-0.27848
243	0.1375	0.0502	0.1006	0.36509	0.73164	-1.00761	-0.31247
252	0.1385	0.0478	0.0965	0.34513	0.69675	-1.06384	-0.36133
261	0.1394	0.0487	0.0918	0.34935	0.65854	-1.05167	-0.41774
270	0.1403	0.0467	0.0889	0.33286	0.63364	-1.10004	-0.45627
279	0.1412	0.0457	0.0852	0.32365	0.60340	-1.12808	-0.50518
288	0.142	0.0436	0.0811	0.30704	0.57113	-1.18077	-0.56014
297	0.1432	0.0437	0.0776	0.30517	0.54190	-1.18689	-0.61267
306	0.1432	0.0424	0.0757	0.29609	0.52863	-1.21709	-0.63746
315	0.1438	0.0412	0.0726	0.28651	0.50487	-1.24999	-0.68346
324	0.1433	0.0393	0.0701	0.27425	0.48918	-1.29372	-0.71502
333	0.145	0.0373	0.068	0.25724	0.46897	-1.35774	-0.75723
342	0.1455	0.0377	0.0657	0.25911	0.45155	-1.35052	-0.79508

Table B-3(13). Data generated measuring integral area vs. time at [std/*endo*-OTBS **192**] = 1

Time (s)	benzene	standard	end-OTBS	std/C_6H_6	sub/C_6H_6	ln[std/C_6H_6]	ln[sub/C_6H_6]
125	0.542	0.2526	0.2053	0.4661	0.3788	-0.7635	-0.9708
150	0.553	0.2543	0.1926	0.4599	0.3483	-0.7768	-1.0547
175	0.5627	0.2552	0.1821	0.4535	0.3236	-0.7907	-1.1282
200	0.5708	0.2564	0.1727	0.4492	0.3026	-0.8003	-1.1955
225	0.5786	0.2571	0.1643	0.4443	0.2840	-0.8111	-1.2589
250	0.5853	0.2579	0.1567	0.4406	0.2677	-0.8196	-1.3178
275	0.5918	0.2584	0.1498	0.4366	0.2531	-0.8287	-1.3739
300	0.5974	0.2592	0.1435	0.4339	0.2402	-0.8350	-1.4263
325	0.602	0.2597	0.1383	0.4314	0.2297	-0.8407	-1.4708
350	0.6076	0.26	0.1324	0.4279	0.2179	-0.8488	-1.5237
375	0.6133	0.2602	0.1264	0.4243	0.2061	-0.8574	-1.5794
400	0.6169	0.2603	0.1227	0.4219	0.1989	-0.8629	-1.6150
425	0.6213	0.2608	0.1179	0.4198	0.1898	-0.8681	-1.6620
450	0.6252	0.2612	0.1136	0.4178	0.1817	-0.8728	-1.7054
475	0.6294	0.2608	0.1098	0.4144	0.1745	-0.8810	-1.7461
500	0.6343	0.2607	0.1049	0.4110	0.1654	-0.8892	-1.7995
525	0.6377	0.2606	0.1017	0.4087	0.1595	-0.8949	-1.8358
550	0.6398	0.2612	0.0989	0.4083	0.1546	-0.8959	-1.8670
575	0.6442	0.2613	0.0946	0.4056	0.1468	-0.9023	-1.9184
600	0.6477	0.2612	0.0912	0.4033	0.1408	-0.9081	-1.9604
625	0.6497	0.2611	0.0892	0.4019	0.1373	-0.9116	-1.9856
650	0.6533	0.2611	0.0856	0.3997	0.1310	-0.9171	-2.0324
675	0.6562	0.2611	0.0827	0.3979	0.1260	-0.9216	-2.0712
700	0.6596	0.2605	0.0799	0.3949	0.1211	-0.9290	-2.1109
725	0.6615	0.2603	0.0782	0.3935	0.1182	-0.9327	-2.1352
750	0.6659	0.2599	0.0742	0.3903	0.1114	-0.9408	-2.1944
775	0.6679	0.2595	0.0725	0.3885	0.1085	-0.9454	-2.2206
800	0.6705	0.2596	0.07	0.3872	0.1044	-0.9489	-2.2595
825	0.674	0.2592	0.0668	0.3846	0.0991	-0.9556	-2.3115

Table B-4(24). Data generated measuring integral area vs. time at [std/ketone **1**] = 4

Time (s)	standard	ketone	TMS	std/TMS	sub/TMS	ln[std/TMS]	ln[sub/TMS]
45	0.5219	0.1332	0.3291	1.5858	0.4047	0.4611	-0.9045
54	0.5199	0.1338	0.3297	1.5769	0.4058	0.4555	-0.9018
63	0.5181	0.1341	0.3313	1.5638	0.4048	0.4471	-0.9044
72	0.5154	0.1351	0.3343	1.5417	0.4041	0.4329	-0.9060
81	0.5118	0.1352	0.337	1.5187	0.4012	0.4179	-0.9133
90	0.5097	0.135	0.3385	1.5058	0.3988	0.4093	-0.9192
99	0.5062	0.1354	0.3416	1.4819	0.3964	0.3933	-0.9254
108	0.504	0.1361	0.3425	1.4715	0.3974	0.3863	-0.9229
117	0.5018	0.1367	0.3456	1.4520	0.3955	0.3729	-0.9275
126	0.4993	0.1382	0.3467	1.4401	0.3986	0.3647	-0.9198
135	0.4967	0.1379	0.3483	1.4261	0.3959	0.3549	-0.9265
144	0.4943	0.1375	0.3513	1.4071	0.3914	0.3415	-0.9380
153	0.4911	0.1383	0.354	1.3873	0.3907	0.3274	-0.9399
162	0.49	0.1385	0.3542	1.3834	0.3910	0.3245	-0.9390
171	0.4872	0.1392	0.3563	1.3674	0.3907	0.3129	-0.9399
180	0.4835	0.1385	0.3597	1.3442	0.3850	0.2958	-0.9544
189	0.4817	0.1393	0.3605	1.3362	0.3864	0.2898	-0.9509
198	0.4784	0.14	0.3644	1.3128	0.3842	0.2722	-0.9566
207	0.4755	0.1395	0.3669	1.2960	0.3802	0.2593	-0.9670
216	0.4739	0.14	0.3682	1.2871	0.3802	0.2524	-0.9670
225	0.4701	0.1411	0.3714	1.2658	0.3799	0.2357	-0.9678
234	0.4672	0.1407	0.3736	1.2505	0.3766	0.2236	-0.9766
243	0.4643	0.1412	0.3761	1.2345	0.3754	0.2107	-0.9797
252	0.4626	0.1414	0.3774	1.2258	0.3747	0.2036	-0.9817
261	0.4597	0.142	0.3795	1.2113	0.3742	0.1917	-0.9830
270	0.4561	0.143	0.3817	1.1949	0.3746	0.1781	-0.9818
279	0.4538	0.1429	0.3843	1.1808	0.3718	0.1662	-0.9893
288	0.4505	0.1429	0.3882	1.1605	0.3681	0.1488	-0.9994
297	0.4477	0.1439	0.3896	1.1491	0.3694	0.1390	-0.9960
306	0.4457	0.1434	0.391	1.1399	0.3668	0.1309	-1.0031
315	0.4428	0.144	0.3939	1.1241	0.3656	0.1170	-1.0063
324	0.4401	0.1445	0.3963	1.1105	0.3646	0.1048	-1.0089
333	0.4364	0.1454	0.3986	1.0948	0.3648	0.0906	-1.0085
342	0.4335	0.1458	0.4008	1.0816	0.3638	0.0784	-1.0112
351	0.4314	0.1466	0.4012	1.0753	0.3654	0.0726	-1.0068
360	0.4285	0.1467	0.4058	1.0559	0.3615	0.0544	-1.0175
369	0.4251	0.1466	0.408	1.0419	0.3593	0.0411	-1.0236
378	0.4214	0.1473	0.4114	1.0243	0.3580	0.0240	-1.0271
387	0.4187	0.1473	0.4143	1.0106	0.3555	0.0106	-1.0341
396	0.4174	0.1478	0.4139	1.0085	0.3571	0.0084	-1.0298

Table B-5(32). Data generated measuring integral area vs. time at [std/Methylene **204**] = 1

Time	C_6H_6	Standard	Methylene	std/C_6H_6	sub/C_6H_6	ln[std/C_6H_6]	ln[sub/C_6H_6]
144	0.3588	0.3316	0.3096	0.9242	0.8629	-0.0788	-0.1475
168	0.3752	0.3306	0.2942	0.8811	0.7841	-0.1266	-0.2432
192	0.3919	0.3293	0.2789	0.8403	0.7117	-0.1740	-0.3402
216	0.409	0.3268	0.2643	0.7990	0.6462	-0.2244	-0.4366
240	0.4246	0.3247	0.2507	0.7647	0.5904	-0.2682	-0.5269
264	0.4403	0.3225	0.2372	0.7325	0.5387	-0.3114	-0.6186
288	0.4552	0.3194	0.2254	0.7017	0.4952	-0.3543	-0.7029
312	0.4688	0.3158	0.2154	0.6736	0.4595	-0.3951	-0.7777
336	0.4839	0.3129	0.2032	0.6466	0.4199	-0.4360	-0.8677
360	0.4976	0.309	0.1934	0.6210	0.3887	-0.4765	-0.9450
384	0.511	0.3052	0.1838	0.5973	0.3597	-0.5154	-1.0225
408	0.5236	0.3014	0.175	0.5756	0.3342	-0.5523	-1.0959
432	0.5366	0.2971	0.1663	0.5537	0.3099	-0.5912	-1.1715
456	0.5463	0.2942	0.1595	0.5385	0.2920	-0.6189	-1.2311
480	0.5589	0.2895	0.1516	0.5180	0.2712	-0.6578	-1.3047
504	0.5706	0.284	0.1454	0.4977	0.2548	-0.6977	-1.3672
528	0.5796	0.2812	0.1392	0.4852	0.2402	-0.7233	-1.4264
552	0.5915	0.2767	0.1318	0.4678	0.2228	-0.7597	-1.5014
576	0.6003	0.2725	0.1272	0.4539	0.2119	-0.7898	-1.5517
600	0.6109	0.2674	0.1217	0.4377	0.1992	-0.8262	-1.6134
624	0.6195	0.2642	0.1163	0.4265	0.1877	-0.8522	-1.6727
648	0.6296	0.2596	0.1108	0.4123	0.1760	-0.8859	-1.7374
672	0.6385	0.2554	0.1061	0.4000	0.1662	-0.9163	-1.7947
696	0.6479	0.2502	0.1019	0.3862	0.1573	-0.9515	-1.8497
720	0.6545	0.2466	0.0989	0.3768	0.1511	-0.9761	-1.8898

APPENDIX C
LIST OF GRAPHS FOR KINETIC STUDIES

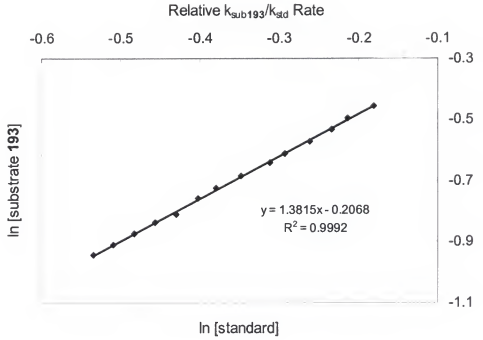

Graph C-1. Data generated measuring integral are vs. time for [std/substrate **193**] = 1

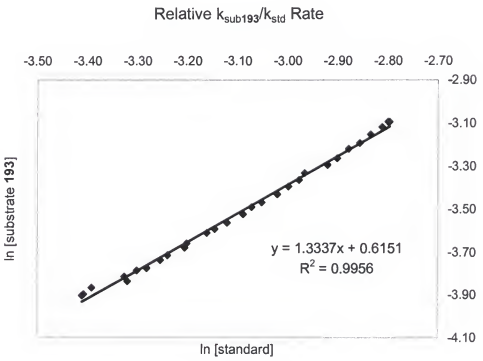

Graph C-2. Data generated measuring integral are vs. time for [std/substrate **193**] = 1

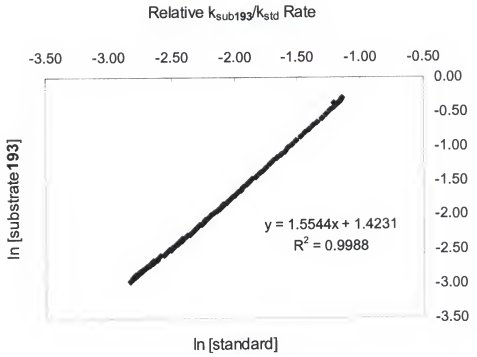

Graph C-3. Data generated measuring integral are vs. time for [std/substrate **193**] = 0.25

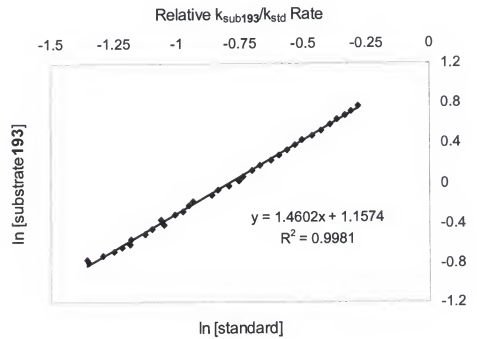

Graph C-4. Data generated measuring integral are vs. time for [std/substrate **193**] = 0.25

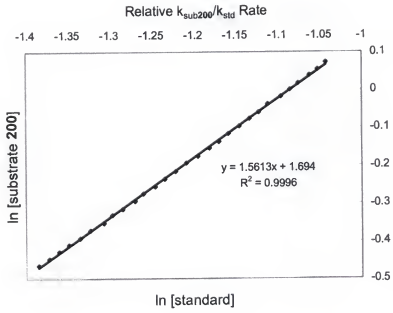

Graph C-5. Data generated measuring integral are vs. time for [std/substrate **200**] = 0.25

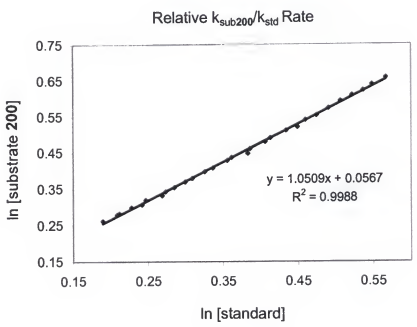

Graph C-6. Data generated measuring integral area vs. time for [std/substrate **200**] = 1

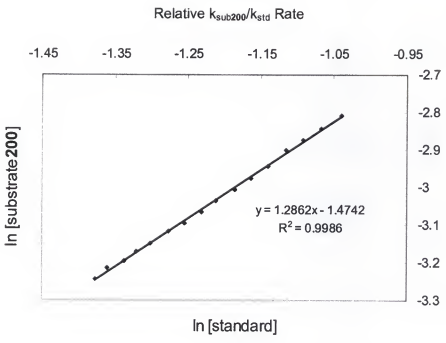

Graph C-7. Data generated measuring integral area vs. time for [std/substrate **200**] = 4

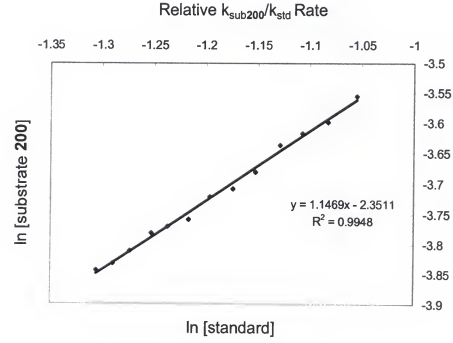

Graph C-8. Data generated measuring integral area vs. time for [std/substrate **200**] = 8

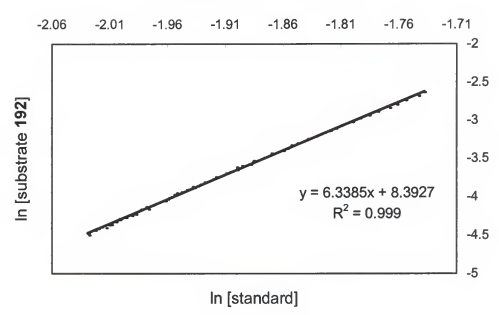

Graph C-9. Data generated measuring integral area vs. time for [std/substrate **192**] = 1

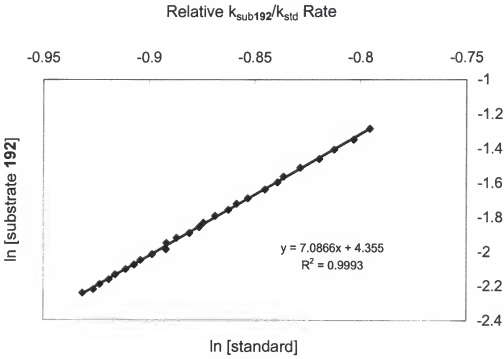

Graph C-10. Data generated measuring integral area vs. time for [std/substrate **192**] = 1

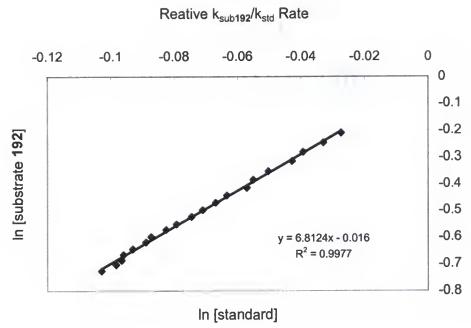

Graph C-11. Data generated measuring integral area vs. time for [std/substrate **192**] = 1

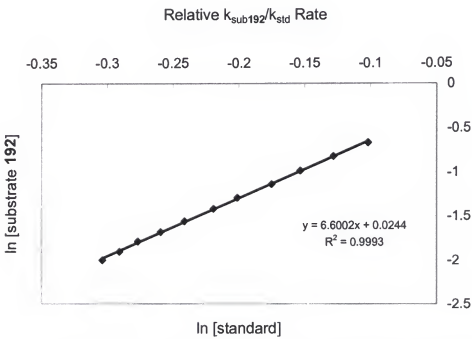

Graph C-12. Data generated measuring integral area vs. time for [std/substrate **192**] = 1

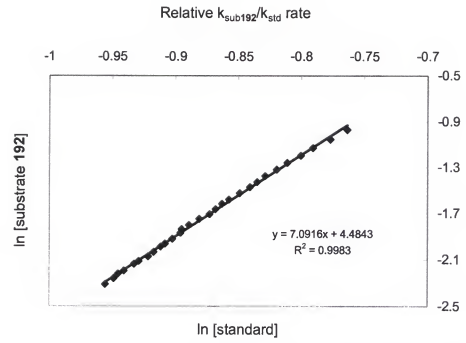

Graph C-13. Data generated measuring integral area vs. time for [std/substrate **192**] = 1

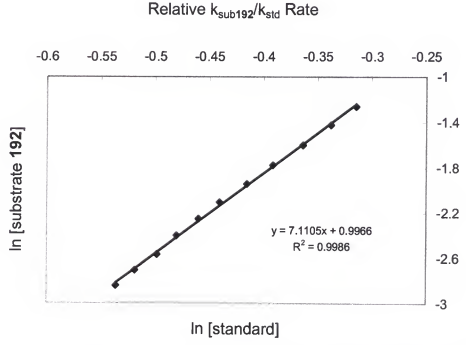

Graph C-14. Data generated measuring integral area vs. time for [std/substrate **192**] = 1

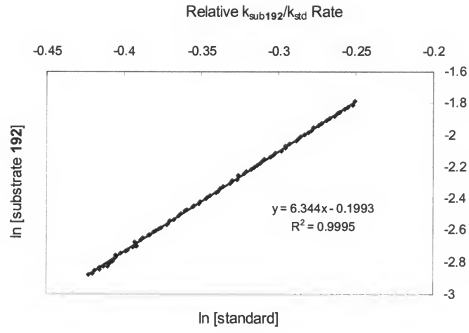

Graph C-15. Data generated measuring integral area vs. time for [std/substrate **192**] = 4

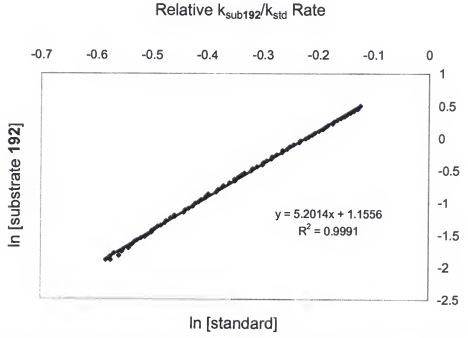

Graph C-16. Data generated measuring integral area vs. time for [std/substrate **192**] = 0.25

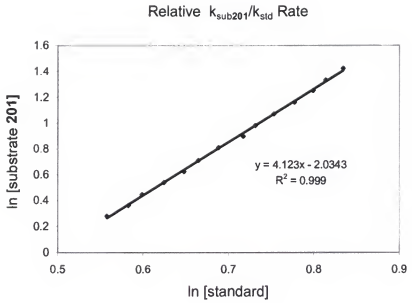

Graph C-17. Data generated measuring integral area vs. time for [std/substrate **201**] = 0.25

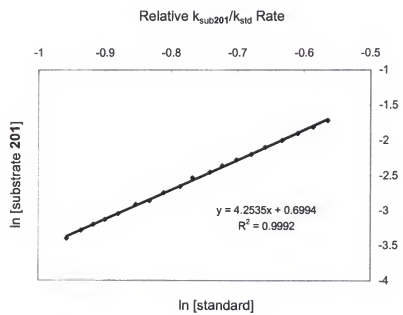

Graph C-18. Data generated measuring integral area vs. time for [std/substrate **201**] =1

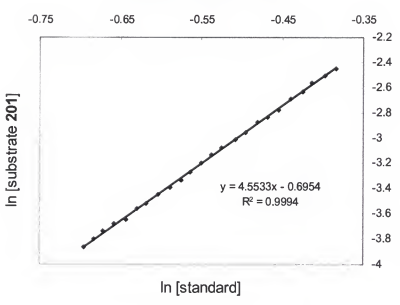

Graph C-19. Data generated measuring integral area vs. time for [std/substrate **201**] = 4

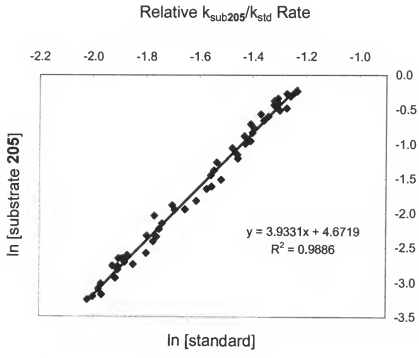

Graph C-20. Data generated measuring integral area vs. time for [std/substrate **205**] = 0.25

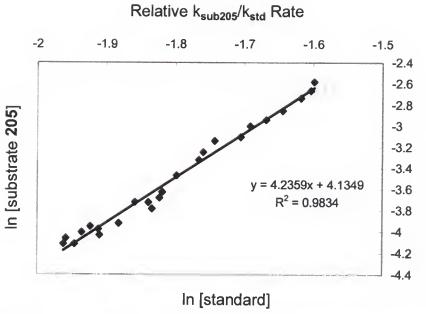

Graph C-21. Data generated measuring integral area vs. time for [std/substrate **205**] = 1

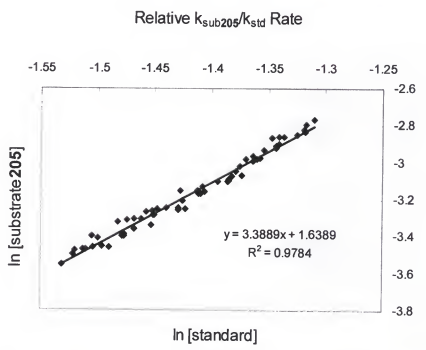

Graph C-22. Data generated measuring integral area vs. time for [std/substrate **205**] = 4

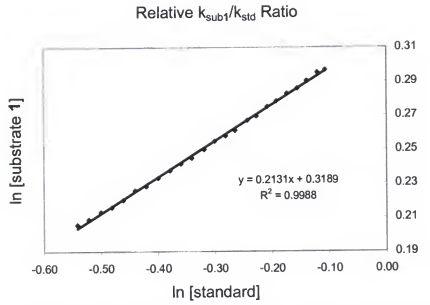

Graph C-23. Data generated measuring integral area vs. time for [std/substrate **1**] = 1

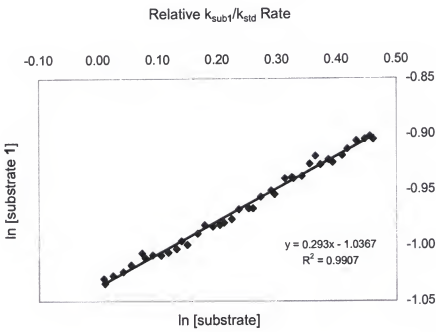

Graph C-24. Data generated measuring integral area vs. time for [std/substrate **1**] = 4

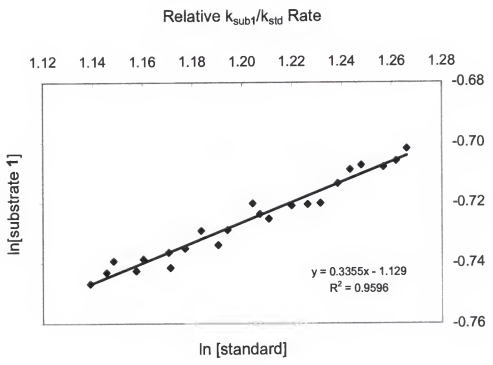

Graph C-25. Data generated measuring integral area vs. time for [std/substrate 1] = 8

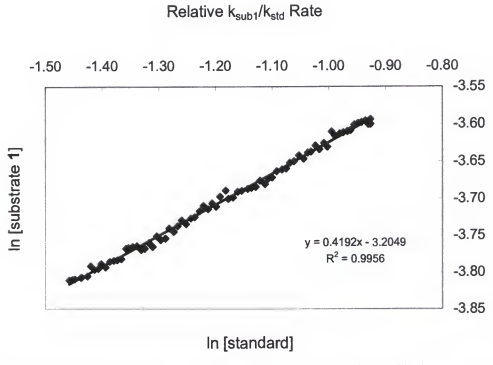

Graph C-26. Data generated measuring integral area vs. time for [std/substrate 1] = 16

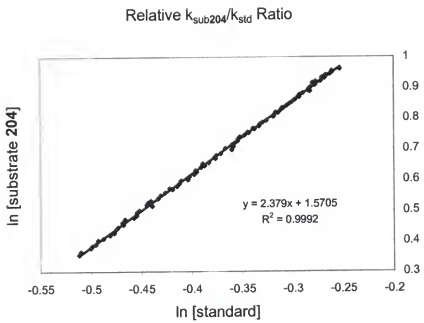

Graph C-27. Data generated measuring integral area vs. time for [std/substrate **204**] = 0.25

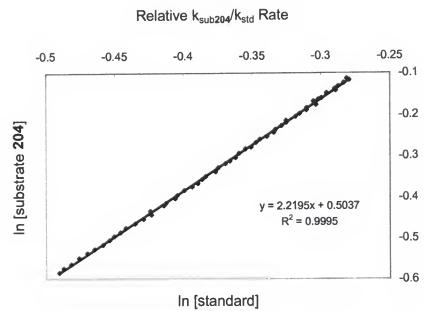

Graph C28. Data generated measuring integral area vs. time for [std/substrate **204**] = 1

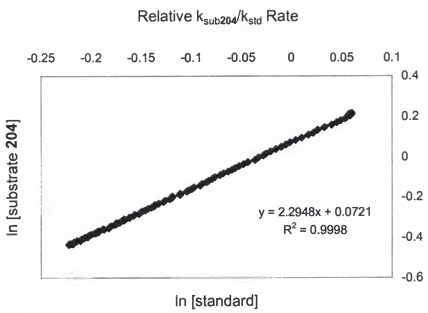

Graph C-29. Data generated measuring integral area vs. time for [std/substrate **204**] = 1

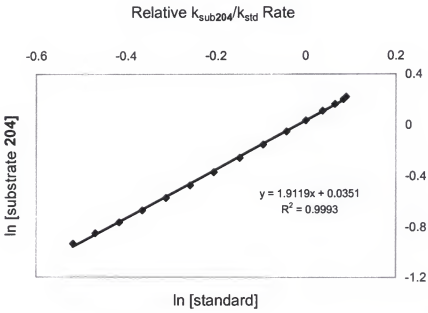

Graph C-30. Data generated measuring integral area vs. time for [std/substrate **204**] = 1

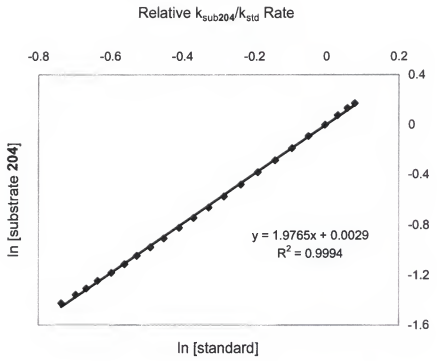

Graph C-31. Data generated measuring integral area vs. time for [std/substrate **204**] = 1

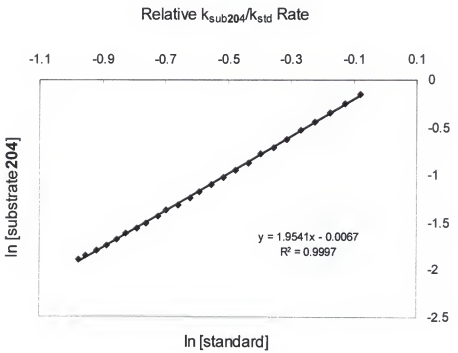

Graph C-32. Data generated measuring integral area vs. time for [std/substrate **204**] = 1

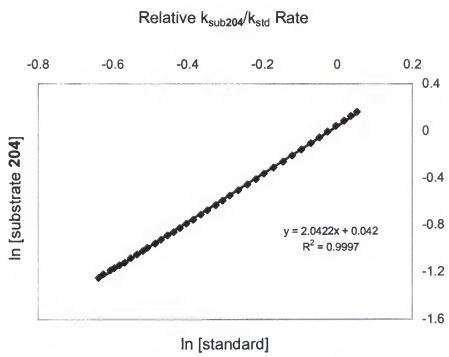

Graph C-33. Data generated measuring integral area vs. time for [std/substrate **204**] = 1

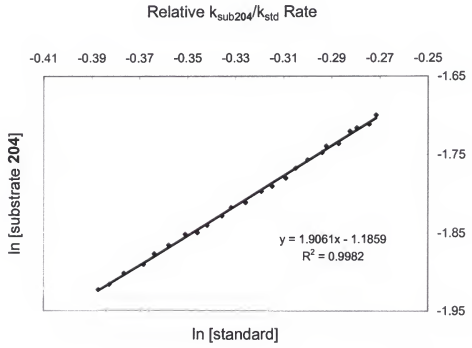

Graph C-34. Data generated measuring integral area vs. time for [std/substrate **204**] = 4

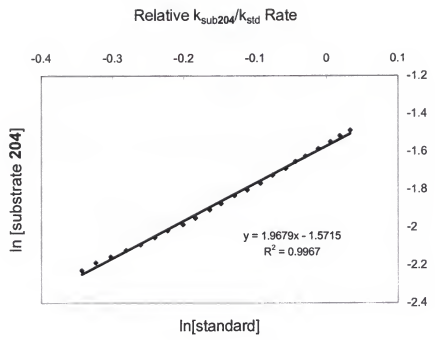

Graph C-35 Data generated measuring integral area vs. time for [std/substrate **204**] = 4

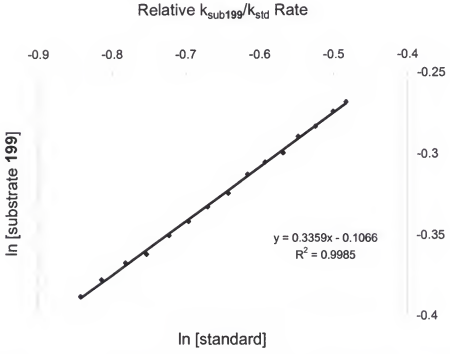

Graph C-36. Data generated measuring integral area vs. time for [std/substrate **199**] = 1

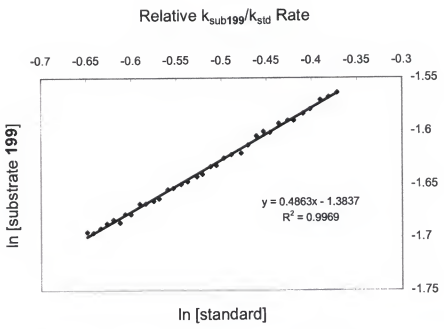

Graph C-37. Data generated measuring integral area vs. time for [std/substrate **199**] = 4

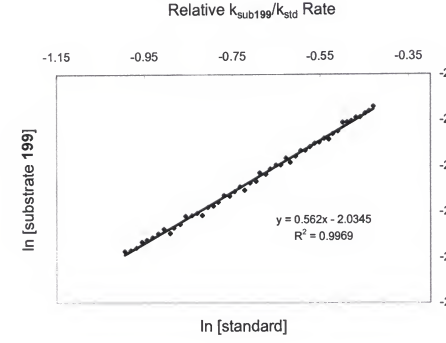

Graph C-38. Data generated measuring integral area vs. time for [std/substrate **199**] = 8

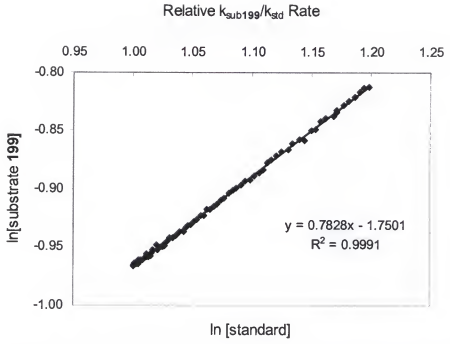

Graph C-39. Data generated measuring integral area vs. time for [std/substrate **199**] = 8

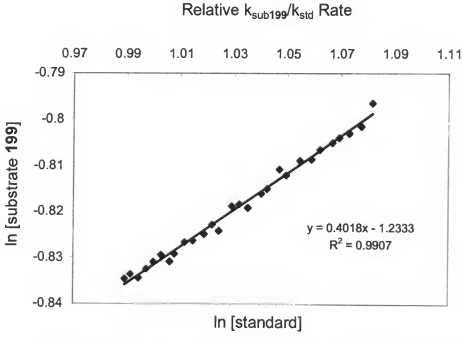

Graph C-40. Data generated measuring integral area vs. time for [std/substrate **199**] = 8

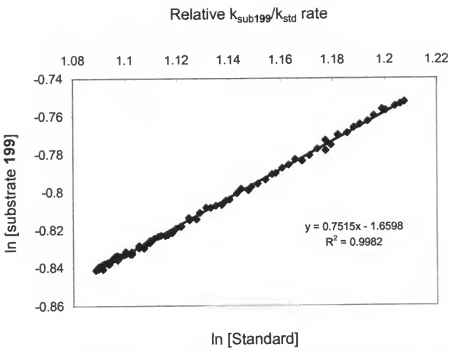

Graph C-41. Data generated measuring integral area vs. time for [std/substrate **199**] = 8

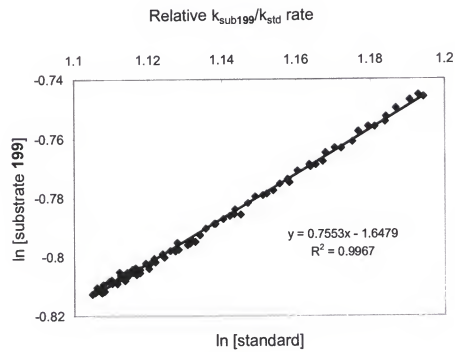

Graph C-42. Data generated measuring integral area vs. time for [std/substrate **199**] = 8

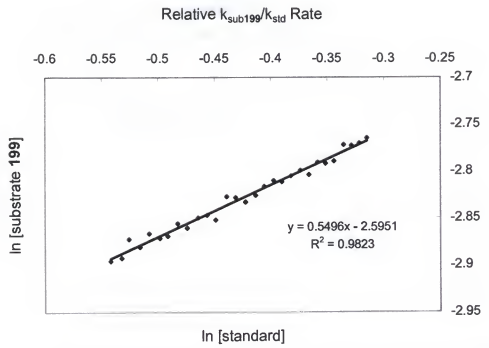

Graph C-43. Data generated measuring integral area vs. time for [std/substrate **199**] = 16

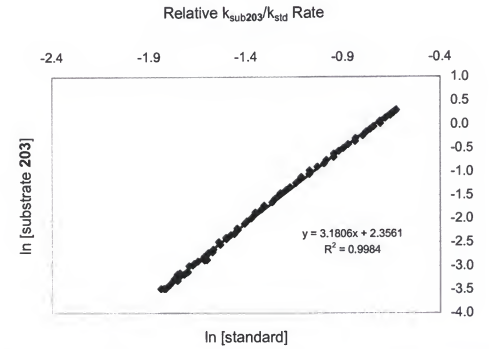

Graph C-44. Data generated measuring integral area vs. time for [std/substrate **203**] = 0.25

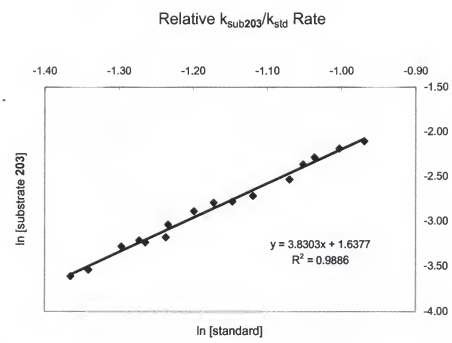

Graph C-45. Data generated measuring integral area vs. time for [std/substrate **203**] = 1

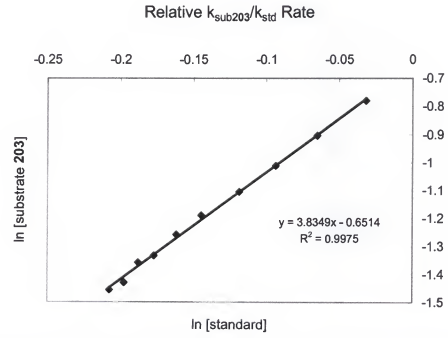

Graph C-46. Data generated measuring integral area vs. time for [std/substrate **203**] = 1

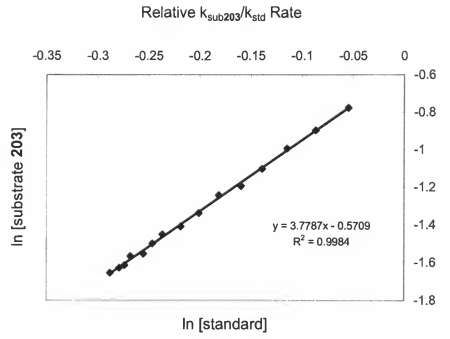

Graph C-47. Data generated measuring integral area vs. time for [std/substrate **203**] = 1

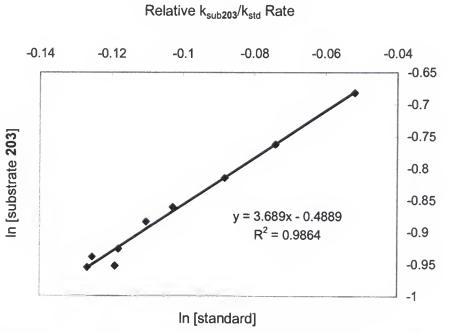

Graph C-48. Data generated measuring integral area vs. time for [std/substrate **203**] = 1

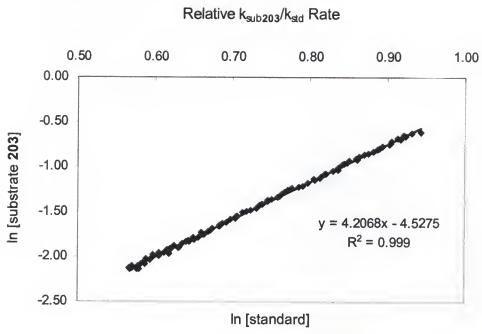

Graph C-49. Data generated measuring integral area vs. time for [std/substrate **203**] = 4

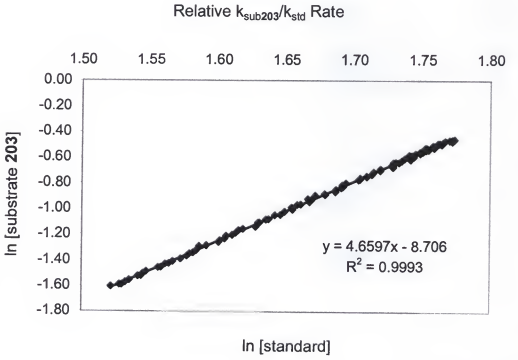

Graph C-50. Data generated measuring integral area vs. time for [std/substrate **203**] = 8

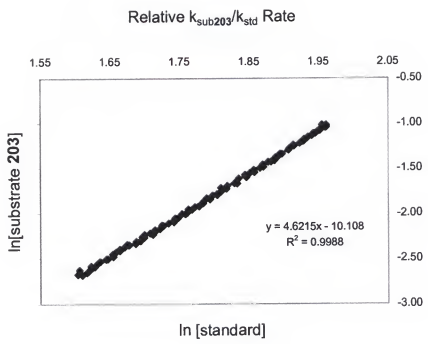

Graph C-51. Data generated measuring integral area vs. time for [std/substrate **203**] = 16

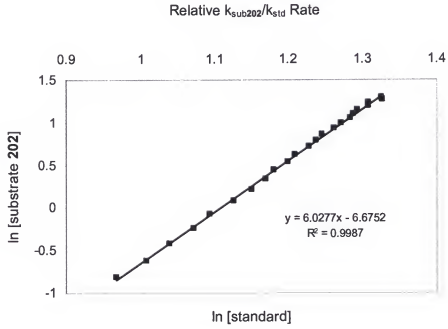

Graph C-52. Data generated measuring integral area vs. time for [std/substrate **202**] = 1

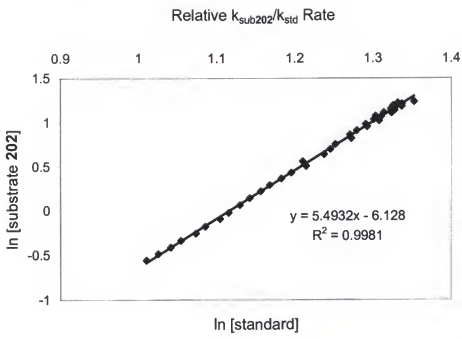

Graph C-53. Data generated measuring integral area vs. time for [std/substrate **202**] = 1

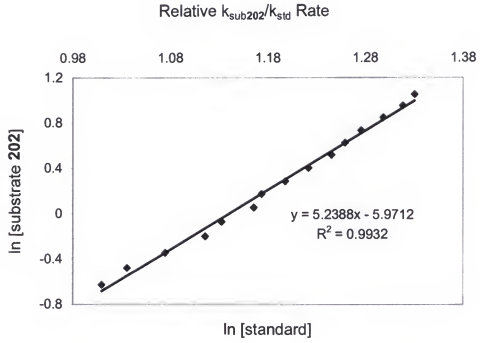

Graph C-54. Data generated measuring integral area vs. time for [std/susbtrate **202**] = 1

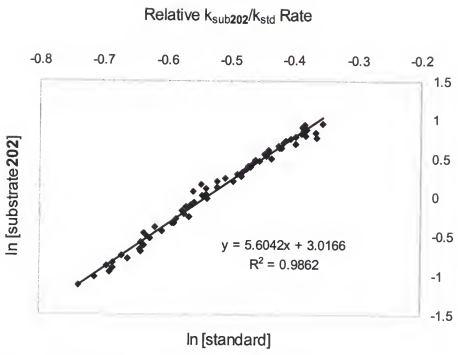

Graph C-55. Data generated measuring integral area vs. time for [std/susbtrate **202**] = 0.25

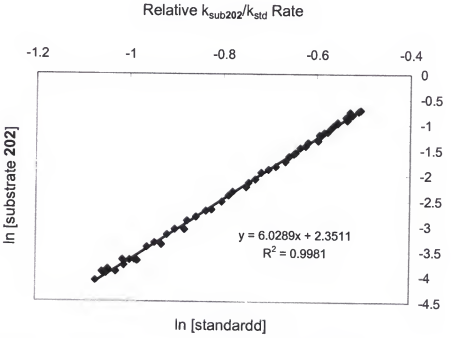

Graph C-56. Data generated measuring integral area vs. time for [std/substrate **202**] = 1

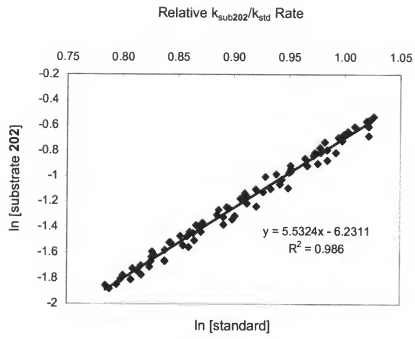

Graph C-57. Data generated measuring integral area vs. time for [std/substrate **202**] = 4

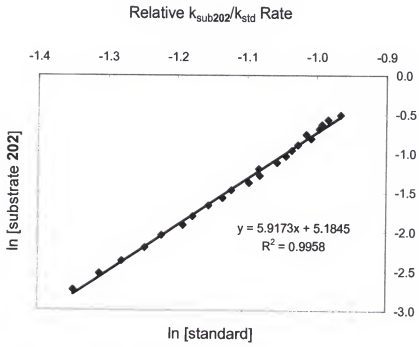

Graph C-58. Data generated measuring integral area vs. time for [std/substrate **202**] = 0.25

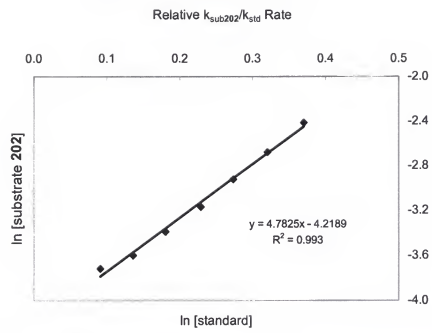

Graph C-59. Data generated measuring integral area vs. time for [std/substrate **202**] = 4

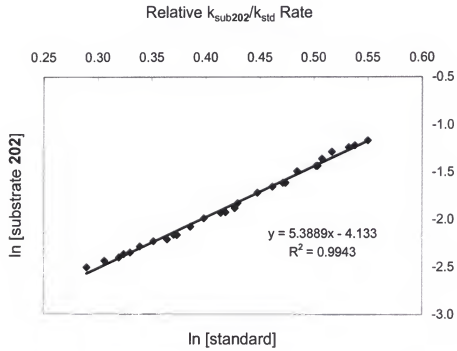

Graph C-60. Data generated measuring integral area vs. time for [std/substrate **202**] = 4

LIST OF REFERENCES

1. Chieu, P.; Lautens, M. In Stereoselective Heterocyclic Synthesis I; Metz, P., Ed.; Wiley & Sons: New York, 1997, vol. 189, p 1.

2. (a) Noyori, R.; Sato, T. *Bull. Chem. Soc. Jpn.* **1978**, 51, 2745. (b) Ashcroft, M. R.; Hoffmann, H. M. R. *Organic Synthesis Collective vol VI* **1988**, 512, 17. (c) Mann, J.; Usmani, A. A.; Cowling, A. P. *J. Chem. Perkin. Trans I* **1981**, 2116. (d) Murray, D. H.; Albizati, K. F. *Tetrahedron Letters* **1999**, 29, 4109.

3. (a) Föhlish, B.; Gehrlach, E.; Geywitz, B. *Chem. Ber.* **1987**, 120, 1815. (b) Föhlish, B.; Krimmer, D.; Gehrlach, E.; Kashammer, D. *Chem. Ber.* **1988**, 121, 1585.

4. For a review on the [4+3] cycloaddition: (a) Rigby, J. H.; Pigge, F. C. In Organic Reactions; Paquette, L. A., Ed.; Wiley and Sons: New York, 1997; Vol. 51, p351.

5. (a) Davies, H. M. L.; Ahmed, G.; Churchill, M. R. *J. Am. Chem. Soc.* **1996**, 118, 10774. (b) Lautens, M.; Aspiotis, R.; Colucci, J. *J. Am. Chem. Soc.* **1996**, 118, 10930. (c) Harmata, M.; Jones, D.; Kahraman, M.; Sharma, U.; Barnes, C. L. *Tetrahedron Lett.* **1999**, 40, 1831. (d) Hoffmann, H. M. R.; Stark, C. B.; Wartchow, R.; Pierau, S. *Chem. Eur. J.* **2000**, 6, 684. (e) Montaña, P. M.; Grima, *Tetrahedron* **2002**, 58, 4769.

6. (a) Hoffmann, H. M. R.; Lampe, T. F. J. *Tetrahedron: Asymmetry* **1996,** 7(10), 2889. (b) Cha, K. J.; Kim, H.; Ziani-Cherif, C.; Oh, J. *J. Org. Chem.* **1995**, 60, 792. (c) Lautens, M.; Ma, S.; Yee, A. *Tetrahedron Lett.* **1995,** 36, 4185.

7. Yadav, J. S.; Srinivas Rao, C.; Chandrasekhar, S.; Rama Rao, A.V. *Tet. Lett.* **1995**, 36(42), 7717.

8. (a) Hoffmann, H.M.R.; Vakalopoulos, A.; Smits, R. *Eur. J. Org. Chem.* **2002**, 1538. (b) Hoffmann, H.M.R.; Kim, H. *Eur. J. Org. Chem.* **2000**, 2195. (c) Hoffmann, H.M.R.; Vakalopoulos, A. *Org. Lett.* **2001**, 3(2), 177.

9. (a) Hoffmann, H.M.R.; Lampe, T.F.J. *Tetrahedron Letters* **1996**, 37(43), 7695. (b) Hoffmann, H.M.R.; Lampe, T.F.J.; Vakalopoulos, A. *Org. Lett.* **2001**, 3(6), 929.

10. Hoffmann, H. M. R.; Wolbers, P. *Tetrahedron* **1999**, 55, 1905.

11. Hoffmann, H. M. R.; Misske, A. M. *Tetrahedron* **1999**, 55, 4315.

12. Hoffmann, H. M. R.; Nowakowski, M. *Tetrahedron Letters* **1997**, 38(6), 1001.

13. Hoffmann, H. M. R.; Treu, J.; Dunkel, R. *Tetrahedron: Asymmetry* **1999**, 10, 1539.

14. Hoffmann, H. M. R.; Dunkel, R.; Mentzel, M. *Tetrahedron* **1997**, 53(44), 14929.

15. Sato, T.; Hayakawa, Y.; Noyori, R. *Bull. Chem. Soc. Jpn.* **1984**, 57, 2515.

16. Simpkins, N. S.; Cox, P. J.; Bunn, B. J. *Tetrahedron* **1993**, 49, 1, 207.

17. Grieco, P. A.; Hunt, K. W. *Org. Lett.* **2001**, 3, 3, 481.

18. Grieco, P. A.; Hunt, K. W. *Org. Lett.* **2002**, 3, 2, 245.

19. Lautens, M. *Pure & Appl. Chem.* **1992**, 64, 12, 1873.

20. Lautens, M.; Chiu, P.; Colucci, J. T. *Angew. Chem. Int. Ed. Engl.* **1993**, 32, 281.

21. Lautens, M.; Di Felice, C.; Huboux, A. *Tetrahedron Letters* **1989**, 30, 49, 6817.

22. Lautens, M.; Abd-El-Aziz, A. S.; Lough, A. *J. Org. Chem.* **1990**, 55, 5305.

23. Cha, J. K.; Lee, J. C. *J. Am. Chem. Soc.* **2001**, 123, 3243.

24. Cha, J. K.; Jin, S.; Lee, J. C.; *J. Org. Chem.* **1998**, 63, 2804.

25. Cha, J. K.; Cho, S. Y.; Lee, J. C. *Tetrahedron Letters* **1999**, 40, 7675.

26. Cha, J. K.; Lee, K. *J. Am. Chem. Soc.* **2001**, 123, 5590.

27. Föhlish, B.; Sendelbach, S.; Bauer, H. *Liebigs Ann. Chem.* **1987**, 1.

28. Mann, J.; Barbosa, L. C. A.; Wilde, P. D. *Tetrahedron* **1989**, 45, 4619.

29. (a) Blechert, S.; Schuster, M.; *Angew. Chem. Int. Ed. Engl.* **1997**, 36, 2036. (b) Grubbs', R. H.; Chang, S. *Tetrahedron*, **1998**, 54, 4413. (c) Wright, D. *Current Organic Chemistry* **1999**, 3, 211. (d) Fürstner, A. *Angew. Chem. Int. Ed. Engl.* **2000**, 39, 3012.

30. Chauvin, Y.; Hérisson, J. L.; *Makromol. Chem.* **1971**, 141, 161.

31. (a) Basset, J. –M.; Descotes, G.; Ramja, J.; Pagano, S. Tetrahedron Lett. 1994, 35, 7379. (b) Basset, J. –M.; Couturier, J. –L.; Tanaka, K.; Leconte, M.; Ollivier, J. *Angew. Chem. Int. Ed. Engl.* **1993**, 32, 112.

32. (a) Schrock, R. R. *Tetrahedron* **1999**, 55, 8141. (b) Schrock, R. R. *Acc. Chem. Res.* **1990**, 23, 158.

33. Grubbs, R. H.; Nguyen, S. T.; Ziller, J. W. *J. Am. Chem. Soc.* **1993**, 115, 9858.

34. Grubbs, R. H.; Schwab, P.; France, M. B.; Ziller, J. W. *Angew. Chem. Int. Ed.* **1995**, 34, 2039.

35. Grubbs, R. H.; Scholl, M.; Trnka, T. M.; Morgan, J. P. *Tetrahedron Lett.* **1999**, 40, 2247.

36. Stinson, S. *Chem. Eng. News* **2000**, 78, 35, 6.

37. Grubbs, R. H.; Nguyen, S. T.; Dias, E. L. *J. Am. Chem. Soc.* **1997**, 119, 3887.

38. Buchmeiser, M. R. *Chem Rev.* **2000**, 100, 1565.

39. Schrock, R. R.; Saunders, R. S.; Cohen, R. E.; Wong, S. J.; *Macromolecules* **1992**, 25, 2055.

40. Héroguez, V.; Amedro, E.; Grande, D.; Fontanille, M.; Gnanou, Y. *Macromolecules* **2000**, 33, 7241.

41. Schrock, R. R.; Cummins, C. C.; Cohen, R. E. *Chem. Mater.* **1992**, 4, 27.

42. Langer, R. *Acc. Chem. Res.* **2000**, 33, 94.

43. Nguyen, S. T.; Watson, K. J.; Anderson, D. R. *Macromolecules* **2001**, 34, 11, 3507.

44. Wagener, K. B.; Hopkins, T. E.; Pawlow, J. H.; Koren, D. L.; Deters, K. S.; Solivan, S. M.; Davis, J. A.; Gómez, F. J. *Macromolecules* **2001**, 34, 7920.

45. Crowe, W. E. Zhang, Z. J. *J. Am. Chem.* **Soc. 1995**, 115, 10998.

46. Crowe, W. E.; Goldberg, D. R.; Zhang, Z. J. *Tetrahedron Lett.* **1996**, 37, 2117

47. blechert ex of just trans CM: Blechert, S.; Brümmer, O.; Rückert, A. *Chem. Eur. J.* **1997**, 3, 441.

48. Grubbs, R. H.; Chatterjee, A. K. Sanders, D. P. *Org. Lett.* **1999**, 1, 1751.

49. Grubbs, R. H.; Chatterjee, A. K.; Morgan, J. P.; Scholl, M. *J. Am. Chem. Soc.* **2000**, 122, 3783.

50. Grubbs, R. H.; Chatterjee, A. K.; Choi, T. L. *Angew. Chem. Int. Ed.* **2000**, 39, 1277.

51. Grubbs, R. H.; Morrill, C. *J. Org. Chem.* **2003**, 68, 15, 6031.

52. Miyaura, N.; Yammamoto, Y.; Takahashi, M. *Synlett* **2002**, 128. (b) Grubbs, R. H.; Goldberg, S. D. *Angew. Chem. Int. Ed.* **2002**, 41, 807.

53. Roy, R.; Das, S. K. *Chem. Commun.* **2000**, 519.

54. Han, S.-Y.; Chang, S. In Handbook of Metathesis; Grubbs, R. H., Ed.; Wiley-VCH: Germany, 2003; Vol. 2, p 5.

55. Hanessian, S.; Margarita, R.; Hall, A.; Johnstone, S.; Tremblay, M.; Parlanti, L. *J. Am. Chem. Soc.* **2002**, 124, 13342.

56. (-)-Griseoviridin: Meyers, A. I.; Dvorak, C. A.; Schmitz, W. D.; Poon, D. J.; Pryde, D. C.; Lawson, J. P.; Amos, R. A. *Angew. Chem. Int. Ed.* **2000**, 39, 9, 1664.

57. Mori, M.; Kinoshita, A.; *J. Org. Chem.* **1996**, 61, 8356.

58. ROCM: Snapper, M. L.; Randall, M. L.; Tallarico, J. A. *J. Am. Chem. Soc.* **1995**, 117, 9610.

59. (a) Blechert, S.; Schneider, M. F.; Lucas, N.; Velder, J. *Angew. Chem. Int. Ed Engl.* **1997**, 36, 257. (b) Blechert, S.; Schneider, M. F. *Angew. Chem. Int. Ed Engl.* **1997**, 35, 411.

60. Arjona, O.; Plumet, J.; Csáky, A. G.; Murcia, M. C. *J. Org. Chem.* **1999**, 64, 9739.

61. Szeimies and Feng: Szeimies, G.; Feng, J. Eur. *J. Org. Chem.* **2002**, 2942.

62. Grubbs, R. H.; Bowden, N. B.; Zuercher,W. J.; Kim, S. H. *J.Org. Chem.* **1996**, 61, 1073.

63. Blechert, S.; Stragies, R. *Tetrahedron* **1999**, 55, 8179.

64. Arjona, O.; Plumet, J.; Csákÿ, A. G.; Mendel, R. *J. Org. Chem.* **2002**, 67, 1380.

65. Schrock, R. R.; Wolf, J. R.; McConville, D. H. *J. Am. Chem. Soc.* **1993**, 115, 4413

66. Grubbs, R. H.; Fujimura, O. J. am. Chem. Soc. 1996, 118, 2499

67. Schrock, R. R; Hoveyda, A. H.; Cefalo, D. R.; La, D. S.; Alexander, J. B. *J. Am. Chem. Soc.* **1998**, 120, 4041

68. Schrock, R. R; Hoveyda, A. H.; Cefalo, D. R.; La, D. S.; Zhu, S. S.; Jamieson, J. Y.; Davis, W. M. *J. Am. Chem. Soc.* **1999**, 121, 8251.

69. Burke, S. D.; Müller, N.; Beaudry, C. M. *Org. Lett.* **1999**, 1, 11, 1827.

70. Schrock, R. R; Hoveyda, A. H.; Weatherhead, G. S.; Ford, J. G.; Alexanian, R. R. *J. Am. Chem. Soc.* **2000**, 122, 8071.

71. Hoveyda, A. H.; Cefalo, D. R.; La, D. S.; Harrity, J. P. A.; Visser, M. S. *J. Am. Chem. Soc.* **1998**, 120, 2343.

72. Schrock, R. R.; Hoveyda, A. H.; Ford, J. G.; Sattely, E. S.; La, D. S. *J. Am. Chem. Soc.* **2001**, 123, 7767.

73. Hoveyda, A. H.; Schrock, R. R.; Aeilts, S. L.; Cefalo, D. R.; Bonitatebus, P. J. Houser, J. H. *Angew. Chem. Int. Ed.* **2001**, 40, 1452.

74. Hoveyda, A. H.; Schrock, R. R.; Hultzsch, K.; Jernelius, J. A. *Angew. Chem. Int. Ed.* **2002**, 41, 589.

75. Grubbs, R. H.; Seiders, T. J.; Ward, D. W. *Org. Lett.* **2001**, 3, 3225.

76. Hoveyda, A. H.; Van Veldhuizen, J. J.; Garber, S. B.; Kingsbury, J. S. *J. Am. Chem. Soc.* **2002**, 124, 4954.

77. Kashman, Y.; Groweiss, A.; Shmueli, U. *Tet. Lett.* **1980**, 21, 3629.

78. (a) Spector, I.; Shochet, N.R.; Kashman, Y.; Groweiss, A. Science, February, **1983**, 219, p493. (b) Néeman, I.; Fishelson, L.; Kashman. Y.; *Mar. Biol.* 30, 293, **1975**.

79. Kashman, Y.; Groweiss, A.; Lidor, R.; Blasberger, D.; Carmely, S. *Tet. Lett.* **1985**, 41, 10, 1905.

80. Blasberger,D.; Carmely, S.; Cojocaru, M.; Spector, I.; Shochet, N. R.; Kashman, Y. *Justus Liebigs Ann. Chem.* **1989**, 1171.

81. Zibuck, R.; Liverton, N. J.; Smith III, A. B. *J. Am. Chem. Soc.* **1986**, 108, 2451.

82. Fürstner, A.;De Souza, D.; Parra-Rapado, L.; Jensen, J.T. *Angew.Chem. Int. Ed.* **2003**, 42, 5358.

83. (a) Smith, A.B.; Noda, I.; Remiszewski, S. W.; Liverton, N. J.; Zibuck, R. *J. Org. Chem.* **1990**, 55, 3977 (b) White, J. D.; Kawasaki, M. *J. Am. Chem. Soc.* **1990**, 112, 4991.

84. (a) White, J.D.; Kawasaki, M. *J. Am. Chem. Soc.* **1990**, 112, 4991 (b) White, J.D.; Kawasaki, M. *J. Org. Chem.* **1992**, 57, 20, 5292.

85. Wright, D.L.; Usher, L.C.; Estrella-Jimenez, M.E. *Org. Lett.*, **2001**, 3, 4277.

86. Usher, Lynn C. Ring-Opening Metathesis/Cross Metathesis and Domino Metathesis of 8-oxabicyclo[3.2.1]octene Derivatives: An Approach to Pyran Containing Natural Products **2003**, PhD dissertation, University of Florida

87. Cuny, G.D.; Cao, J.; Sidhu, A.; Hauske, J.R. *Tetrahedron* **1999**, 55, 8169 and with ethylene: Harmata, M.; Shao, L.; Kurti, L.; Akeywardane, A. *Tetrahedron Lett.* **1999**, 40, 1075.

88. Crowe, W. E.; Goldberg, D. R.; *J. Am. Chem. Soc.* **1995**, 117, 5162.

89. (a) Hoffmann, H. M. R.; Lampe, T. F. *J. Chem. Commun.* **1996**. 1931. (b) Lautens, M. Ma, S. *Tetrahedron Lett.* **1996**, 37, 1727.

90. Hoffmann, H. M. R.; Lampe, T. F. J. *Tetrahedron: Asymmetry* **1996**, 7, 10, 2889.

91. Ager, D. J.; In *Organic Reactions*, Wiley & Sons: New York, 1990, 38, 1-223.

92. Grubbs, R. H.; Kirkland, T. A. *J. Org. Chem.* **1993**, 58, 5057.

93. Wright, D.L.; Usher, L.C.; Estrella-Jimenez, M.E.; Ghiviriga, I. *Angew.Chem. Int. Ed.* **2002**, 41, 23, 4560.

94. Mann, J.; Bowers, K. G.; Markson, A. J. *J. Chem. Research* **1986**, 424.

95. (a) Anderson, C. B.; Sepp, D. T. *Tetrahedron* **1968**, 24, 1707. (b) Lemieux, R. U. *Pure Appl. Chem.* **1971**, 27, 527.

96. Sheldon, R. A.; Kochi, J. K. In *Organic Reactions*, Wiley & Sons: New York, 1972, 19, 279-421.

97. (a) Suárez, E.; González, C. C.; Francisco, C. G. *Tetrahedron Lett.* **1997**, 38, 23, 4141. (b) Suárez, E.; Concepción, J. I.; Francisco, C. G.; Freire, R.; Hernández, R.; Salazar, J. A. *J. Org. Chem.* **1986**, 51, 3, 402. (c) Suárez, E.; Boto, A.; Hernández, R. *Tetrahedron Lett.* **1999**, 40, 32, 5945.

98. Hoveyda, A. H.; Gillingham, D. G.; Kataoka, O.; Garber, S. B. *J. Am. Chem. Soc.* **2004**, 126, 12288.

BIOGRAPHICAL SKETCH

María E. Estrella-Jiménez was the first born of three, born in New York on May 8, 1977, from Sheila Jiménez and Félix A. Estrella. After living in New York with her mother for seven months, they moved to Puerto Rico to meet her father. She grew up in Puerto Rico, were she attended the Colegio de la Inmaculada to obtain her high school diploma. Then, she earned her Bachelor of Arts in chemistry from the University of Puerto Rico, Río Piedras Campus, where she first experienced working with organic chemistry doing undergraduate research with Professor John A. Soderquist. During her undergraduate research, she earned the Pfizer fellowship, which gave her the opportunity to participate in a summer internship. After she completed her B.S., she spent three months working at Pfizer in Groton, CT. Then, she started her graduate studies in organic chemistry on August 2000 at the University of Florida under the supervision of Professor Dennis L. Wright. Upon completion of her Ph.D., she will move to Texas, University of Texas Medical Branch, to be a postdoctoral fellow of Dr. Scott R. Gilbertson. After that experience, she plans to work in industry.

I certify that I have read this study and that in my opinion it conforms to acceptable standards of scholarly presentation and is fully adequate, in scope and quality, as a thesis for the degree of Doctor of Philosophy.

Dennis L. Wright, Chairman
Associate Professor of Chemistry

I certify that I have read this study and that in my opinion it conforms to acceptable standards of scholarly presentation and is fully adequate, in scope and quality, as a thesis for the degree of Doctor of Philosophy.

Merle A. Battiste, Cochair
Professor of Chemistry

I certify that I have read this study and that in my opinion it conforms to acceptable standards of scholarly presentation and is fully adequate, in scope and quality, as a thesis for the degree of Doctor of Philosophy.

William R. Dolbier Jr.
Professor of Chemistry

I certify that I have read this study and that in my opinion it conforms to acceptable standards of scholarly presentation and is fully adequate, in scope and quality, as a thesis for the degree of Doctor of Philosophy.

David H. Powell
Scientist of Chemistry

I certify that I have read this study and that in my opinion it conforms to acceptable standards of scholarly presentation and is fully adequate, in scope and quality, as a thesis for the degree of Doctor of Philosophy.

Kenneth Sloan
Professor of Medicinal Chemistry

This thesis was submitted to the Graduate Faculty of the Department of Chemistry in the College of Liberal Arts and Sciences and to the Graduate School and was accepted as partial fulfillment of the requirements for the degree of Doctor of Philosophy.

May 2005

_____

Dean, Graduate School